Mechanisms of nuclear receptor resistance in prostate cancer

by

Craig L Doig

A thesis submitted to The University of Birmingham

For the degree of

DOCTOR OF PHILOSOPHY

School of Clinical & Experimental Medicine

The University of Birmingham

February 2011

"Does the body rule the mind or does the mind rule the body?
I dunno."

-Morrissey

ABSTRACT

Nuclear receptors (NRs) are essential transcription factors that participate in a diverse number of cellular functions. Operating as sensors of both endogenous and exogenous ligands they are able to direct gene expression in both a positive and negative manner. Many NRs exhibit attractive chemotherapeutic potential due to their ability to govern key pathways of cellular differentiation, growth arrest and programmed cell death. Interestingly, there are numerous examples of NR signaling becoming disrupted in human malignancies including the prostate. Mechanisms that give rise to impaired receptor signalling are investigated herein; these include pre-receptor regulation of NR ligand availability and epigenetically mediated hypoacetylation of N-terminal histone tails. This work attempts to overcome or circumvent their transcriptional disruption and also unveils the molecular mechanisms behind NR transcriptional potency in prostate cancer.

Prereceptor ligand metabolism has been previously demonstrated as an important factor in the regulation of nuclear receptor activity. During progression, CaP cells acquire the ability to upregulate the formation of AKR1C3, this enzyme may be responsible for conversion of prostaglandin intermediates. This study attempted to restore the actions of the anti-tumourigenic nuclear receptor PPARγ through reduction in the levels of AKR1C3. This may increase the levels of the ligand PGJ_2 available for PPARγ activation. From these studies it was identified found that reducing the levels of AKR1C3 and co-treatment with PGD_2 and SAHA was unable to restore activation of this NR. This is in opposition to studies in leukaemic cells and suggests a distinct molecular mechanism of PPARγ activation by prostaglandins in human prostate cancer.

In additional studies, one member of the NR family was chosen for further analysis, namely the vitamin D receptor (VDR). This thesis consistent with previous investigations describes malignant metastatic PC-3 prostate tumour cell lines to be selectively insensitive to the biologically active form of vitamin D. Several of the genes regulated by VDR in immortalized non-transformed RWPE-1 cells become unresponsive when challenged with active vitamin D in the PC-3 malignant cell line. Furthermore, the disruption was also shown to be present in the isogenic RWPE-2 cell line suggesting NR deregulation is acquired prior to androgen deprivation therapy resistance (ADT-R).

Nuclear receptor insensitivity is shown in Chapter 5 of this work with PC-3 and RWPE-2 cells selectively deregulating the VDR. In accordance with this finding studies of the VDR basal levels of expression in PC-3 cells become altered. Thus, levels of VDR expression are lost in correlation to its target genes and this reflects the ability of VDR to exert its anti-proliferative actions prostate cancer.

Furthermore, the networks of gene targets within VDR signaling motifs also become skewed in prostate cancer. The incoherent feedforward response observed within VDR-MCM7 signalling contains a microRNA (MiR106b) whose activity was shown in this work to become disrupted in cancer. Not only does the proliferative MCM7 protein become upregulated but also the miR106b that targets *CDKN1A* transcript for degradation becomes upregulated. Therefore, the hypothesis proposed was that MiR106b is a proto-oncogene capable of indicating the VDR resistant/responsive status of CaP cases. To continue this work it was suggested that the serum analysis of human patients with various stages of prostate disease should be analysed and compared alongside control groups to determine a risk stratification profile for prostate cancer patients.

The vitamin D receptor and its target gene *CDKN1A* were then examined for recruitment of VDR, nuclear corepressor (NCOR1) and RNA p-polymerase II to response elements. Using the non-malignant prostate epithelial cell line RWPE-1, and PC-3 prostate cancer cell line, to represent stages of prostate disease progression, the spatio-temporal binding characteristics in response to ligand were measured. These findings identified aberrant nuclear corepressor recruitment to the transcription start site of *CDKN1A* in the malignant disease model cell line. Taken together, these investigations serve to enhance the understanding of nuclear receptor activity within prostate cancer with a particular focus on the VDR.

ACKNOWLEDGEMENTS

I would like to thank my supervisors Dr. Moray Campbell and Prof. Chris McCabe for their fantastic support, advice and expertise throughout this project.

Having been accepted into this research group in 2007 I have found my all of my colleagues during the 4 years to be considerate, generous and fun to be with. The first few weeks of working in a research laboratory is a daunting and confusing experience. Luckily I had two excellent friends (Dr. James Thorne and Dr. Sebastiano Battaglia) to teach me where everything was kept, how to keep cells in top condition and the various techniques used in this thesis. Therefore, I would like to express my gratitude to them and I owe you a few beers next time we meet. Everyone else on the IBR 2nd floor have been extremely helpful (but I can't afford to buy you all drinks).

Dr. Moray Campbell relocated to Roswell Park Cancer Institute (Buffalo, New York) six months after I joined the group. No, I don't think it was something I said. However, this did provide the opportunity to integrate with other groups within Birmingham. And as part of this I spent a large portion of my time working alongside Dr. Laura O'Neill whom was always friendly, charitable with her time, expertise and reagents (!).

In January 2009 I relocated with Morays group to Buffalo, New York to continue my studies at Roswell Park Cancer Institute, where I spent 15 months. Everyone here was very welcoming and always polite. I must thank Moray for giving me somewhere to stay upon my arrival and also Dr. Orla Maguire and her husband Connor for sharing that burden. I was never short of friends in Buffalo and Orla, Connor, Laura, Joe, Jason, Michelle, Sobo and Seb were always around to hang out with. I will miss Friday drinking Spaten in Ulrichs Tavern (unlike the bathroom facilities in that place, which I am happy never to see again!). Thanks to Buffalo and thanks Roswell Park Cancer Institute.

Throughout all of this and more there has been one person who has kept me sane, and encouraged me to keep going. My wife Kelly has been understanding, hugely supportive, and consistently amazing. Thank you x

ABBREVIATIONS

Acute Myelogenous Leukemia	AML
Acute Promyelocytic Leukemia	APL
Aldoketoreductase 1C3	AKR1C3
Androgen Deprivation Therapy-Recurrent	ADT-R
Androgen Receptor	AR
Adenosine Triphosphate	ATP
Chromatin Immunoprecipitation	ChIP
Chromatin Immunoprecipitation with microarray	ChIP-ChIP
Chromatin Immunopreciptiation with DNA sequencing	ChIP-Seq
Coactivator	CoA
Corepressor	CoR
Corepressor Nuclear Receptor Box	CoRNR box
Cyclin Dependent Kinase	CDK
Cycloheximide	CHX
Deoxyribonucleic Acid	DNA
DNA Binding Domain	DBD
DNA Methyltransferases	DNMT
Epidermal Growth Factor	EGF
Epidermal Growth Factor Receptor	EGF-R
European Prospective Investigation into Cancer	EPIC
Feedforward Loop	FFL
Genome Wide Association Studies	GWAS
Glucocorticoid Receptor	GR
Histone Acetyltransferase	HAT
Histone Deacetylase	HDAC
Histone Deacetylase Inhibitor	HDACi
Histone 3 Lysine 4	H3K4
Histone 3 Lysine 4 Monomethylation	H3K4me
Histone 3 Lysine 4 Dimethylation	H3K4me2
Histone 3 Lysine 4 Trimethylation	H3K4me3

Histone 3 Lysine 9 Acetylation	H3K9ac
Histone 3 Lysine 9 Dimethylation	H3K9me2
Histone 3 Lysine 27 Trimethylation	H3K27me3
Human Papilloma Virus	HPV
Ligand Binding Domain	LBD
Nuclear Corepressor	NCOR1
Nuclear Receptor	NR
Oesrogen Receptor	ER
Peroxisome Proliferator Activated Receptor	PPAR
Postranslational Modifications	PTMs
Proliferating Cell Nuclear Antigen	PCNA
Prostaglandin D_2	PGD_2
Prostaglandin J_2	PGJ_2
Prostate Cancer	CaP
Prostate Specific Antigen	PSA
Prostatic Intraepithelial Neoplasia	PIN
Retinoblastoma	Rb
Retinoic Acid Receptor	RAR
Retinoid X Receptor	RXR
Ribonucleic acid	RNA
Silencing Mediator of retinoic acid and thyroid hormone receptor	NCOR2/SMRT
Simian Virus 40	SV40
Sirtuin	SIRT
Sodium Butyrate	NaB
Steroid Receptor Coactivator	SRC
Suberoylanilide hydroxamic acid	SAHA
Tosyl-phenylalanyl chloromethyl ketone	TPCK
Transcription Start Site	TSS
Thyroid Hormone Receptor	TR
Transgenic Adenocarcinoma of the Mouse Prostate	TRAMP
Trichostatin A	TSA

Vitamin D Receptor	VDR
Vitamin D Response Element	VDRE

TABLE OF CONTENTS

LIST OF FIGURES

LIST OF TABLES

Chapter 1: General Introduction

1.1 The Prostate

1.1.1 Prostate Malignancy

The prostate forms part of the male reproductive system, and is situated beneath the bladder. Post-embryonic growth occurs principally during puberty and the organ develops to encapsulate the urethra. Activity of the prostate tissue is regulated through androgens such as testosterone, which also control its rate of proliferation. The prostate's primary function is to regulate the semen, ensuring a suitable environment in which the sperm can survive.

The first stage of prostate cancer (CaP) tumourigenesis is thought to be prostatic intraepithelial neoplasia (PIN) in luminal cells (Figure 1.1), occurring in either a low or high grade manner. Reviewed in Abate-Shen & Shen [1], high grade PIN has been shown to be a precursor of CaP with cells losing expression of important differentiation markers such as E-cadherin. Furthermore, development from PIN leads to loss of the basal lamina contributing to an invasive carcinoma that can escape the confines of the prostate capsule. However, a recent study has demonstrated that basal cells are also able to stimulate growth of benign prostate tissue [2]. This finding suggests that immunohistochemical studies of prostate cancers can be misleading, thus emphasizing the importance that molecular studies are conducted in parallel when investigating cell origins.

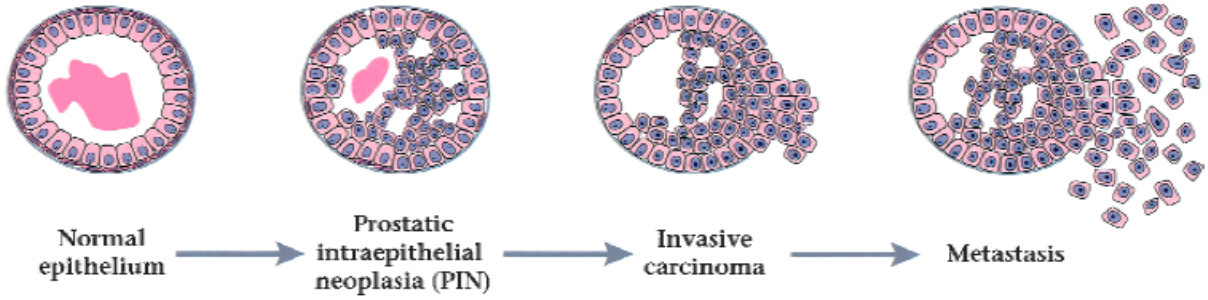

Figure 1.1 Progression of human prostate cancer (CaP). The multistage process of cancer begins with an abnormal proliferation of luminal cells disrupting the regular structure of the epithelium. This develops and obtains invasive qualities that lead to further malignant characteristics like metastasis and angiogeneisis. Adapted from Abate-Shen and Shen [1].

1.1.2 Epidemiology of prostate cancer

CaP is one of the most common forms of malignancy in men in the Western world. Currently, there are approximately 200,000 new cases and it is responsible for the deaths of 30,000 men in the USA every year [3]. The United Kingdom has a similarly proportional rate with CaP being the second most common cause of cancer death in males [4]. Therefore, substantial resources are aimed at treating this hormonally initiated disease. Contributing factors are numerous, with ethnicity, diet, lifestyle and genetic background all having high influence in development of the disease [5]. There are also significant geographical differences observed in the level of CaP incidence. For example South East Asia has a far lower incidence, but when individuals migrate to Western Europe and the USA their incidence increases [6]. Therefore, it is probable that there is interplay of all of these different factors that interact with contributing genetic components.

The evidence that dietary interactions can provide a protective relationship against CaP (such as various fruit and vegetable consumption) is compelling and detailed by Mills et al 1989 [7]. In this cohort study of 14,000 Seventh-day Adventist men (this

group have a history of low CaP occurrence and live on a strict vegetarian diet) it was found that in particular vegetables and dried fruit were cancer protective. However, the impact of such dietary factors will depend also upon the individual's hormone and metabolic enzyme levels, and their intake of compounds such as the heterocyclic amines. As the majority of people in the Western hemisphere have an omnivorous diet the actions of heterocyclic amines cannot be ignored. These have a strong association with both genotoxic and non-genotoxic effects [8]. Accordingly, levels of CaP show correlation with geographical areas where red meats are a major component of the diet [9]. Conversely, countries such as Japan with a high intake of fish and lower intake of red meat have a lower incidence rate of CaP [9]. However this finding may be more reflective of the anti-tumour effects of either ω−3 fatty acids or vitamin D that are present at high levels in fish [10, 11].

The prostate is highly responsive to hormonal signals and CaP development is hormonally driven. Physiological androgens such as testosterone increase the growth rate of cells, and the prostate is highly efficient at converting hormonal precursors into active testosterone and dihydrotestosterone by 5-α reductase type II. These are then able to bind to the androgen receptor (AR) and activate a battery of pro-growth target genes associated with an increased rate of cell division. Concordant with this, androgen ablation results in 80% of patients showing partial or complete response [12]. However, remission only lasts approximately 12 to 18 months before tumours then become Androgen Deprivation Therapy-Recurrent (ADT-R) [13].

Therefore, despite the impressive initial response rate to androgen deprivation and sustained prostate specific antigen (PSA) monitoring there is need for improvement. This is particularly vital when considering the success of long term treatment as the 10 year survival rate of prostate cancer is currently 60% in England [14].

The full extent and interaction between each of these factors remains largely unknown and so are subject to constant research efforts. For example, emerging large-scale prospective epidemiological studies such as the EPIC (European Prospective Investigation into Cancer) in the EU [15] will evaluate which of these interactions are important. Going forward it is likely that these findings will be integrated with Genome Wide Association studies (GWAs) [16] to illuminate true cancer risk factors.

1.1.3 Vitamin D in Prostate Cancer

The inverse proportionality between skin cancer and prostate cancer was revealed with the collection, unification and comparison of worldwide cancer statistics in the 1970s. Only then was it discovered that the incidence of CaP in Caucasian populations throughout Europe and the United States increased with geographical latitude [17, 18]. In addition, it was also found that development of skin cancer was associated with a significantly decreased likelihood of CaP occurrence [19, 20]. The evidence therefore suggested that exposure to UV sunlight produced a protective response, delaying the transformation of cells in the prostate. Therefore, it was hypothesised that a UV mediated effect influenced growth decisions made by the prostate, slowing or preventing prostate cancer initiation or progression.

The biologically active isoform of vitamin D ($1\alpha,25(OH)_2D_3$) is formed in the presence of UV sunlight and therefore it became heavily correlated with cancer protective processes [21]. This original finding was linked with colon cancer but statistics for CaP showed a similar level of significance, and therefore $1\alpha,25(OH)_2D_3$ activity was for the first time linked to prostate anti-cancer response. This was further supported with the identification that an increase of 25nmol/lit in plasma $25,(OH)D_3$ levels resulted in a 29% reduction in colon cancer related deaths and a 17% decrease in the number of cases [22].

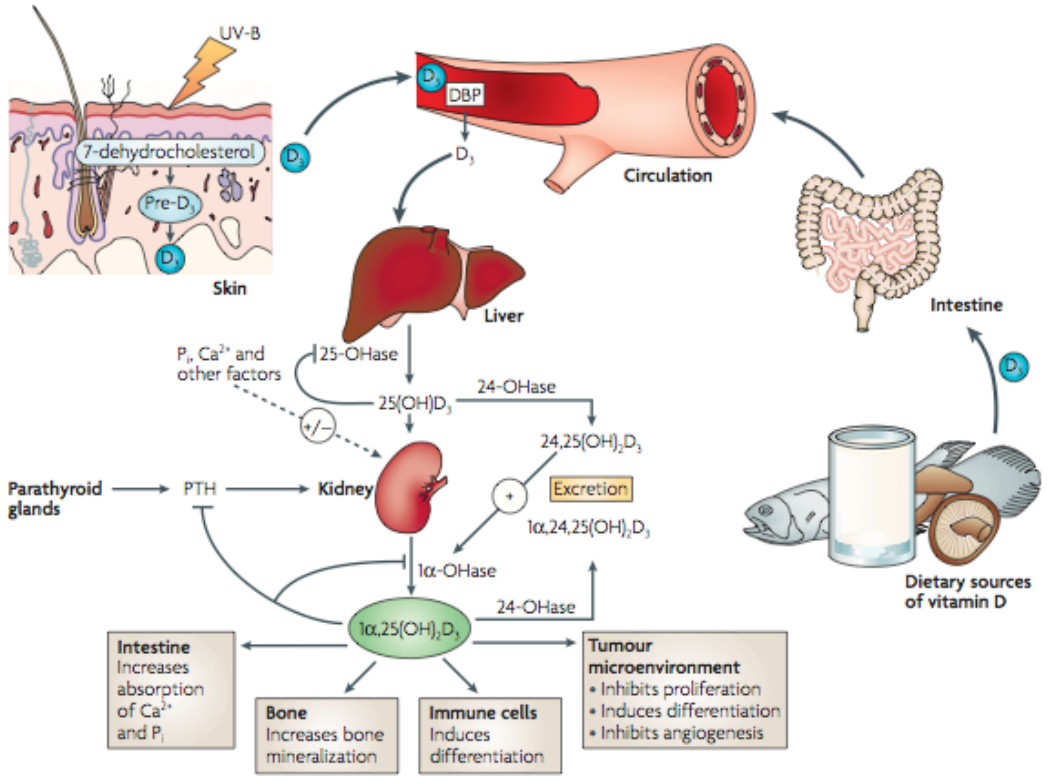

Figure 1.2 Formation of vitamin D. 7-dehydrocholesterol is converted to pre-vitamin D3 in response to sunlight. Vitamin D3 binds to vitamin D-binding protein (DBP) in the bloodstream, and is transported to the liver. This is then hyroxylated by 25-hydroxylase producing 25-hydroxycholecalciferol. Upon reaching the kidney $25(OH)D_3$ is 1α-hydroxylated $1\alpha,25(OH)_2D_3$. The rate of synthesis is positively regulated by parathyroid hormone levels and negativley regulated by Ca^{2+}, P_i and $1\alpha,25(OH)_2D_3$. The main effects of vitamin D upon the main target tissues are depicted. Adapted from Deeb et al [23].

The human body is unable to synthesize the precursor form of vitamin D ($25(OH)_2D_3$) and relies on the dietary intake of vitamin D, obtained from foods such as dairy products and fish (Figure 1.2). These are high in 7-dehydrocholesterol, the pro-vitamin whose conversion to $25(OH)_2D_3$ (pre-vitamin D_3) occurs in epidermal cells upon exposure to UV B radiation. This provides enough energy to cleave the 9-10 bond in the B ring of the circulating 7-dehydrocholesterol to produce $25(OH)_2D_3$ which is then isomerized to yield the physiologically active $1\alpha,25(OH)_2D_3$ [24].

Conversion and metabolism of the various forms of vitamin D occurs through the action of the cytochrome P450 superfamily of haem-containing mono-oxygenases. *CYP24A1* encodes the main metabolic enzyme responsible for the hydroxylation of $1\alpha,25(OH)_2D_3$ to a biologically less active molecule [25]. Over the past 30 years research has investigated the risks of $1\alpha,25(OH)_2D_3$ deficiency and its relationship with disease including malignancy of the prostate [26, 27].

1.2 Cell and animal models of the prostate

1.2.1 Non-malignant prostate cell lines

To understand the processes in the development of CaP, cell line models are used to represent specific stages of tumourigenesis. Human cells are a highly desirable model with which to study cancer as extrapolation towards *in vivo* conditions is more comparable. All human cancer cell lines used for *in vitro* work have become immortalized during disease progression. However, models of normal epithelial cells are not transformed and therefore require transfection with viral genetic components able to

overcome normal senescence. This gives a robust and maintainable source of cells that retain the properties of non-malignant cells.

The RWPE-1 cell line was selected for this study as a model of the normal non-malignant prostate epithelium. These cells originated from the prostate of a Caucasian male without CaP undergoing cystoprostatectomy. Immortalisation of the extracted cells was conducted by introduction of a psHPV-18 m plasmid containing the complete HPV-18 gene. Transfection with this gene has been demonstrated in other cell lines and leads to retention of characteristics of growth and differentiation control [28, 29]. RWPE-1 cells have been shown to have an epithelial morphology with functional PSA and AR status, and stain positively for p53 [30]. Specifically, these cells are androgen responsive and cultured in the presence of the epidermal growth factor (EGF). The RWPE-1 cells are thought to be a luminal-basal intermediate of the prostate that are partially differentiated. They express prostatic cytokeratins 8 and 18 and are not invasive so unable to form tumours when injected in nude mice. These data further supports their use as a suitable and reproducible model of non-malignant prostate epithelial cells.

1.2.2 Prostate cancer cell lines

The use of isogenic cell lines within comparative studies is often a way of controlling biological and experimental variation. Analysis of cell lines with the same genetic background may reduce inherent differences between cells derived from different individuals. To address this, transformed isogenic cell lines of RWPE-1, called RWPE-2 were also used in the current study. RWPE-2 cells contain the same HPV 18 adenovirus transfection as the RWPE-1 cells. Additionally they have v-Ki-RAS introduced, which activates production of the v-Ki-RAS oncogene, that found to be mutated in 25% of

human CaP [31]. As a result RWPE-2 cells are able to manifest tumour growth when injected in nude mice and show a moderate invasive profile *in vitro* [30]. Therefore, the RWPE-2 cell lines represent human CaP at an early stage of transformation.

More aggressive CaP cell lines such as PC-3, DU 145 and LNCaP were derived from different primary tumours [32]. PC-3 cells were derived from a prostatic lumbar vertebra metastasis [33], and are classed as poorly differentiated prostate adenocarcinoma. Upon analysis they were found to express elevated levels of the proliferative protein EGF-R [34]. PC-3 cells represent advanced grade CaP that is ADT-R, a classification which makes them similar to DU 145 cells. These cells were derived from a metastatic tumour in the central nervous system of a 69-year-old Caucasian male [35]. LNCaP cells were derived from the lymph node metastasis of a 50-year-old Caucasian male. They are moderately differentiated and represent metastasis with a lower proliferative rate than that of PC-3 or DU 145 cells. As with PC-3 and DU 145 cells they are able to form tumours when injected into nude mice, but LNCaP cells retain some degree of androgen responsiveness [36]. Also similar to the RWPE-1 cells, LNCaP cells have an isogenic variant that is used to assess the acquisition of ADT-R phenotype. The LNCaP C4-2 cells were produced by co-injection of LNCaP and human bone osteosarcoma cell line MS into castrated nude mice. This produced development of the ADT-R sub-line of cells capable of forming tumours [37]. Characterisation of the tumours confirmed they were able to induce angiogenesis and vascularisation. Together, these cell lines provide key investigational models for spectrum of cancer states.

1.2.3 TRAMP mouse as a prostate cancer model

This work utilizes the **TR**ansgeneic **A**denocarcinoma of the **M**ouse **P**rostate (TRAMP) murine model. The TRAMP mouse was produced with a prostate epithelium specific transgene SV40 (linked with the probasin promoter) [38]. This gene is induced in the adolescent animal under the control of the AR receptor producing a progressive form of prostate neoplasia recapitulating human disease. TRAMP mice exhibit mild hyperplasia by 10 weeks and invasive adenocarcinoma at approximately 18 weeks. As the development of the tumour is dependent upon physiological androgens, castration of the mice at 12 weeks of age is partially curative with a success rate of 20% (the remaining 80% develop an ADT-R CaP). Among the advantages of the TRAMP model, there is 100% incidence of CaP and the histologic analysis of progression from PIN to invasive carcinoma is reflective of the human form of disease. Shown in Figure 1.3 is a time line illustration of the TRAMP model stages of progression.

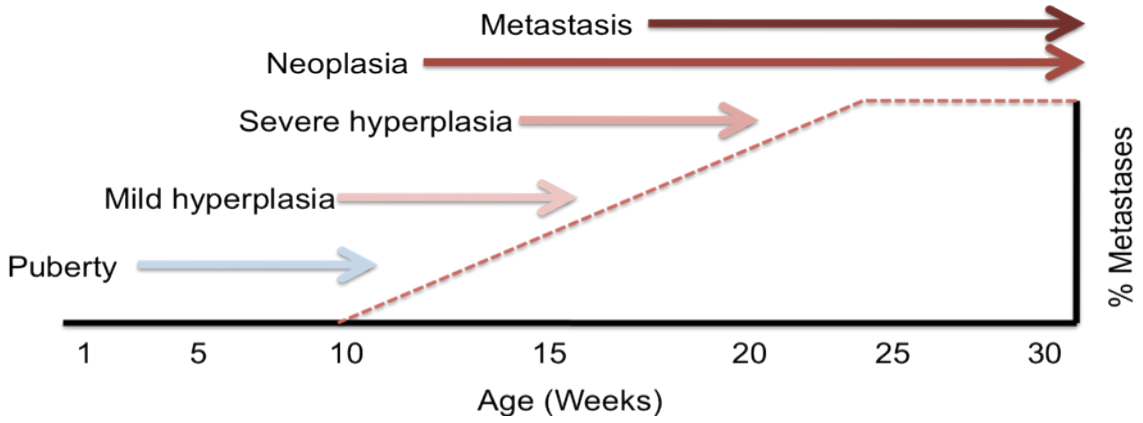

Figure 1.3 Illustration of the TRAMP murine model development. The probasin gene begins expression between 4 and 6 weeks of age, leading to hyperplasia by 12 weeks and poorly differentiated adenocarcinoma by 24 weeks. All TRAMP mice develop CaP.

1.3 Nuclear Receptor (NR) functions

1.3.1 Nuclear receptor structure and function

There are 48 different types of nuclear receptors making them the largest family of transcription factors in humans [39]. NR superfamily members include the steroid hormone receptors (thyroid hormone receptor (TR), oestrogen receptor (ER) and glucocorticoid receptor (GR)) and the non-steroidal binding NRs such as the retinoic acid receptor (RAR) and the vitamin D receptor (VDR). As with other transcription factors, NRs have various functional domains encoded into their genomic sequences. Each of these regions is responsible for encoding a motif that exerts a specified molecular action, such as precise DNA binding, ligand binding recognition and cofactor interactions (Figure 1.4).

NRs bind to DNA as homodimers or heterodimers, with other members of the nuclear receptor family (for example VDR and RARs bind with RXR (Retinoid X Receptor to form a heterodimer [40])). Therefore, NR target gene specificity arises in part from the ability to recognise specific nucleotide sequences within promoter and enhancer regions. Using their ability to select these sites of binding, each NR activates and represses cohorts of genes. This allows regulation of essential biological responses including reactions to intrinsic hormonal signals (such as oestrogen and testosterone) and extrinsic stimuli such as dietary derived vitamin D, retinoic acid and xenobiotics. Thus, NRs have combined roles of both receptors, in their ability to detect and respond to ligand, and transcription factors in their gene regulatory effects.

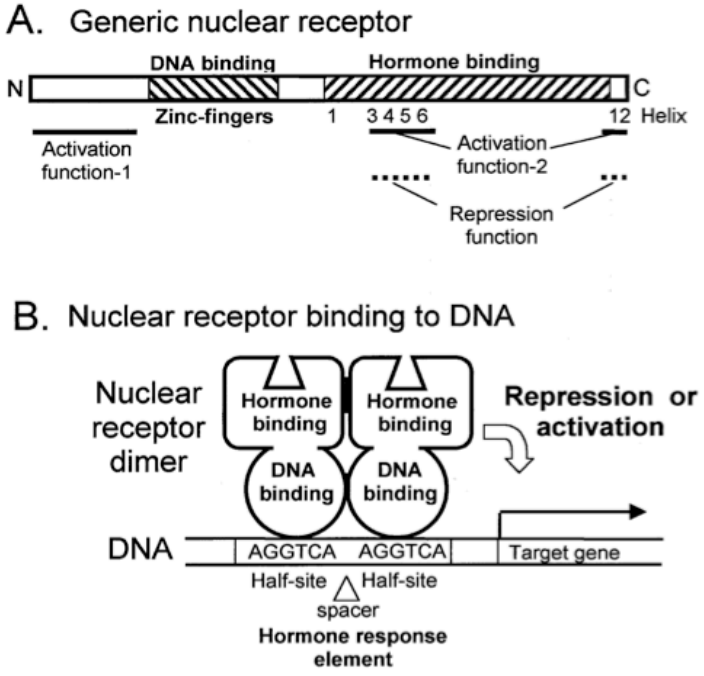

Figure 1.4 Basic NR structure and DNA binding. A) All NRs contain a ligand/hormone binding domain (LBD) and a DNA binding domain (DBD). The LBD contains helical motifs that undergo conformational change in the presence of ligand. The DBD contains two zinc finger motifs whose sequence varies dependent upon the NR. This helps to dictate binding sequence specificty. B) NRs bind to the DNA as a dimer. This example shows a response element containing two AGGTCA in a direct repeat separated by a spacer sequence. Taken from Privalsky [41].

However, the response of each NR is integrated within multiple networks of signalling pathways. Thus, important cellular processes including the cell cycle and inflammation are governed through networks that integrate signals to mediate NR activity. Therefore, the crosstalk with other pathways produces a highly intricate level of control over their transcriptional targets. Examples are shown in Figure 1.5 whereby multiple growth factors using transition of phosphoryl groups as a means of transmitting signals and can phosphorylate the ligand binding domain (LBD) of retinoic acid receptor (RAR) [42]. This alters the activation potential of the NR increasing its likelihood of association with the core co-integrator CBP/P300 and subsequently the transcriptional machinery complexes leading to gene activation. Additional to these signals ubiquitin

protein groups can be added to the NRs and their bound components. These are recycling flags that mark proteins for degradation by large proteosomal complexes. Thus, marking the various cofactors of NR mediated transcription with ubiquitin groups leads to their removal and subsequent breakdown.

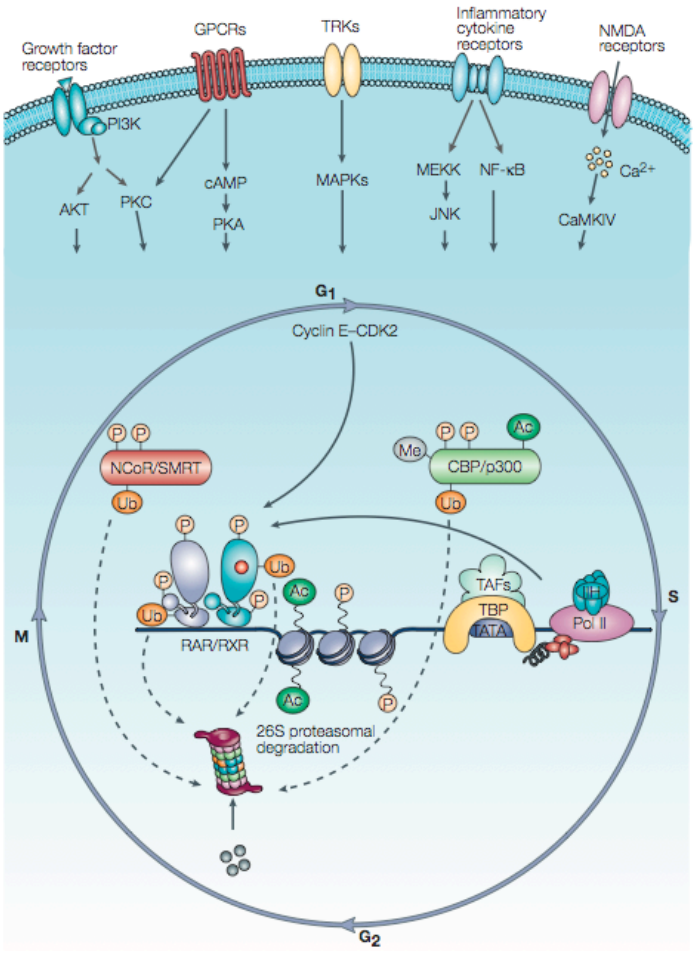

Figure 1.5 Signalling pathways provide a network of feedback influencing NR mediated transcription of target genes. Fluctuation in the NRs transcriptional output is produced by numerous signal transduction pathways, G-Protein coupled receptors (GPCRs), and growth factors. These signals occur in a cell cycle dependent nature to temporaly influence the proliferative rate. The Retinoic acid receptor (RAR) Retinoid X receptor (RXR) heterodimer is shown here as an example of NR functioning. Coregulator proteins such as NCOR1, NCOR2/SMRT and the CBP/P300 complexes are shown. These bind to the NR mediating recruitment of activation or repressive complexes. Addition of phosphorylation marks to proteins that are involved in NR target gene transcription alters their activity. Placement of ubiquitin marks upon proteins flags them for removal and breakdown by the proteosome. Taken from [43].

Therefore, the NRs utilise a wide number of cellular inputs to carry out their sigalling potency. Furthermore, there are additional protein complexes within the nucleus that modify their functioning. These provide an important element of flexibility into their response allowing increasingly complex transcriptional outputs.

Essential to their regulatory activity, the NRs rely upon the presence of supporting proteins collectively named coregulators. These coregulators mediate the transcriptional activation or repression of target genes produced in the presence of NR ligand. This leads to the central dogma behind NR gene regulation; ligand binding induces conformational change lowering NR affinity for corepressors (CoRs). This has the effect of promoting NR binding of coactivators (CoAs). Release of the CoR from the DNA bound NR induces the recruitment of a number of different CoAs.

Many CoA proteins exist in large multi-protein complexes with distinct activity. For example; histone tail modifying enzymes that modify the surrounding chromatin, placing post-translational modifications (PTMs) such as methylation and acetylation marks on histone amino acid residues. ATP dependent chromatin remodeling machinery: as the name indicates these require ATP for their activity and are responsible for the dismantling and repositioning of the nucleosome subunits. Mediator complex, this acts as a bridge attached to the activator complexes and recruiting the transcriptional machinery to the gene. Additionally, there are numerous other proteins found in the CoA complexes with roles that are as yet undefined. However, it is suggested these may be concerned with the placement, reading, and removal of PTMs to the histone tails.

CoRs act in opposition to CoA and repress transcription genes. The two major CoRs that bind to NRs were identified as the silencing mediator of retinoic acid and

thyroid hormone receptor (NCOR2/SMRT) and nuclear corepressor (NCOR1) proteins [44]. These are very similar in structure and contain an N-terminal section with various repression domains and a C-terminus that allows NR interaction of the CoRs (Figure 1.6). Individual knockout murine models of NCOR1 [45] and NCOR2/SMRT [46] show embryonic lethality at different timepoints. This suggests they have distinct and essential roles in development that cannot be replaced. Therefore, although the two corepressors are shown to have some functional redundancy they also have some highly specific roles. In accordance with this certain NRs exert a preference for either NCOR1 or NCOR2/SMRT.

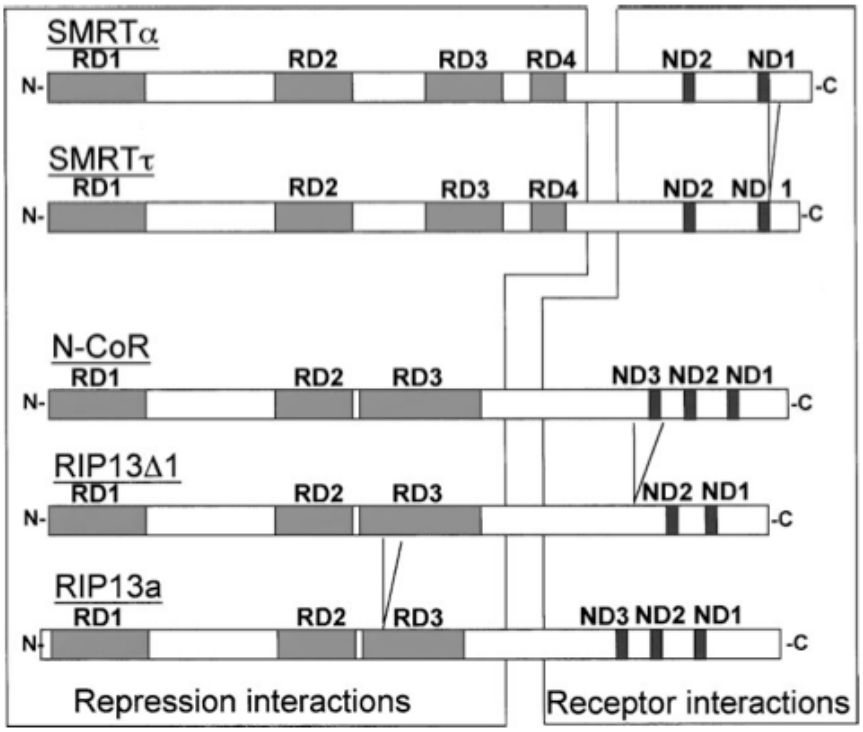

Figure 1.6 The two main corepressors of NR activity (NCOR2/SMRT and NCOR1). The splice variants of the two CoRs are shown containing truncationed isoforms. These CoRs contain repressive and receptor interacting regions. The C-terminal domain binds to NR and the N-terminal contains various repression domains responsible for recruiting chromatin remodelling machinery. Thus the CoRs act as a platform, attaching to NRs and mediating epigenetic modifcations in the local chromatin environment. Taken from Privalsky [41].

For example RARs bind with NCOR2/SMRT in preference to NCOR1, and TR recruits NCOR1 in preference to NCOR2/SMRT [47, 48] (a dependency that may relate to the lethality of murine knockouts as RARs are indispensable for embryonic development). The repression domains contained in the CoRs enforce suppression of a genes activity. This is produced by histone modifying enzymes bound to the CoRs such as the histone deacetylase 3 (HDAC3) [49]. NCOR1, NCOR2/SMRT have been demonstrated to bind allosterically to HDAC3 and few if any, other HDAC members [50]. This suggests the HDAC3 enzyme is integral for the biological effect of NCOR1 and NCOR2/SMRT upon NR mediated transcription. The relationship that CoAs and CoRs have with NRs makes them key regulators of biological pathways.

1.3.2 Key NRs within the prostate

- **Androgen Receptor (AR)**

The AR is centrally linked with prostatic tumourigenesis, reviewed in [51]. Endogenous AR ligands are all cholesterol-derived steroids. It has been demonstrated that the biosynthesis pathways responsible for steroidogenesis are upregulated in CaP tissues [52]. It is the availability of androgens that drive the activity of the AR target genes. These in turn act to stimulate the proliferative pathways such as AKT and cMYC [53]. Therefore, the main therapeutic intervention has been to block the ARs activity by minimising the concentration of ligand to interact with or blocking the receptors from binding DNA. Late stage CaP cells are able to alter their requirements for proliferation, becoming self sufficient in growth signals. This results in the AR becoming constitutively active in the absence of ligand [54].

- **Peroxisome Proliferator Activated Receptor-γ (PPARγ)**

PPARγ has been associated with many anti-tumourigenic actions [55-57]. In particular it has been demonstrated to have pro-differentiating [58] and anti-proliferative [59] responses in murine and human prostate cancer cell lines. In conflict with this, the anti-cancer potential of PPARγ is confounded by publications detailing pro-tumourgenic properties of activation and overexpression in some cancers [60, 61]. However, strong evidence remains for therapy using PPARγ targeting, such as xenograft models of colon cancer in rodents decreasing in cancer development to troglitazone treatment [62]. The agonist Troglitazone is able to reduce the occurrence of colitus [63], an inflammatory condition associated with colon cancer in many mammals including humans.

In parallel with these observations, many PPARγ target genes are linked with cell cycle arrest and inhibition of the E2F transcription factor [64]. PPARγ stimulation also decreases the phosphorylation status of retinoblastoma (Rb), limiting cell cycle progression. Additionally, PPARγ increases the expression of cyclin dependent kinase inhibitors like $p21^{(waf/cip)}$ [65], inducing a G1 growth arrest and suggesting NRs have important anti-tumourgenic actions.

- **Retinoic Acid Receptors (RARs)**

Retinoic acids are signaling molecules that are have been demonstrated to be essential for embryonic development and cellular differentiation (Reviewed in [66]).

Of the three isoforms of RAR (α, β and γ) RARβ has been shown in previous studies to inhibit the growth of prostate cancer when used in combination with $1\alpha,25(OH)_2D_3$ [67, 68]. Co-treatment of 9cRA with $1\alpha,25(OH)_2D_3$ induced cell cycle arrest in LNCaP cells through the altered expression of $p21^{(waf1/cip1)}$and $p27^{(kip1)}$ [69]. A

further study was also conducted in CaP using PC-3 cells. This revealed that combinatorial treatment of 9cRA and $1\alpha,25(OH)_2D_3$ is able to reduced the growth of cells in culture and when injected into nude mice [70]. Therefore, targeting of the retinoic acid receptors is emerging as an efficient anticancer strategy.

- **Vitamin D Receptor (VDR)**

The VDR was first cloned in humans in 1988 [71]. Located on chromosome 12, it is composed of 11 exons that encode the functional protein. The translated protein contains various elements permitting hormone binding and DNA binding activity (reviewed by [72]). The VDR recognises and binds to VDRE's within the genome. These are usually two hexonucleotides that are repeats and spaced by a varying number of base pairs. Occupation of the response element by the heterodimer requires VDR to attach to the 5' and RXR on the 3' end. Though it must be stated that the composition and binding ability of the response elements varies greatly.

Amongst many VDR targets is the *CDKN1A* gene, which encodes the $p21^{(waf1/cip1)}$ protein. $p21^{(waf1/cip1)}$ is a member of the Cip family of proteins and plays a key regulatory role in the control of the cell cycle by activating the G1 phase block. The role of $p21^{(waf1/cip1)}$ as a potent tumour suppressor gene is not only linked to the p53 protein. The effects of $p21^{(waf1/cip1)}$ have been demonstrated to activate numerous anti-proliferative and pro-differentiation pathways independently of p53 [73-76].

$p21^{(waf1/cip1)}$ exerts its action via the binding and inhibition of the cyclin dependent kinases CDKs (Figure 1.7), and blocks the cell cycle progression. In addition, $p21^{(waf1/cip1)}$ inhibits the PCNA dependent DNA polymerase responsible for DNA replication required during S-phase. Inactivation of the CDKs by $p21^{(waf1/cip1)}$ occurs by prevention of its

phosphorylation activity. A motif contained within the protein permits the binding of CDK subunits, deregulating the interaction between CDK and its substrate CDK-cyclin.

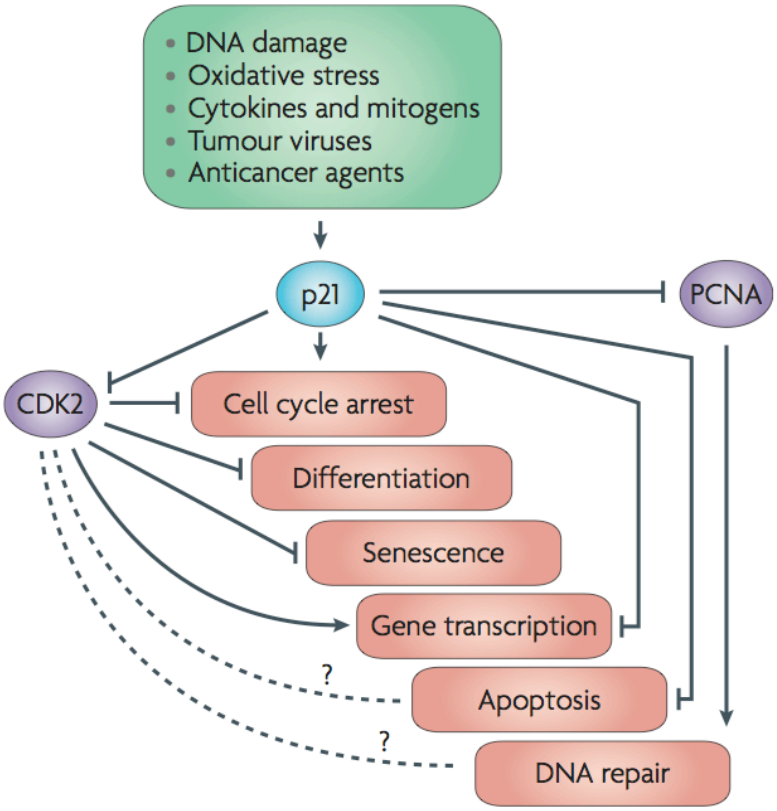

Figure 1.7 The role of p21$^{(waf1/cip1)}$ in cell growth regulation. Specific stimuli (DNA damage, oxidative stress etc...) are able to induce the activation of *CDKN1A* gene transcription and translation into protein. The primary role is in the inhibition of the cyclin dependent kinases (CDKs) and inhibiton of the proliferating cell nuclear antigen (PCNA). Some of the anti-proliferative actions of p21 are mediated through its protein-protein interactions and its effect on transcriptional activity are generally inhibitory. Both of these factors are required to be active for the cell to commence S Phase replication. Thus by their inhibiton CDKN1A exibits a G1 Phase arrest upon activation. Taken from Abbas and Dutta [77].

This mechanism generates considerable potential for p21$^{(waf1/cip1)}$ to inhibit tumour growth and inflict significant anti-proliferative, apoptotic damage. However, in addition to these effects there are also emerging data suggesting p21$^{(waf1/cip1)}$ holds anti-apoptotic actions. For instance, p21$^{(waf1/cip1)}$ has been shown to inhibit the CDKs in response to

ionising radiation, resulting in a reduced level of apoptosis in cell populations [78]. In addition there are several additional pathways that support the anti-apoptotic response of $p21^{(waf1/cip1)}$. These include the binding of $p21^{(waf1/cip1)}$ to the apoptotic proteins pro-caspase 3 [79], caspase 8 and 10 [80] inhibiting their activity. Therefore, whilst the consequences of $p21^{(waf1/cip1)}$ activation are largely anti-tumourigenic, there are pro-survival pathways that require $p21^{(waf1/cip1)}$ for their activity.

1.4 Disruption of NR signalling

1.4.1 Altered CoR activity restricts transcription

In accordance with these findings new technology has enhanced our understanding of NR actions. Genome wide ChIP-ChiP and ChIP-Seq assays have shown there to be a variety of NR responses [81, 82]. The distortion of the ARs transcriptome has been shown to occur in prostate malignancy with an enhanced transcription of proliferative target genes and downregulation of anti-proliferative genes [83]. An example of which is the TMPRSS2/ETS fusion gene becoming constitutively active by distorted AR signalling in CaP [84]. The restoration of homeostatic NR activity has become an important therapeutic target. Therefore, restoration of appropriate NR signalling within malignancy may produce growth restrictive outcomes slowing or halting disease progression.

Current research suggests the abilities of NRs become ‘selectively filtered’ in malignancy. Transcriptional programs are skewed toward pro-growth target genes and downregulation of growth inhibition genes.

Furthermore, CoRs have been heavily implicated in many human cancers such as leukaemias (reviewed in [85]). Mechanistic examples of CoR dysfunction in disease include genetic translocations producing a fusion protein that results in aberrant NCOR1 and NCOR2/SMRT binding.

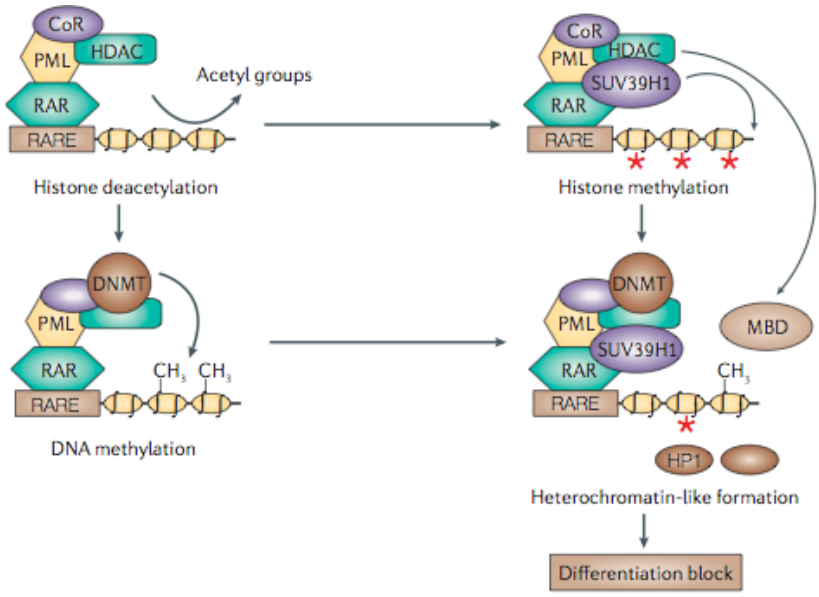

Figure 1.8 CoR deregulation through PML/RAR fusion protein in APL. In acute promyelocytic leukaemia (APL) the PML/RaR fusion protein binds to CoRs which in turn recruit HDACs. The PML/RAR then recruits chromatin modifiers such as the DNA methyltransferases DNMT1 and DNMT3. The resulting modified chromatin then acts as a binding site for acessory componants that are able to bind methylated DNA including MBD1. In addition the methylated histones are bound by the heterochromatin associated protein 1 (AP1) 'compacting' the histones conformation. Consequently, pro-differentiation genes are deactivated ehancing proliferation of the leukaemia. Taken from Pelicci et al [86].

A common illustration is the PML/RARα fusion protein. Acute promyeloid leukaemia (APL) is a subtype of acute myelogenous leukaemia (AML). It develops when the RARα gene found on chromosome 17 becomes reciprocally translocated to the promyelocytic gene (PML) located on chromosome 15 resulting in a fusion gene and protein [87]. This fusion is remarkably consistent in the manifestation of disease with 97% of APL patients [88]. The oncogeneic actions of the PML/RARα

fusion protein have been widely studied and its mode of action is in part due to PMLs dimerisation domain. This is potent and induces the formation of very stable heterodimers. Heterodimers of PML/RARα are able to recruit and maintain the stablisation of CoR complexes (Figure 1.8). This has the effect of silencing the anti-proliferative and pro-differentiation target genes of RARα [89]. However, APL can now be effectively treated by combining chemotherapy with All Trans-Retanoic Acid (ATRA) treatment and is a success story of modern medicine. Therapeutic doses of ATRA are able to bind the PML/RARα fusion proteins ligand-binding domain. This induces the release of corepressor complexes that have been inappropriately recruited and stabilized. This beneficial effect is improved further with additional HDAC inhibitor treatment.

1.4.2 Epigenetic regulation and deregulation of NR transcription.

In addition to these actions the DNA itself can be methylated. DNA methylation occurs on cytosine bases of CpG dinucleotides. Placement of methyl groups is conducted by one of three DNA methyltransferases (DNMTs) that are essential for embryonic development (reviewed by [90]). Methylation of the DNA remains one of the major mechanisms the cell uses to induce inheritable transcriptional silencing of genes. The best-known example of which is X-chromosome inactivation, used to give long term silencing of one copy of the X- chromosome in females.

The ability of chromatin to modulate changes in gene transcription is also mediated through DNA methylation of local CpG islands. Previous studies have shown that unmethylated DNA is wrapped around nucleosomes that were found to have largely acetylated histone tails [91, 92]. In conjunction with these findings, methylation levels of

DNA correlate with nucleosomes containing non-acetylated histone tails and more compact chromatin conformation [93]. The consequences of DNA methylation have also been observed upon specific histone modifications as well as general overall changes. For example methylation of DNA has been shown to produce H3K9 methylation, responsible for gene silencing and inhibition of H3K4 methylation [94]. Genes silenced by DNA-methylation can also be re-expressed with the application of de-methylating compounds such as 5-azacytidine and 5-aza-2'-deoxycytodine. These have been shown to have clinically relevant effects at low doses and they are now being used as treatments for leukaemia [95].

The histone code hypothesis suggests that gene regulatory process extend to the post-translational modifications (PTMs) placed upon the histone amino acid subunits. It is thought these influence transcription of genes recruiting downstream 'reader' and 'effector' proteins [96]. One of the most commonly investigated PTMs thought to regulate transcription is the histone 3 lysine 4 (H3K4) methylation mark. This residue is able to be mono, di or tri methylated [97]. Furthermore, the presence of these modifications in the promoter of a gene impacts upon likelihood of the genes expression. As mentioned H3K4me3 is strongly linked with actively transcribed genes. In addition it is enriched at the Transcription Start Site (TSS) of active genes in comparison to surrounding regions. Methylation of specific histone amino acid subunits has been also observed to occur in correlation with the methylation of DNA. Addition of tri-methylation marks to histone 3 lysine 4 (H3K4) is associated with active genes and has been shown to be present at CpG poor promoters only when the gene is transcribed [98]. However, areas high with CpG's are constitutively methylated at H3K4 regardless of the

transcriptional activity of the gene [99]. This demonstrates that the features contained within the DNA are able to establish an epigenetic state. This then directly influences the accessibility of transcription factors and machinery to the DNA. Furthermore, in the absence (or low levels) of CpG sequences the cells use histone modifications to influence gene activity.

DNA methylation is central to epigenetic control of gene expression in cancer and CpG methylation has been used as a marker of both disease predisposition [100] and progression [101].

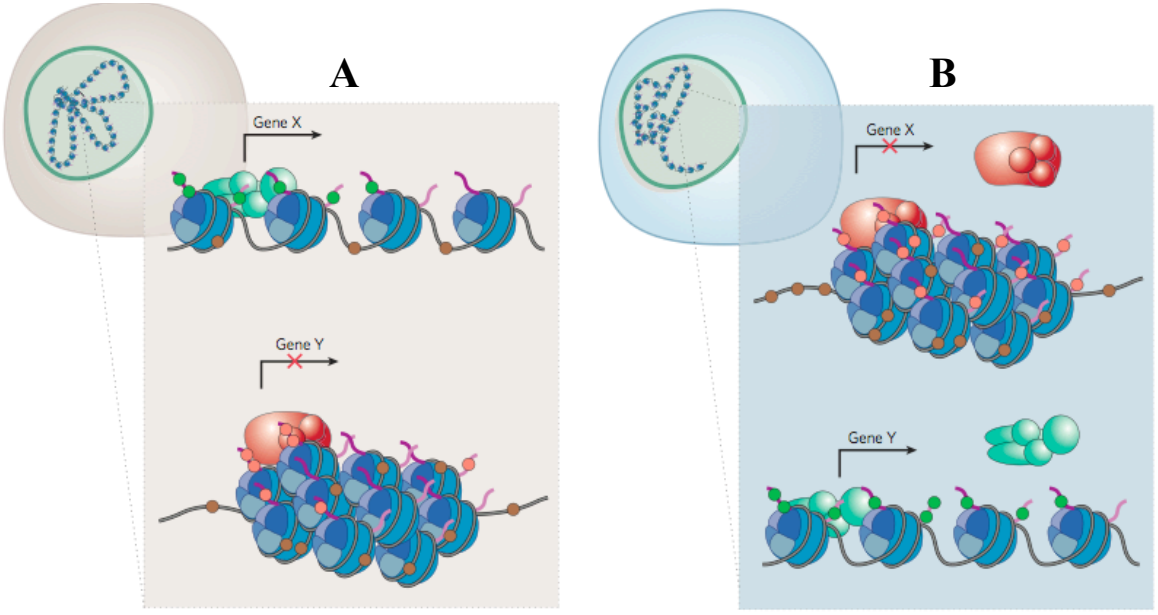

Figure 1.9 Epigenetic corruption of gene expression. A) Gene X has low levels of DNA methylation (brown circles) and is transcriptionally active. It has an open chromatin conformation, accordingly, many transcriptional complexes are bound (green circles). H3K9 acetylation and H3K4 methylation marks are also present. Gene Y is inactive, and contains high CpG methylation and inactivating marks such as H3K27me3 (pink circles) and repressive protein complexes (red circles). B) Transformed cells alter gene expression through silencing normally active genes and activating normally silent genes. Using the aberrant placement of histone modifications and changes recruitment of protein complexes (activating or repressing) epigenetic corruption of the transcriptome can be achieved. Adapted from Feinberg [94].

There are very few studies examining direct effects of DNA methylation upon NR signalling and the present evidence suggests DNA methylation status maybe able to influence local NR activity. However, the LXR nuclear receptor has been demonstrated to have areas of hypermethylation across its promoter in murine models [102]. Also the gene encoding the ER-a nuclear receptor (ESR1) shows a strong correlation of promoter methylation and prostate cancer progression. In particular, this study found that the higher the gleason grade of prostate cancer the higher the extent of ESR-1 promoter DNA methylation [103].

Epigenetic maintenance of gene repression is also mediated through the H3K27me3 mark [104]. This is also known as the polycomb repression mark placed by polycomb repressive complex 2 (PRC2). However, the presence of both H3K4me3 and H3K27me3 at a promoter leads to an activating and a repressive mark being in place at the same time. This is known as 'bivalency' and its purpose is not clear but may play some role in regulating genes important for differentiation [105]. Although it may also serve as an additional mechanism by which the cell uses to reduce transcriptional noise of genes.

Specific amino acids can also be subject to different changes, for example H3K9me2 holds a repressive influence where as H3K9ac is a mark associated with gene transcription. In support the activation effect of H3K9ac a genome wide study of human tissues often found both H3K9ac and H3K4me3 to occupy the promoters of most genes alongside RNA polymerase II [106]. This indicates that they are hallmarks of transcriptionally active genes.

In opposition to this the H3K27me3 mark is often found to be at silenced genes ([107]). Thus, the distribution of both activating and repressive marks can influence genes activity. Therefore, NRs ability to recruit and remove certain histone PTMs will provide alterations in target gene transcription. Furthermore, changes in PTMs have been found to be associated with different malignancies [108]. This leads to the conjecture of there being a strong epigenetic component to the pathology of cancer.

In order to exert their activity the H3K4me3 relies upon the binding of proteins with a particular domain known as the plant homeodomain fingers (PHD fingers). Proteins (such as P300, CBP and nucleosome remodeling factor (NURF)) with this domain are able to 'read' the chromatin and the H3K4me3 mark provides the 'ligand' for their 'activation'[109]. Such factors upon binding to H3K4me3 are able to recruit transcriptional machinery often found associated with RNA polymerase II. Thus the previous finding of elevated H3K4me3 at promoter regions of genes is thought to anchor protein complexes important for transcriptional activation processes.

This gives the H3K4me3 mark a high degree of importance, one that is emphasised with evidence of its deregulation being contributory to prostate tumourigenesis (reviewed in [110]). Furthermore, there are proteins with other chromatin binding properties that indicate a deregulation between the reading, placement and effects of the histone marks can impact upon CaP development. Alterations in histone marks produced by aberrant NR binding patterns may provide a causative mechanism for propagation of an aberrant transcriptome.

Such mechanisms are already being identified and again leukaemia provides a pertinent example. The MLL gene has been demonstrated to be a prominent H3K4

specific methyltransferase. Its activity is shown to induce gene transcription through the placement of this mark. However, in Acute Myelogenous Leukaemia MLL gene rearrangements are commonly reported [111]. One such study investigated the MLL-PTD duplication (MLL exon 4 to 11 or 4 to 12 duplication). Using a mouse knock-in model it was shown that MLL-PTD produces an elevation in the levels of H3K4me2 at HOXA genes. Furthermore, this was found to be in conjunction with histone acetylation at the same cluster. An elevation in the expression levels of these genes is shown to induce leukaemia indicating aberrant histone methylation influencing tumourigenesis [112].

Another example of a corruption in the placement of histone marks occurs with the H3K27me3 specific methyltransferase named enhancer of zeste homolog 2 (EZH2). This enzyme has often found to be upregulated in cancers including the prostate [113]. Concordantly, reduction in its levels attenuated the growth of prostate xenograft tumour models [114]. It has also been demonstrated the mutation of a single amino acid in the EZH2 protein nullifies its H3K27 trimethylation activity [115]. These findings emphasise the ease with which the placement of PTMs can be perturbed, leading to epigenetic corruption of a genes activity.

Alongside the errors in PTM placement, their inappropriate removal is also a mechanism by which transcription can be influenced. Aberrant histone demethylase (HDM) activity has particular pertinence at the H3K4 and H3K27 amino acids. A recent discovery, the presence of HDMs such as LSD1 has provided and extra pathway of regulation. LSD1 was demonstrated to be a stable element within HDAC containing CoRs [116]. Excessive removal of the methyl marks at H3K4 by elevation of LSD1 was shown to produce anti-tumourigeneic actions in breast cancer. Conversely, reduction in

LSD1 increased the invasiveness of malignant cells [117]. However, the anti-/pro-tumourigenic nature of this activity depends upon the gene at which it is located. For example LSD1 is able to remove methylation of H3K4 at the AR providing transcriptional activation of the AR target genes within CaP [118].

1.4.3 NR and CoR interactions in transcription.

Bound coregulator complexes also govern the activity of all NRs. These induce the changes in chromatin remodelling and previously described placement of histone PTMs to activate genes. In comparison to CoAs the CoRs activities and roles in gene expression are less well understood.

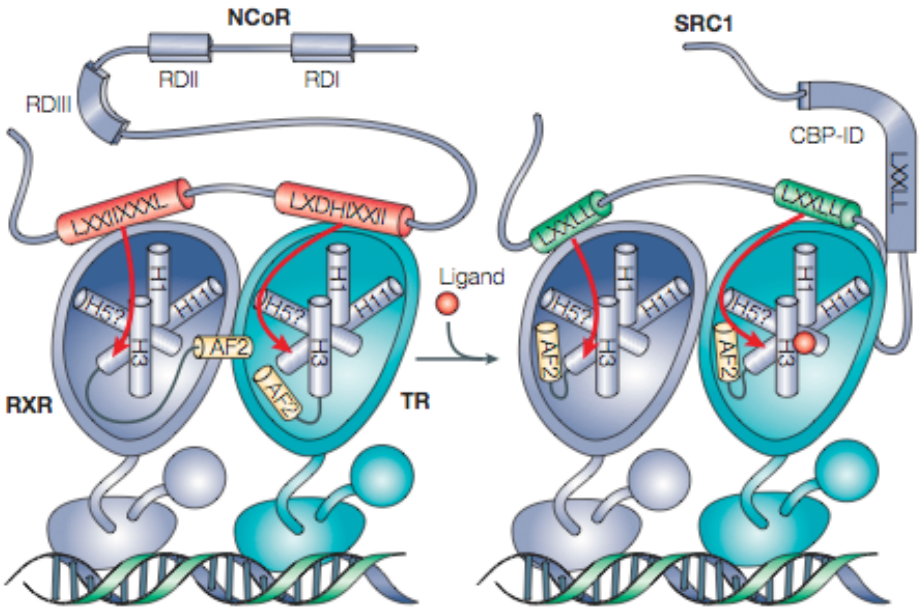

Figure 1.10 NR interacting motifs in CoR and CoA. In the absence of ligand the NRs (shown examples here are RXR and TR) are bound to the CoRs. These coregulators contain an extended CoRNR box motif (LxxH/IIxxxI/L) that occupies the hydrophobic pocket with the NR. Ligand binding induces confirmational shift of helix 12 re-shaping the hydrophobic pocket. This induces the rejection of CoR for association with the CoA (example here is the steroid receptor coactivator (SRC)) containing both a CBP interacting domain and the shorter LXXLL motif able to bind the hydrophobic pocket. Taken from Rosenfeld [43].

Initially formed upon the identification of interacting regions within their sequence is the conventional model of CoR release during transcriptional activation. Here an activating ligand binds to an already CoR bound receptor occupying a specific DNA sequence.

Ligand presence induces release of CoR and recruitment of CoA and in turn histone acetyltransferase (HAT) enzymes. The mechanism behind this is focussed upon structural differences between the CoAs and CoRs. A motif contained within the CoRs called the **Cor**epressor **n**uclear **r**eceptor (CoRNR) box, interacts with the hydrophobic groove of the NRs structure. Ligand binding to the NR displaces the bound CoR through conformational changes in the helix 12 positioning (found in the AF-2 region) (shown in Figure 1.10). As the CoRNR box is an elongated motif containing an LxxH/IIxxxI/L sequence it is too large to occupy the NRs newly configured hydrophobic pocket.

These changes allow selective binding of only CoA proteins, as they contain the LxxLL binding motif that is a shorter sequence compared to the CoRNR box. This alternation between coregulators in association with the NR allows recruitment of histone acetyltransferases (HATs). Thus producing activation of chromatin remodelling and histone PTMs that activate gene transcription.

However, more recent findings have shown the classical view of CoR and CoA exchange inducing gene transcription to be over simplified. Using the ERα as a model previous work has shown numerous interactions between coregulators and NRs. Furthermore, these occurred in response to ligand treatment over a timeframe of several minutes [119]. As part of this study a panel of transcription factors, histone modifying enzymes, and chromatin remodeling complexes were all screened for their promoter

presence. Using these data it was demonstrated that there were reoccurring fluctuations in histone methylation and acetylation. This suggested there were repeating recruitment and release patterns of CoAs and CoRs at the ERα bound response element. Furthermore, changes in these levels related to the recruitment and loss of the various chromatin modification enzymes [120]. This not only supported the histone code hypothesis (that gene activation required and induces changes in the PTMs on histone tail amino acids [121-123]) but also revealed that transcription is a highly dynamic process with frequent exchanges at the genomic template as well as the different coregulator proteins.

Therefore, this was one of the first studies to show that NR mediated gene transcription is a cyclical procedure. In addition, it requires both activating and repressive events to occur on a genetic and epigenetic level. The changes in associated complexes were mediated by the NR undergoing repeatable clearance and recruitment patterns of the coregulators.

The same group revealed the fluidity involved in NRs mediated gene regulation, they found that both unbound and ligand bound ERα can bind to target gene promoters in a cyclical manner [124]. It is conjectured that unliganded NR binding to the DNA may enforce repression of genes preventing unnecessary activation. In addition it may assure a rapid mRNA response to the detection of ligand.

Together, these investigations indicate that gene activation required sequential recruitment and release of coregulators that exhibits cyclical qualities (Figure 1.11). Furthermore, such cyclical turnover of complexes bound to NRs may serve as a sampling process. The cell may use this to measure the concentration of ligand available, therefore,

detecting change. This in turn allows the fine-tuning of mRNA output to suit environmental requirements.

However, observations of other NR models although they suggest similar cyclical release and recruitment it is shown to occur on a differing temporal scale. The previously described investigations with the ERα detailed above demonstrate cycles occurring within minutes of ligand exposure. In contrast, experiments in CaP using the AR binding to the PSA promoter as a model show that this has a prolonged cyclical nature lasting approximately 16 hours [125]. Therefore, it is clear in terms of NR specificity there are many differing gene targets, the transcriptional regulation varies between tissues and NRs.

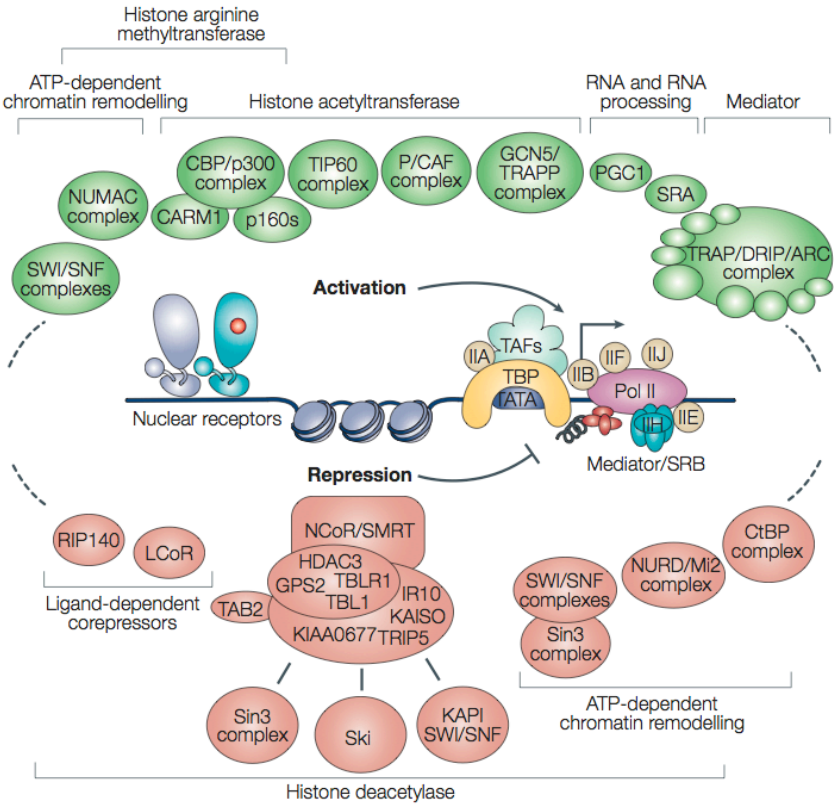

Figure 1.11 Cyclical recruitment and release of coregulators. There are a huge number of coregulatory complexes (activators in green and repressors in red) that interact with NR to modulate transcription. The NR passes through cycles of association with each type of coregulator during transcription in order to produce specific mRNA kinetics. Taken from [43].

Spatio-temporal studies of the VDR demonstrate that, similar to the ERα and AR, it is also able to undergo re-occurring recruitment to promoters. This also suggests there is cyclical recruitment and loss of both CoA and CoR at VDREs. For example a previous study determined that there were three active VDREs encoded within the *CDKN1A* gene (encodes $p21^{(waf1/cip1)}$). These were shown to bind VDR upon ligand activation displaying varied kinetics [75]. This study continued further by using ChIP experiments showing recruitment of the CBP protein to the VDR bound VDRE. Furthermore, the presence of these factors varied overtime in response to $1\alpha,25(OH)_2D_3$ as did their accumulation at each response element.

Additional work linked the VDR mediated events with histone PTMs within the local chromatin environment [126]. As a result it was discovered during each cycle the loss of CoR NCOR1 was followed by an accumulation of H3K9 acetylation mark at the transcription start site (TSS) of *CDKN1A*. At the same timepoints they were able to show enrichment of the activating CBP HAT. This work also reveals the importance of CoRs and their associated proteins, as knockout of either NCOR-1 or HDAC3 perturbed the mRNA kinetics of the gene. Interestingly, however, knockout of CBP had no effect upon transcriptional outcome.

Therefore, VDR target gene activation appears to undergo repeated 'programmes' to enable sampling of the environment and assess ligand concentration. These changes vary in rapidity dependent upon the NR being observed. Also these 'programmes' place specific histone modifications that change in parallel with fluctuations in mRNA expression.

Oscillations in the mRNA levels of target genes can be of critical importance to homeostasis and development (Reviewed in [127]). These changes are in part mediated through accumulation patterns of many CoA and CoR at their promoters [119, 128] (described above). However, malignancy renders cells unable to mediate the anti-proliferative actions of many NRs (such as RAR, PPARs and VDR). Concordantly, many of the NR target genes have been shown to become transcriptionally unresponsive or resistant.

Investigations into the mechanisms of this resistance within bladder cancer cells have revealed the importance and continuity of corepressors in transcriptional regulation. Bladder cancer tissues overexpress NCOR1, this in turn increased the growth rate of cells and mediated insensitivity to VDR and PPARγ ligands [129]. By using siRNA this work demonstrated reducing NCOR1 in combination with HDACi treatment (Suberoylanilide hydroxamic acid, SAHA) treatment enhanced the cells response to ligand. Significantly, this was shown by a measurable biological phenotype using proliferation rate in comparison to single treatments. Furthermore, it was identified that a reduction in levels of NCOR1 produced a similar level of proliferation as HDAC inhibition alone. Therefore, these data strongly suggest the importance of NCOR1 as a mediator of HDAC activity. Also it shows an aberrant increase of NCOR1 in cancer may contribute to transcriptional repression through epigenetic changes at NR target genes. These previous works indicate the potential significance of using HDAC inhibition as a therapeutic strategy.

Analysis using other malignant cell models supported the significance of these findings. Co-treatment of $1\alpha,25(OH)_2D_3$ with the HDACi Trichostatin A (TSA) has been found to overcome the gene repression exerted by NCOR1 and HADC3 in breast cancer

cells [130, 131]. This suggests the mechanistic nature of NR mis-regulation share some similarity between cancers of originating from different tissues.

In addition prostate malignancy demonstrates a similar response. Using a range of CaP cell lines it was revealed that HDAC inhibition with NaB (Sodium butyrate) or TSA in co-treatment with $1\alpha,25(OH)_2D_3$ increased the sensitivity of CaP cell lines (DU 145, PC-3 and LNCaP) [132]. As in bladder and breast malignancy the proliferative rate of these cells was attenuated in comparison to the single treatment conditions. Using primary human prostate tissues additional work showed that NCOR2/SMRT was elevated in cancer compared to normal controls [133]. Upon further examination with CaP cells it was demonstrated that a reduction in NCOR2/SMRT levels increased expression of cell cycle arrest genes such as GADD45α. These findings all support there being an imbalance in corepressor levels in malignant cells. Furthermore, this selectively distorts the actions of NRs (in this case VDR) through elevated HDAC recruitment and hypoacetylation of local chromatin.

Alternative models of prostate malignancy provided additional support to this hypothesis. A study using CWR22 xenograft models examined the proliferative actions in response to VDR stimulation. It was shown that NCOR1 and NCOR2/SMRT were elevated in cells insensitive to VDR stimulation and their activity was vital to repress VDR target genes [134]. The investigation showed that down-regulating either NCOR1 or NCOR2/SMRT was sufficient to restore VDR activated gene expression. In addition this study revealed important knowledge regarding $1,25(OH)_2D_3$ properties within the cell. They demonstrated that the expression of vitamin D transporters and ligand binding affinities were similar in resistant and responsive cells.

Therefore, these studies supported the hypothesis that NR insensitivity is not caused by alterations in the NR itself. Alternatively, the data show corruption of epigenetic mechanisms being responsible for the deregulation of NR target genes. Moreover, the activity of CoRs and HDACs were heavily implicated in this role.

Thus, aberrant CoR levels emerged as a pivotal factor in cancer development by controlling the transcriptional actions of NRs. Investigations into non-malignant and malignant cells show that in cancer NRs have a restricted ability to activate genes. For the majority of cases in non-malignant cells, unliganded NRs do not activate gene expression and exist bound to coregulators. It is the elevated CoR configuration of these complexes that can contribute to the differential amplitude of transcriptional response (Figure 1.12).

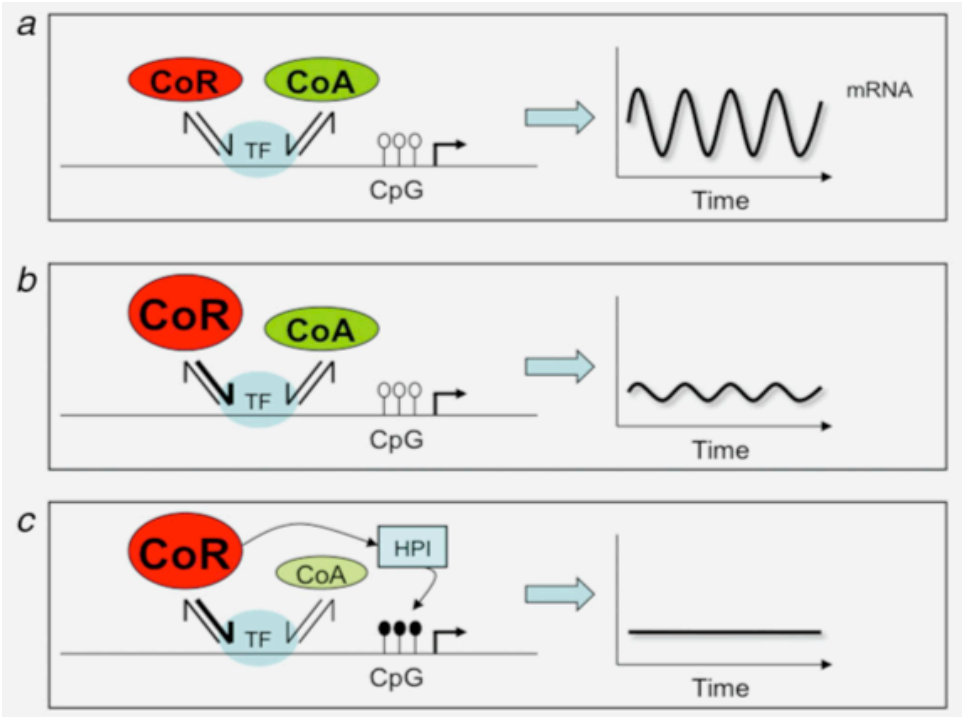

Figure 1.12 Model for corruption of co-repressor activity in malignacy. (a) Non-malignant cells use a balance of co-activators and co-repressors to mediate dynamic gene transcription (right). (b) Increases in co-reppressor activity occuring during transformation produce a prodominatly repressed response. (c) Sustained overexpression of co-repressors produces a repressed chromatin environment enhancing the presence of inheritable epigenetic changes (CpG methylation). Taken from Battaglia et al [85].

However, the importance of cell type specific effects cannot be overlooked. All of the studies examining NR and coregulator exchange described above use malignant cell models. As yet unaddressed is the nature of these dynamics within the non-malignant environment. Whilst there has been identification of aberrant CoR and HDAC levels in comparison to normal cells, there has been no study into the transcriptional kinetics within these systems.

Therefore, investigations are needed that examine the recruitment and loss of co-repressors at NR target genes in non-transformed cells. In addition to this, a comparative analysis of recruitment in malignancy is required. Such experiments may reveal a deeper understanding of aberrant CoR interactions within normal physiology and malignant disease.

1.4.4 Prereceptor regulation of nuclear receptor activity

Pre-receptor regulation of NRs involves the control of ligand availability through metabolic enzymes. Pre-receptor ligand metabolism has now been shown to occur in a number of NRs including the AR and GR [135, 136]. Therefore, aberrant activity or altered level of enzymes may exert ligand regulation to impair NRs target gene expression.

Upregulation of androgen converting enzymes in CaP tissue and cells has been widely reported [137]. In particular, it has been shown that Aldoketoreductase 1C3 (AKR1C3) is overexpressed in prostate cancer tissue samples and cell lines [138]. AKR1C3 is also referred to as type 2 3α-HSD or 17-beta-hydroxysteroid dehydrogenase type 5 and is involved in the conversion of androstenedione to testosterone [139]. In

correlation with this ADT-R CaP cells have been shown to overexpress AKR1C3 protein and lack its primary substrate 5α-dihydrotestosterone [140] (Figure 1.13).

The prostaglandin catabolic pathway in untransformed cells produces the PPARγ ligand 15ΔPGJ$_2$. However, in malignancy it is hypothesized that excess AKR1C3 may utilise PGD$_2$, converting it into the 9α,11β prostaglandin F$_2$, that has proliferative actions [141].

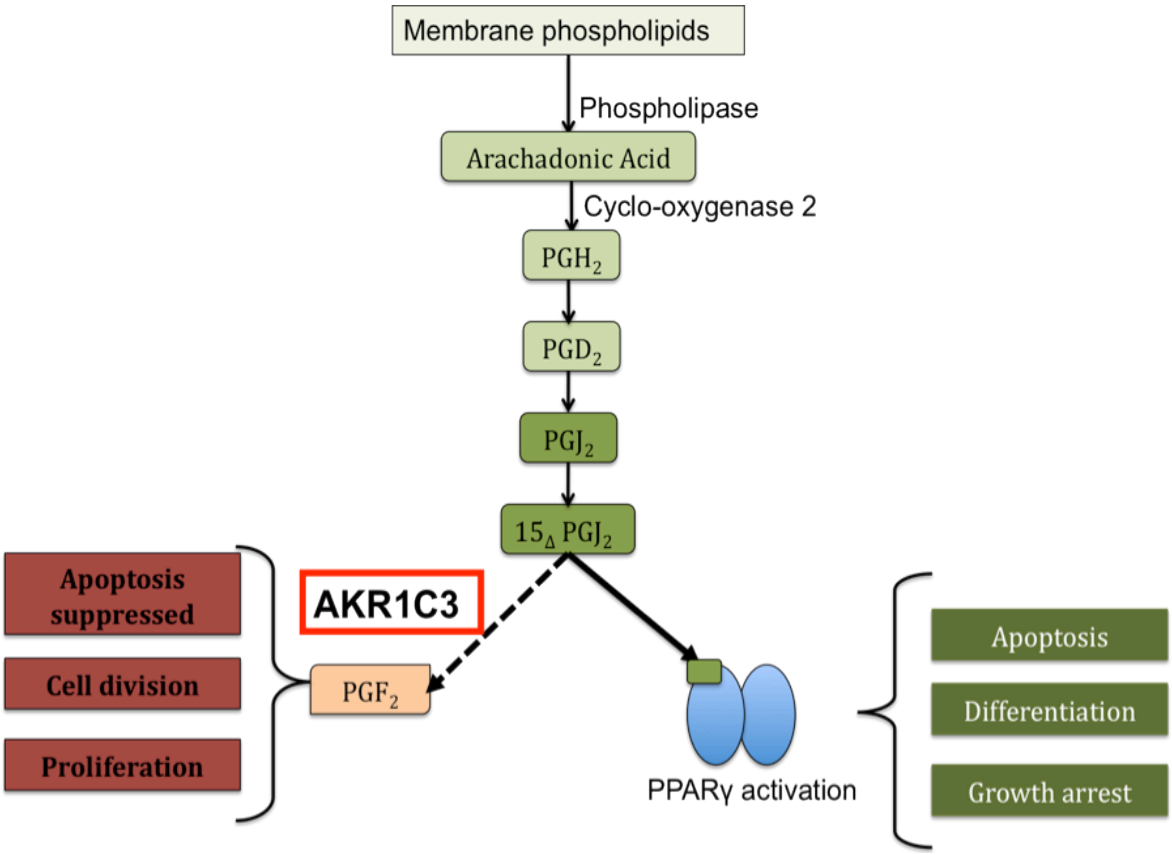

Figure 1.13 Elevated level of AKR1C3 found in cancers diverts conversion of PGJ$_2$ into PGF$_2$. Non-malignant cell lines do not have elevated AKR1C3, and PGJ$_2$ is non-enzymatically converted in to 15ΔPGJ$_2$, a ligand for PPARγ inducing activation of anti-tumourgenic target genes. An inappropriate conversion to PGF$_2$ increases cellular cascades inducing pro-tumourgenic actions. Adapted from Campbell et al [142].

Through this mechanism AKR1C3 may deprive the PPARγ of activating ligand. In the absence of elevated AKR1C3 represented in normal tissue PGD$_2$ is non-

enzymatically converted into a PPARγ ligand inducing anti-growth response genes. Therefore, inhibition of AKR1C3 levels in CaP may restore previously lost PPARγ activation.

1.4.5 Sirtuin activity induces aberrant NR activity.

The action of HDACs has been long studied, and among the many groups of HDAC enzymes are the Sirtuin family. HDACs are classified into four families (Class I, II, III, IV) named in regard to their similarity to yeast derivatives. Sirtuins fall into the Class III nicotinamide adenine dinucleotide (NAD)-dependent deacetylases. Indeed the activity of many transcription factors (including nuclear receptors) can be significantly altered by acetylation through HATs or deactylation by HDACs [143, 144] (Figure 1.14). All mammals have seven variants of Sirtuins, and various studies have shown that the HDAC activity of Sirtuin family can become deregulated in cancer [145, 146].

This family of proteins has wide reaching actions and understanding the activity of the Sirtuins in cancer may provide important insight into the consequences of their upregulation. It was in 1914 Peyton Rous (whom a few years earlier had been the first person to boldly hypothesise cancer could be transmitted by a virus [147]), discovered that rats on a calorie controlled diet showed reduced tumour sizes and decreased morbidity [148]. The biological mechanism behind the observation eluded both Rous and the entire scientific community for decades to come. However, the benefits of a calorie restrictive diet continued to be measured in many organisms ranging from yeast to higher apes. A significant finding came with the discovery in yeast [149] and mice [150] that the increased life span effect produced by calorie reduced diet was nullified with Sirtuin knockout models.

CaP incidence increases with age suggesting factors effecting lifespan may be associated with development. Accordingly, changes in global histone acetylation and methylation status have been used to predict CaP recurrence in patients [151].

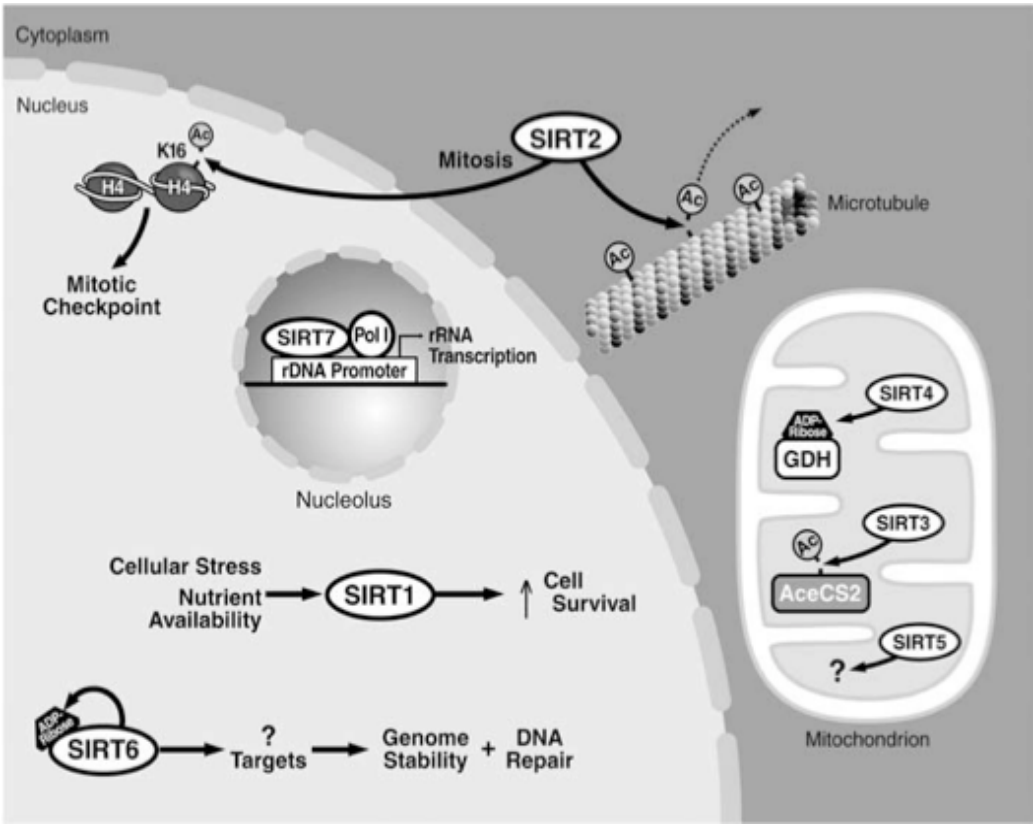

Figure 1.14 Cellular localisation and actions of Sirutins. SIRT1 is involved in nutrient sensing and promoting cell survial. SIRT2 is able to cross the nuclear membrane and deacetlyate histone tails to prevent advancement through the cell cycle in presence of DNA damage. SIRT3, 4 and 5 are found exclusively in mitchondria. SIRT 3 activates acetyl-CoA sythetase to increase actly-CoA production. SIRT 4 represses glutamate dehydrogenases repressing insulin signaling pathways. The actions of SIRT5 are yet to be identified. SIRT6 activates upon genomic damage and promotes DNA repair, through unidentified target genes. SIRT7 mediates Pol I transcription of rRNA genes. Taken from Saunders and Verdin [156].

Studies in mouse and human CaP have shown that SIRT1 is overexpressed [152], and so Sirtuins may have an integral role in disease development. Specific effects of SIRT1 on NRs in CaP have also been published with conflicting results. Studies have found SIRT1 inhibition to decrease the growth of ADT-R CaP cells [153], but contrasting

work on SIRT1 has demonstrated deacetylation of the AR act as an additional corepressor [154, 155].

Therefore, SIRT1 has been associated with both pro and anti-tumourgenic actions in CaP. In addition to this Sirtuins have also been shown to directly regulate the activity of NRs and in particular the PPARs through modification of histones [157], thus influencing their signaling ability. As such targeting the aberrant activity of Sirtuins in cancer through inhibition may restore NR mediated actions. Combining their inhibition with exogenously added ligands targeting PPARγ may produce anti-proliferative, pro-differentiating effects.

1.5 VDR regulated epigenetic events

1.5.1 *CDKN1A* Regulation in RWPE-1 cells.

NR target gene expression has been frequently studied with particular focus upon the receptor binding to DNA response elements. The changes in NR binding have been shown to produce mRNA fluctuations that vary in their magnitude and timing dependent upon the NR being studied. However, all of these previous studies use models of malignancy to test their hypothesis.

Therefore, there is a need for an investigation of NR mediated events that lead to transcription within non-malignant cells. This will establish a ‘baseline’ of normal untransformed cell functioning reflective of *in vivo* NR activity.

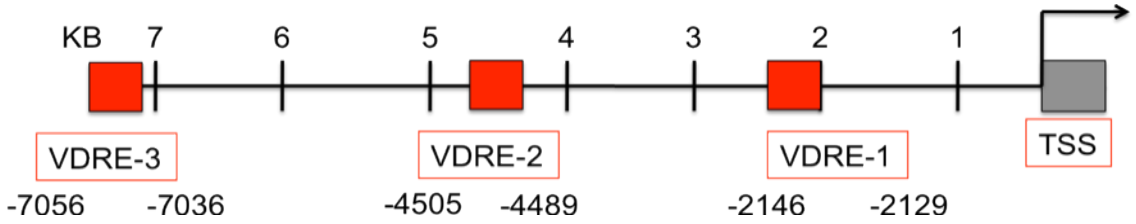

Figure 1.15 Functional VDREs within the *CDKN1A* promoter. Analysis of the human *CDKN1A* promoter revealed three responsive VDREs within the first 10kb upstream of the TSS. Response element positions relative to the transcription start site. Adapted from Samaraki et al [75].

The *CDKN1A* gene as shown in this work and also by other groups [126, 158] is a VDR regulated gene. Multiple response elements have been identified within the *CDKN1A* and these include numerous binding sites for p53 amongst other transcription factors. Screening of the gene found it to contain numerous putative VDRE binding sites that hold the consensus sequence RGKTCA (R = A or G, K = G or T) and variants of this configuration (Direct Repeats (DR3, DR4), Inverted repeats (IR3) or Everted Repeats (ER9)). Previous findings by this laboratory include identification of the mRNA kinetics of VDR target genes in response to $1\alpha,25(OH)_2\ D_3$ (100nm) exposure [76]. This study used the non-malignant RWPE-1 cell line to represent the normal untransformed prostate epithelial condition.

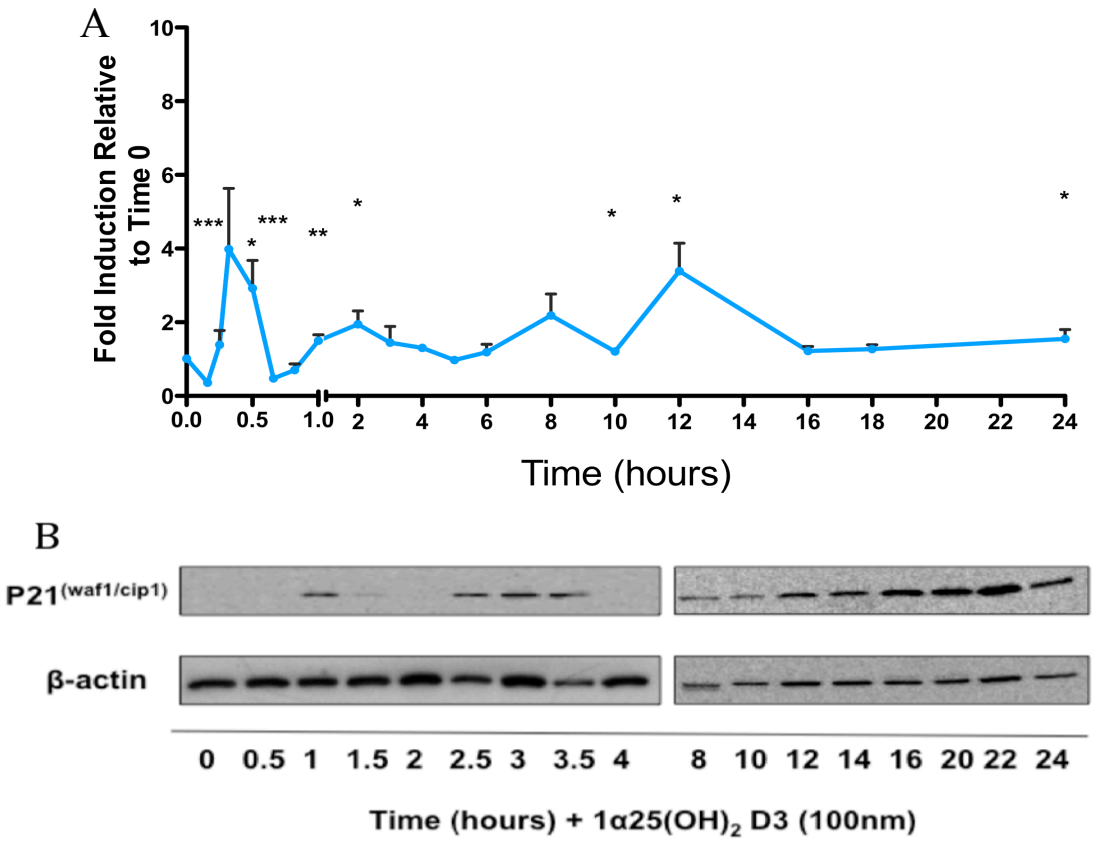

Figure 1.16 CDKN1A response in RWPE-1 cells with 1α25,$(OH)_2D_3$ (100nm). RWPE-1 cells were treated with 1α,25$(OH)_2D_3$ (100 nM) or EtOH and mRNA was extracted at the indicated time points, and accumulation of indicated genes measured by TaqMan Q-RT–PCR. Each data point represents the mean of triplicate experiments in triplicate wells ±SEM (*P<0.05, **P<0.01, ***P<0.001). All measurements performed in technical and biological triplicate. (B) Total cell proteins were isolated from cells treated as above at the indicated time points (1α,25$(OH)_2D_3$ (100nm)) and subjected to western immunoblotting. Representative blots are shown for $p21^{(waf1/cip1)}$. β-Actin used as a loading control. Adapted from Thorne et al [76].

From the data shown in Figure 1.16 20 at 30 minutes post exposure to 1α,25$(OH)_2D_3$ (100nm) there is a statistically significant (p-value<0.05) rise in *CDKN1A* mRNA. This early peak is followed by an mRNA profile that fluctuates between significant changes compared to the vehicle only treatment. These data demonstrate that the cyclical changes in VDR mediated *CDKN1A* accumulation are productive, and transcriptional events contributed to changes at the protein level. This maybe a

consequence of the mRNA accumulation measured at 1 and 2 hours. Eight hours post ligand addition there is detectable p21$^{(waf1/cip1)}$ at an increasing rate, at these later stages changes in protein abundance mediated by secondary interactions cannot be excluded. From the above data is it clear that cyclical accumulations of p21$^{(waf1/cip1)}$ message and protein occurs in response to VDR activation.

Previous work in our laboratory studied four histone modifications that were chosen for analysis at the regions of the *CDKN1A* gene shown in Figure 1.15. These time-resolved quantitative ChIP approaches at the described VDREs revealed that histone modifications regulate *CDKN1A* expression [76]. Histone modifications investigated were associated with gene maintenance, H3K4me3 (the trithorax mark) [159] and the H3K27me3 (the polycomb mark) [160].

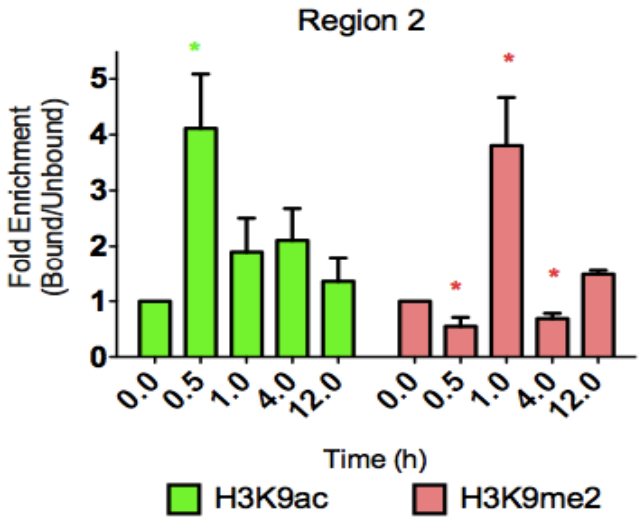

Figure 1.17 VDR-regulated epigenetic events on the promoter of CDKN1A. Changes to histone modifications (H3K9me2 and H3K9ac) were assayed using N-ChIP and normalized using bound over unbound DNA pulled down with specific ChIP grade antibodies. Enrichment was measured by Q-PCR as above. Each data point represents the mean of triplicate experiments in triplicate wells ±SEM (*P<0.05) Adapted from Thorne et al [76].

In addition H3K9ac and H3K9me2 were also examined. This investigation found enrichment of the activating H3K9ac and loss of repressive H3K9me2 0.5 hours post treatment at VDRE-2 (Figure 1.17). This exchange of marks at H3K9 was also reversed after 1 hour indicating a deactivation signal. This suggests a highly dynamic and tightly regulated epigenetic mechanism of gene transcription.

Previous work focusing upon the NCOR1 corepressor has suggested that it may play a significant role in the acquisition of methylation at H3K9. It was found that NCOR1 but not NCOR2/SMRT was able to bind a protein called Kaiso. Upon binding of the Kaiso/NCOR1 complex to promoters there was deacetylation and methylation of the H3K9 subunits [161]. Additionally Kaiso is a methyl CpG binding protein indicating that it can contribute to inheritable repression of genes as well as transcriptional repression through NCOR1 presence.

Therefore, elevated NCOR1 containing Kaiso protein may be responsible for contributing to epigenetic changes in H3K9. The imposed PTMs may then influence changes in transcriptional response to ligand.

Additional work in this group show that the DNA helicase and replication factor *minichromosome maintenance complex 7* (*MCM7*) is emerging as a VDR regulated gene. This exhibits an mRNA expression profile in response to $1\alpha,25(OH)_2D_3$ (100nm) that has similar dynamics to *CDKN1A* expression. MCM7 has a strong correlation between the level of expression of this gene and the level of DNA replication conducted by the cell. In conjunction with this studies have found increased *MCM7* expression to be associated with malignancy in many tissues including the prostate [162-165]. Supplemental to this the *MCM7* gene encodes in its 3'UTR the sequence for a microRNA subfamily [166].

MiR106B is contained within this sequence and its upregulation has been measurement in response to 1α,25(OH)$_2$D$_3$ using real-time PCR. These data have shown a similar response transcriptional to *MCM7* and *CDKN1A*. Analysis of mRNA expression over the first hour post treatment shows that the MCM7 and MiR106B production rise in their levels, these exhibit an 'early' peak of mRNA that precedes the *CDKN1A* peak observed in RWPE-1 cells.

MiR106B is able to target the *CDKN1A* mRNA for degradation, it is therefore hypothesised that 1α,25(OH$_2$)D$_3$ is able to initiate through *MCM7* activation transcription of the microRNA MiR106B. *MiR106B* then marks the *CDKN1A* mRNA for degradation. Thus contributing to the mRNA dynamics observed in response to 1α,25(OH)$_2$D$_3$ providing and additional layer of transcriptional regulation.

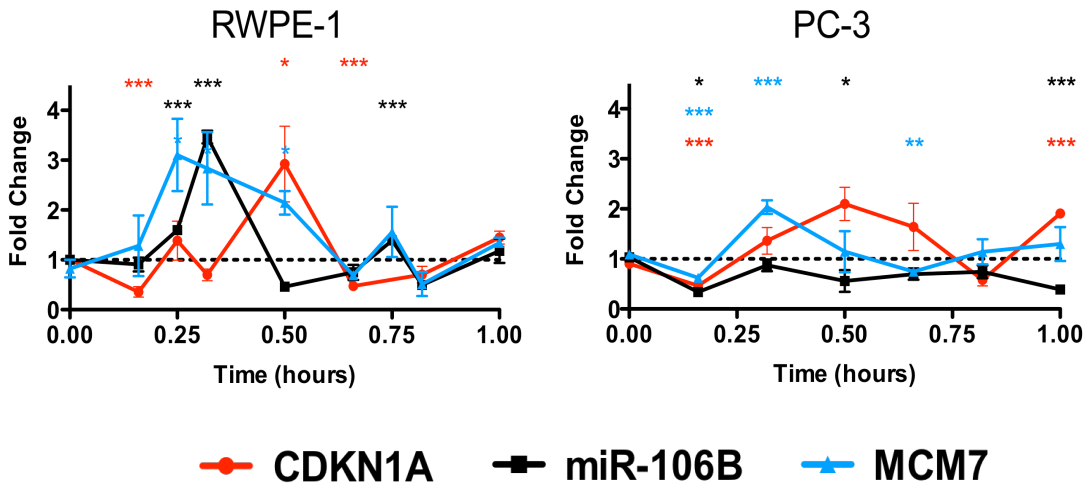

Figure 1.18 mRNA expression of CDKN1A, MCM7 and MiR106B in response to 1α25,(OH)$_2$D$_3$ (100nm). RWPE-1 and PC-3 cells were treated with 1α,25(OH)2D3 (100nM) or EtOH and mRNA was extracted at the indicated time points, and accumulation of indicated genes measured by TaqMan Q-RT–PCR. Each data point represents the mean of triplicate experiments in triplicate wells ±SEM (*P<0.05, **P<0.01, ***P<0.001). All measurements performed in technical and biological triplicate. Conducted by Dr. Orla Maguire.

Upon activation by VDR the MCM7 gene shows detectable rises in mRNA after 15 minutes this appears 15 minutes prior to the early peak in *CDKN1A* suggesting that *MCM7* mRNA is activated first. Further, the sequence for MiR106B can be detected at an increased level after 20 minutes and is situated in-between *CDKN1A* and *MCM7*. All of the early peaks observed are lost by 1 hour treatment. Investigation in the malignant cell line PC-3 shows that although mRNA inducibility is lost in response to VDR, the expression profile of *MCM7* and MiR106B is maintained although its potency is decreased in comparison to RWPE-1 (Figure 1.18).

Therefore, there is a selective distortion of the feedforward loop (FFL) in CaP. This is biased in favour of silencing the anti-proliferative target genes, whilst minimizing disruption of the proliferative genes.

Hypothesis

Nuclear receptors mediate a wide range of growth control events. However, during malignancy their activity becomes distorted. Therefore, the overarching hypothesis of this thesis is that inappropriate overexpression of CoRs NCOR-1 and NCOR2/SMRT contribute to transcriptional silencing in prostate cancer. Elucidation of this may allow identification of new therapeutic targets, which can be exploited to restore NR sensitivity.

Study aims

Experiments designed to test the hypothesis of this thesis were broken down into three specific aims.

1. To investigate the ability of AKR1C3 to regulate PPARγ at a pre-receptor level. Decreasing the levels of AKR1C3 in CaP may restore endogenous PPARγ ligand concentrations producing a decreased proliferation rate.
2. To examine if the transcriptional actions of VDR vary in prostate cell lines representing non-malignant disease. All previous studies of NR and coregulator binding have been performed in malignant cell lines. Therefore, to investigate how VDR regulated epigenetic events influence gene expression RWPE-1 non-malignant cell lines were utilised.
3. To test for differential VDR and cofactor binding in CaP models. Comparison of RWPE-1 binding kinetics to malignant cell lines will reveal the true level of epigenetic mis-regulation giving rise to NR target gene insensitivity.

Chapter 2: Materials and Methods

2.1 Materials and Methods

2.1.1 Cell Culture

Human prostate cell lines used in this work (RWPE-1, RWPE-2, PC-3, LNCaP and DU 145) were purchased from American Type Cell Culture (ATCC) Manassas, Virginia USA. The LNCaP-C42 cells were taken from a stock storage at Roswell Park Cancer Institute, Buffalo, New York, USA. RWPE-1 and RWPE-2 cells were maintained within Keratinocyte serum free medium (K-SFM) (Invitrogen GIBCO). This was combined with the supplements of bovine pituitary extract (0.05mg/ml) (BPE) and human recombinant epidermal growth factor (5ng/ml) (EGF) (Invitrogen GIBCO). LNCaP, LNCaP C-42, PC-3 and DU 145 cells were maintained in RPMI medium (Sigma Aldrich) containing 10% fetal bovine serum (FBS) (Invitrogen) and 2mM L-Glutamine. To minimise chances of infection all cell lines were maintained in 100 units/ml Penicillin and 100μg/ml Streptomycin. All cells were kept in at 37^{o}C in air 95% and 5% CO_2. Confluent cells were washed in sterile PBS, split using Trypsin-EDTA (Sigma Aldrich) and seeded into new flasks containing fresh media. Different cell lines were spilt with differing frequency dependent upon growth characteristics for example; RWPE-1 cells were split at 1:4 ratio bi-weekly. Faster dividing LNCaP, LNCaP C-42, PC-3 and DU 145 cells were split four times weekly at a 1:8 dilution. RWPE-2 cells were maintained within the KSF complete medium and split at a 1:5 ratio three times weekly.

2.1.2 Compounds

- $1\alpha,25(OH)_2D_3$ (BioXell) was stored in a 10mM stock solution in ethanol, protected from sunlight and stored at -20^{o}C.

- Bezafibrate (Sigma Aldrich) was stored in a 1mM stock ethanol solution, protected from sunlight and stored at -20^{o}C.

- Suberoylanilide hydroxamic acid (SAHA) was a kind gift from Merck and stored in a 1mM ethanol solution at -20^{o}C.

- GW9662 (Sigma Aldrich) was stored in a 1mM DMSO stock solution and protected from sunlight by storage at -20^{o}C.

- Sirtinol (Sigma Aldrich) was stored in a 4M stock solution in acetonitrile, protected from the sunlight and stored at -20^{o}C.

For experimental dilutions all compounds were diluted in the corresponding diluent control and treatment commenced alongside vehicle only controls.

2.1.3 Proliferation assays

Principle

Rate of cell division was measured using the ViaLight Plus Kit for high sensitivity cell proliferation (Lonza Rockland Inc.). This used detection of ATP levels within cells to extrapolate their rate of growth. Cells producing ATP were measured using the enzyme luciferase, this catalysed the formation of light using ATP, luciferin and O_2. Under these conditions the below reaction took place. The level of light emitted from each well was directly proportional to the concentration of ATP in the well.

$$\textbf{ATP + luciferin + } O_2 \xrightarrow{\textbf{luciferase}} \textbf{oxyluciferin + AMP + PPi + } CO_2 \textbf{ + } \textit{LIGHT}$$

Procedure

Cells were seeded at differing densities in relation to their inherent differences in proliferation rate. RWPE-1 cells ($4x10^3$) were loaded per well in 96 well plate, PC-3 and DU 145 ($2x10^3$) cells were loaded per well in white walled 96 well plate (Costar). Cells were left to attach to the bottom of well overnight at 37^oc in air 95% and 5% CO_2. Addition of treatment took place the following day and again 48 hours later. Thus the exposure to compound(s) was 72 hours, before the plate was read by the microplate luminometer (Berthold Id Detection System, Fisher Scientific Ltd, UK). Cell lysis reagent (50µl) was added in each well using a multichannel pipette and left at room temperature for 10 minutes. ATP monitoring reagent (100µl) was added and the plate was left for 2 minutes covered with tin foil to exclude sunlight. ATP levels were recorded in Relative Luciferase Units (RLU) with a read time set to 1 second as recommended by the kit manufacturer. Inhibition of proliferation was expressed as a percentage relative to

vehicle treated control. All final results were the result of at least three independent biological experiments performed in triplicate wells. Values were plotted using mean data ± Standard Error of the Mean (SEM) and statistical significance was assessed using Students unpaired t-test where *=p-value <0.05, **=p-value <0.01 and ***=p-value <0.001.

2.1.4 Fluorescence Activated Cell Sorting (FACS) for cell cycle analysis

Principle

As eukaryotic cells grow towards division it passes through specific periods or phases, each phase has a specific role and name. There are four phases to the cell cycle (G_1, G_2, S and M) although a senescence phase, that precedes G_1 called G_0, is often omitted. Throughout each phase the growing cell contains a different amount of DNA. Thus each phase can be detecting by determining the relative amount of DNA in cells by using propidium iodide (Roche). This is intercalating dye binds any present double stranded DNA. As propidium iodide cannot permeate the cell membrane populations must first be lysed and nuclear DNA exposed. This can be performed by exposure to detergents and salt concentrations able to induce swelling and bursting of cellular membranes. The propidium iodide in the stained nuclei is excited by light with a wavelength of 488 nm resulting in fluorescence that can be measured by the flow cytometer.

Between G1 phase where there is one copy of the genome and G2 phase that has two copies of the genome is the S phase. This normally lasts 10–12 hours and duplicates the DNA contained within the cell. Therefore, those cells in G2 and M phase should produce greater signal intensity as they have duplicate copies of DNA. S phase cells are

undergoing duplication and so will yield a greater level of florescence than G1 populations but not as great as G2 populations.

Procedure

T75 cell bind flasks were seeded with sub-confluent, exponentially proliferating cells and allowed to settle overnight. Cells were treated with $1\alpha,25(OH)_2D_3$ (10nm and 100nm) for 24 hours. Cells were harvested by trypsinisation and pelleted by centrifugation at 12,000g for 5mins. Cells were resuspended in 1ml PBS (stored at 4ºc) and transferred to flow cytometry tubes (Falcon). Cells were washed in PBS (1ml) and resuspended in 500µl cell cycle buffer (1 % sodium citrate, 0.1 % Triton X-100, 0.1mM sodium chloride) and 10µg/ml propidium iodide (Sigma Aldrich) protected from light and stored at 4ºC. Samples were vortexed and incubated on ice in the dark for at least 40mins before flow cytometry analysis.

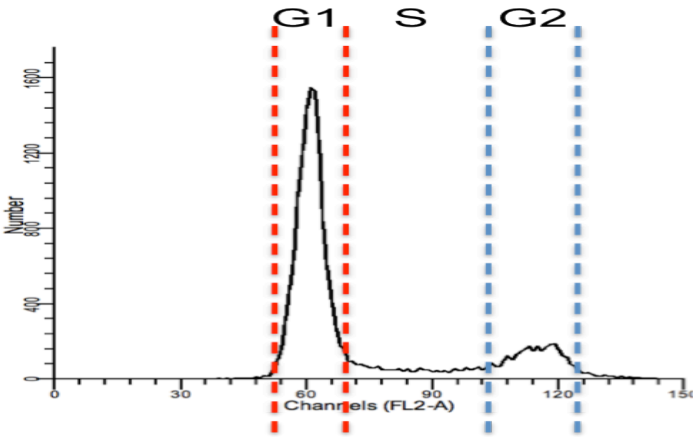

Cell Cycle Phase	% Cells
G1	71.61
S	9.50
G2/M	18.89

Figure 2.1 An example of FACS analysis cell cycle profile in untreated cells. On the x axis is the intensity of the fluorescent signal and the y-axis shows the number of events measured. Cell cycle distribution was determined using a Becton-Dickinson Flow Cytometer and CellFIT Cell-Cycle Analysis software. Analyses were carried out on 10,000 nuclei per sample and each condition was examined in at least three independent experiments.

2.1.5 RNA extraction

Principle

Isolation of pure, good quality RNA can be critical for accurate quantitative analysis in molecular biology. RNA molecules are weak structures that rely on 5' capping and 3' polyadenylation to maintain their conformation. However, RNA molecules are still susceptible to attack by ribonucleases or RNAse and so the quality of samples can degrade rapidly. The following methodology utilised is that detailed by Chomczynski, P. and Sacchi, N. in 1987 [167] whom developed the Guanidinium thiocyanate-phenol-chloroform extraction procedure. Guanidinium thiocyanate-phenol-chloroform is able to preserve to stability of RNA by denaturing the ribonucleases. In addition it degrades tissue and cellular components yielding total RNA whilst maintaining integrity. Addition of chloroform to the Guanidinium thiocyanate-phenol mix allows the separation of phases. Bottom is a red phenol-chloroform phase, an interphase containing DNA and an aqueous phase at the top that contains the total RNA extract. Removal of the aqueous phase and ethanol precipitation of the hydrophillic nucleic acids allows for isolation and resuspension in nuclease free water.

Procedure

1ml of Guanidinium thiocyanate-phenol (Trizol (Invitrogen)) per 5 million cells was added to the well in use. The reagent was then pipetted up and down on the well to maximise lysis of cells and exposure to all areas of the well. The cellular contents now suspended in the Trizol were transferred to an Eppendorf (1.5ml) and left at room temperature for 5 minutes to equilibrate. After 5 minutes, chloroform (200ul) per ml of Trizol added and the samples were then vortexed for 10 seconds then left to incubate at room temperature for 5 minutes. The sample was then centrifuged at 12,000g for 5

minutes at 4°C. The top layer (an aqueous phase containing the RNA) was removed and dispensed into a new Eppendorf (1.5ml) to which isopropanol (propan-2-ol) 500ul (per 1ml of Trizol used) was added. This was then inverted 5 times to mix and kept at -20°c for at least 30 minutes to ensure precipitation of RNA. The sample was then centrifuged for 10 minutes at 12,000g at 4°c to collect a nucleic acid pellet at the bottom of the Eppendorf. The isopropanol was then removed and the pellet was then resuspended in 75% ethanol and centrifuged further for 5 minutes at 12,000g at 4°c to wash the sample. The 75% ethanol was then removed and the sample resuspended in nuclease free water (50ul) and stored at -80°c.

RNA was quantified using the NanoDrop (ND100, Labtech International, UK). Quantification of 2µl of RNA sample was measured through absorbance at 260nm and 280nm with the ratio of 260nm/280nm being an indicator of the purity of RNA sample. Ratios <1.6 indicates partially degraded RNA or a high level of non-nucleic acid present and so was discarded and not used.

2.1.6 Reverse Transcription

Principle

Quantification of isolated mRNA first required conversion of the mRNA into cDNA as RNA is unstable and will degrade rapidly under thermocycling conditions. Therefore, the RNA must be converted to complementary DNA (cDNA) that is stable and receptive to polymerase chain reaction (PCR) conditions. Conversion to cDNA is performed using a commercial cDNA synthesis kit i-script (Biorad). This kit utilises the RNase H1 reverse transcriptase enzyme in a cocktail containing RNase inhibitor, oligo dT and random primers. RNase H1 reverse transcriptase is able to copy the mRNA

sequence whilst degrading the RNA template upon completion. The reverse transcriptase enzyme requires initiation through the binding of oligo dT or random primers. These are able to detect the polyadenylated tail of mRNA or any sequences of oligonucletides respectively. This ensures all present mRNA is converted into cDNA.

Procedure

Previously purified, isolated and quantified RNA was diluted to yield 1µ of RNA in 10µ of nuclease free water (Ambion) per sample. Added to this was the i-Script cocktail and reverse transcriptase in the following volumes:

Components	Volume per reaction (µl)
5x i-Script Reaction Mix	4
i-Script Reverse Transcriptase	1
Nuclease Free Water	5
RNA Template (1µg Total RNA)	10
TOTAL REACTION VOLUME	**20**

Table 2.1 Reverse transcriptase master mix components and volumes

Reaction Protocol
The mix was incubated at the following conditions:

Time (minutes)	Temperature (^{o}c)
5	25
30	42
5	85
∞	4

Table 2.2 Reverse transcriptase reaction thermal conditions.

Resulting cDNA was stored at -20^{o}c.

2.1.7 Quantitative Real-Time Polymerase Chain Reaction (Q-RT-PCR)

Principle

This technique allows accurate detection and quantification of cDNA produced during each PCR amplification cycle. It is an advancement of the traditional polymerase chain reaction procedure. There are three stages in the PCR procedure; denaturation, annealing and extension. Denaturation of the DNA occurs at high temperatures (95^{o}C) and the double stranded DNA unwinds and separates into single strands. The temperature of the reaction mix must then reduce to approximately 40^{o}C below that of the template primers used, this allows them to bind to the single stranded cDNA. In the presence of thermophillic DNA polymerases (Taq) the bound primer and induces 'extension' which is the copying of the primer bound template by the polymerase. This produces an identical strand of DNA, the cycle is then repeated 40 times. In this way the amount of product exponentially increases every cycle. Importantly the primers used must be predesigned to be complimentary to an intron-exon boundary thus preventing any genomic DNA interfering with measurement. The product after 30–40 cycles can then be ran on an agarose gel (1-3%) containing the fluorescent DNA interacting ethidium bromide (0.5μg/ml) and viewed under UV light conditions. However, as this process is exponential and only the end product is viewed it is not an accurate method of measuring abundance and only regarded to be semi-quantitative.

Therefore Q-RT-PCR was developed. This uses an amplicon specific fluorescent probe that is detected upon the specific product being formed. Cleavage of the probe by the DNA polymerase during the extension step of PCR allows detection and extrapolation of fluorescence into a quantifiable value. The probe is also linked to a quencher preventing inappropriate detection, only when the DNA cleaves the probe from the

quencher is its fluorescence detected. This technique allows quantification of amplified product at the end of every cycle of denaturation, annealing and extension. Therefore, the earlier cycle a transcript is detected the more copies of the gene are present in the sample i.e. gene X appearing at cycle 19 is present at a higher level than gene Y which appears at cycle 23. Thus there are more copies of gene X in the sample of isolated cDNA than gene Y.

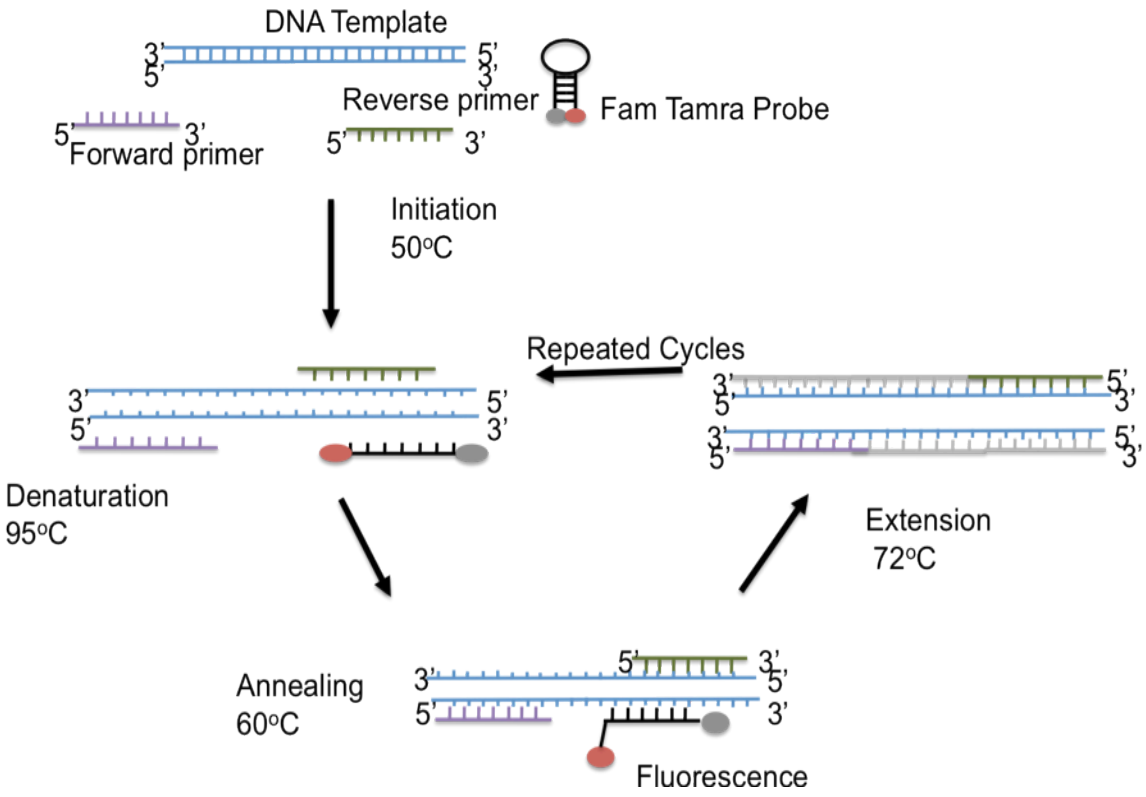

Figure 2.2 Real Time PCR detection using primer and probe combination. The probe oligonucleotide is modified with a fluorescent reporter dye (FAM) and with a quencher (TAMRA). While the probe is intact the dye is proximal to the quencher and prevents fluorescence emission. During the extension phase of the PCR, the taq polymerase (has 5' to 3' exonuclease activity) digests any annealed probe. This induces separation of the reporter dye from the quencher enabling fluorescence detection.

To give individual samples an internal robustness that allows them to be compared to each other there must be an endogenous control. This is quantified within each reaction to account for differences in cDNA amounts between samples. 18s is a ribosomal RNA that is constitutively expressed in all cells in high concentrations. Its expression is consistent between different cell types and changes in levels remain undetectable in exposure to compounds. Comparison of the gene of interest to the 18s internal control gene first then allows direct comparison to samples between treatments.

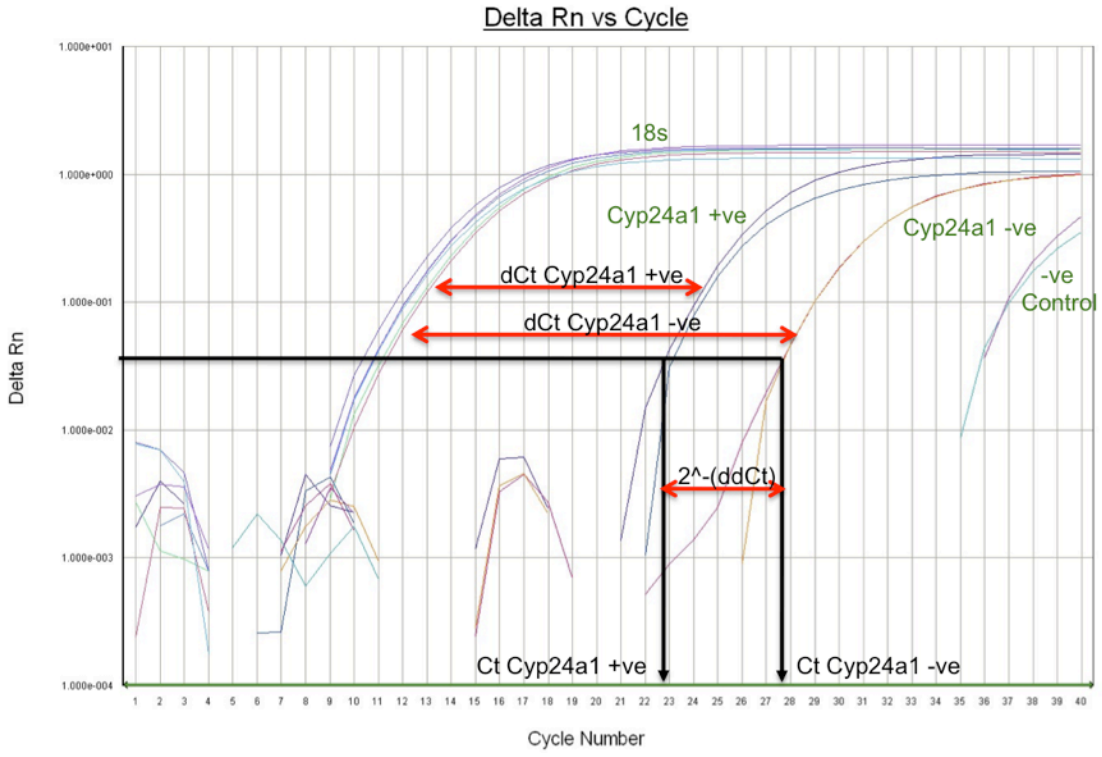

Figure 2.3 An example of the amplification curve of 1α,25(OH)$_2$D$_3$ treated and untreated RWPE-1 cells. Cycle thresholds (Cts) are related to the internal control 18s rRNA Cts and ddct are calculated by comparing the amplification curve. In this example of 1α,25(OH)$_2$D$_3$ treatment upregulated the levels of *CYP24A1* mRNA, this was shown by a shift in the amplification curve to the left in comparison to the untreated sample.

As already stated the amplification process is exponential. The cycle at which a determined level of fluorescence occurs is termed the cycle threshold (Ct) and quantification occurs at the exponential phase of amplification. The Cycle threshold or Ct of the internal control gene can be subtracted from the Ct of the gene of interest. This allows normalisation of the sample termed delta Ct (dCt). Using the delta Ct an untreated control cell can be compared to that of a ligand treated cell. The subtraction of the untreated delta Ct from the treated delta Ct yields the delta delta Ct (ddCt). Conversion of the Ct value into relative fold change by the 2^-ddCt calculation is then performed. The use of 2^ (POWER) is an approximate and hypothetical value used to account for primer amplification efficiency.

Primers and probes used for qRT-PCR were as follows:

Accession Number	Primer Name	Primer Sequence (5'-3')
NM_ 000782	CYP24A1 Forward	CAAACCGTGGAAGGCCTATC
	CYP24A1 Reverse	ACTTCTTCCCCTTCCAGGATCA
	CYP24A1 Probe	ACTACCGCAAAGAAGGCTACGGGCTG
NM_ 000389	CDKN1A Forward	GCAGACCAGCATGACAGATTTC
	CDKN1A Reverse	GGATTAGGGCTTCCTCTTGGA
	CDKN1A Probe	CCACTCCAAACGCCGGCTGATCTT
NM_ 006311	NCOR1 Forward	TGAAGGTCTTGGCCCAAAAG
	NCOR1 Reverse	TTTGTCTTGATGTTCTCATGGTA
	NCOR1 Probe	CTGCCACTGTATAACCAGCCATCAGATACCA
NM_ 001924	GADD45α Forward	AAGACCGAAAGGATGGATAAGGT
	GADD45α Reverse	GTGATCGTGCGCTGACTCA
	GADD45α Probe	TGCTGAGCACTTCCTCCAGGGCAT
NM_ 000376	VDR Forward	CACCCGGCAGTATCATGAGA
	VDR Reverse	CGAGCGTGATTCCTCCTCTT
	VDR Probe	CTTCCGCATCGCCTGGTTTATT
NM_ 000963	PTGS2 Forward	GAATCATTCACCAGGCAAATTG
	PTGS2 Reverse	TCTGTACTGCGGGTGGAACA
	PTGS2 Probe	TGGCAGGGTTGCTGGTGGTAGGA
NM_ 015714	G0S2 Forward	CAGAGAAACCGCTGACATCTAGAA
	G0S2 Reverse	GCAGCAAAACTCAATNMCCCAAA
	G0S2 Probe	TGACCTACCACAAGCATCCACCAAAGG
NM_ 000125	ERα Forward	GGGAAGCTACTGTTTGCTCCTAAC
	ERα Reverse	AAGATCTCCACCATGCCCTCTA
	ERα Probe	TGCTCTTGGACAGGAACCAGGGAAAAT
NM_ 002747	MAPK4 Forward	GCTGATGGCCGCTAACCA
	MAPK4 Reverse	GGCTCACAGGGTACCTGGAA
	MPAK4 Probe	TGACCTACCACAAGCATCCACCAAAGG
NM_ 005916	MCM7 Forward	CGGTGCTGGTAGAAGGAGAG
	MCM7 Reverse	AAACCCTGTACCACCTGTCG
	MCM7 Probe	GCCAATCCTGCGCACTGGGT
NM_ 003739	AKR1C3 Forward	GGGATCTCAACGAGACAAACG
	AKR1C3 Reverse	AAAGGACTGGGTCCTCCAAGA
	AKR1C3 Probe	TGGACCCGAACTCCCCCGGTG

Table 2.3 Primer and probe sequences for Taqman real time RT-PCR. All probes have the fluorescent dye called Fam, attached to the 5' end and the quencher Tamra, bonded to the 3' end, only upon release of the quencher is the fluorescence detected.

Gene Bank Accession Number	Gene name	Product code
NM_000698	5-Lipoxygenase	Hs00167536_m1
NM_030593.1	SIRT2	Hs01560288_m1
NM_016539.1	SIRT6	Hs00213036_m1

Table 2.4 Assay on demand primer and probe mix used in this thesis (Applied Biosystems). Listed above are the accession numbers and product code used for each assay on demand gene.

Primers and probes used previously by the group had been calibrated to guarantee linearity of amplification. Primer efficiency experiments were carried out in order to ensure reliability on mRNA detection. This optimization step was undertaken to ensure a linear relationship between template concentration and Ct values when undertaking a multiplex reaction with both housekeeping genes and target genes. G0S2 primer probes had to be designed using Primer 3 program and ordered from Sigma Aldrich as they were not previously in use. These were tested by using a range of 10 fold cDNA dilutions to examine amplification and multiplex efficiency of primer sequences. The data obtained from this validation is depicted in Figure 2.4. Primer and probe combinations for the ALOX-5 gene were unable to produce a satisfactory efficiency in either singleplex or multiplex conditions. Therefore, an Assay on Demand™ (Applied Biosystems) product was used see Table 2.4 for manufacturers code.

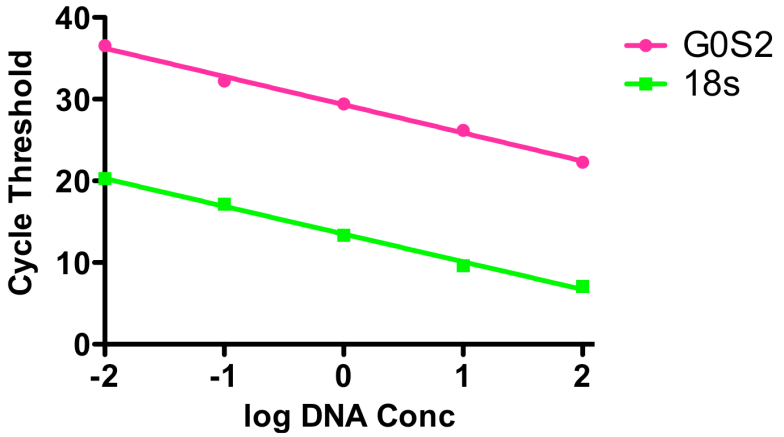

	G0S2	18s	efficiency comparison
Slope	-3.453 ± 0.1340	-3.394 ± 0.1215	-0.05900 ± 0.2374

	G0S2	18s	efficiency comparison
R square	0.9955	0.9962	0.02017

Figure 2.4 An example of multiplex efficiency curves for RT-PCR primer and probe sets displaying the relationship between G0S2 and 18s. Efficiency values were measured using the CT slope method. This method involves generating a dilution series of the target template and determining the CT value for each dilution. A plot of CT versus log cDNA concentration is constructed.

Procedure.

cDNA was amplified in a 20µl reaction containing 1x TaqMan PCR MasterMix (Sensimix dT - QT6T3, Quantace, UK), 125nM FAM-TAMRA labeled probe (Sigma Aldrich) and 1µM of primers (Sigma Aldrich). All reactions were multiplexed with 1x VIC-TAMRA 18s (Applied Biosystems). An ABI 7500 fast real time PCR system was used under the following cycle conditions:

Time	Temperature (°C)	Cycles
2 minutes	50	1
10 minutes	95	1
15 seconds	95	40
1 minute	60	40
30 seconds	72	40

Table 2.5 Thermocycling profile used in the Q-Real-Time PCR.

Final measurements were an average of at least three independent experiments, in triplicate wells for each condition. Assessment of statistical significance was preformed using fold changes of gene expression and was conducted by applying the unpaired t-test.

2.1.8 Microfluidic gene card (Q-RT-PCR$_m$)

Principle

Developed and sold by Applied Biosystems the microfluidic gene card is a 384-well custom array that allows detection of 384 simultaneous quantitative real time PCR reactions. Each card contains the custom ordered genes already pre-loaded into the well and present in duplicate, arranged in 96 wells (96x2x2=384). Therefore, 96 genes can be observed and measured in duplicate per card. The plate is run on an ABI 7900H thermocycler (Applied Biosystems) containing a 96-well plate heating block and analysed as a normal real time PCR reaction.

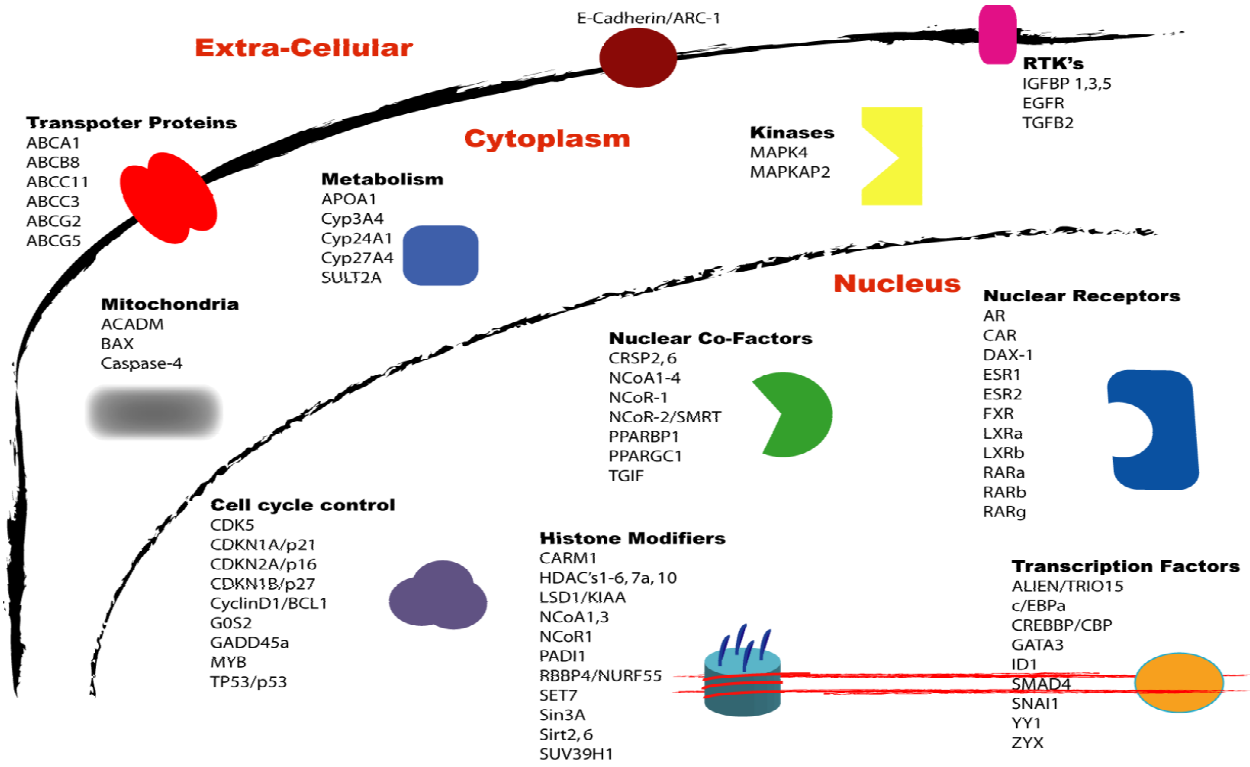

Figure 2.5 Diagrammatic representation of the genes included on the microfluidic card. Included on the card were genes that could be ascribed in to various grouped pertinent to the prostate nuclear receptor network. The picture not only shows their function but also their sub-cellular location. Produced by Dr. James Thorne. Full list in Appendix section.

Procedure

RNA concentrations of each sample were measured using the NanoDrop and diluted accordingly to the lowest within the samples to be analysed. One-step reaction Master-Mix (Qiagen) (200µl) was added to the diluted RNA together with RT mix (4µl) (Qiagen), 100µls of reaction mix were then dispensed per every two rows in the card. This was then centrifuged twice at 10,000g for 2 minutes to distribute sample into each well. The plate was then sealed and run on the ABI 7900 machine under the following cycle conditions:

Time	Temperature (°C)	Cycles
30 seconds	50	1
15 minutes	95	1
45 seconds	95	40
45 seconds	60	40
45 seconds	76	40

Table 2.6 Thermocycling profile used in the microfluidic gene card q-Real-Time PCR.

2.1.9 Western Immunoblotting

Principle

The extraction, purification and quantification of different proteins is an important part of molecular biology, allowing comparative levels of expression. As many proteins have different molecular sizes exploiting their inherent charge differences allows their separation through electrophoresis. Western immunoblotting uses electrophoresis on a polyacrylamide gel (PAGE). Using this background allows the proteins to move through the pores in the gel. Pore size is determined by the levels of acrylamide within the gel and decreases as the concentration of acrylamide increases. Therefore, the combination of protein size, charge, and gel pore size regulates the speed of a protein's migration through the gel. Increasing the acrylamide concentration of a gel will produce a smaller pore size giving a higher resolution of separation between proteins of a smaller molecular weight. In addition the gel is ran under denaturing conditions with 1% Sodium Dodecyl Sulphate (SDS). This has a high negative charge and upon heating with the protein lysates attaches to them increasing the negativity exhibited. An additional benefit of the heating in the presence of SDS and β-mercaptoethanol presence is the reducing of

tertiary and secondary structures producing a linear confirmation. These products when ran on an acrylamide gel form an anionic system with the negatively charged SDS coated proteins migrating from the cathode down through the gel towards the positive anode. Boiled SDS coated protein lysates are loaded into a gel made up of two segments a stacking (or loading) gel and a resolving gel. The stacking gel has a low concentration of buffers and allows the proteins to migrate as a thin band when a current is applied to them. Application of constant voltage to the gel initiates migration of the lysates with the lower molecular weight proteins moving faster through the gel. Upon completion of this stage there will be a separation of the proteins by the molecular weight (kDa) and the contents of the gel is ready for the transfer stage to a protein binding membrane. Polyvinylidene Fluoride (PVDF) is an inert fluoropolymer that has high protein retention. On contact with the acrylamide gel containing the proteins in the presence of a voltage PVDF can hold the proteins that migrate off the gel. Once bound to the surface of the PVDF membrane the proteins are washed in 5% non-fat milk, this blocks nonspecific low affinity interactions of antibody-protein. Following this incubation with specific antibody allows recognition and stable binding. Primary antibody is then recognised and bound by a secondary antibody used for detection purposes. Secondary antibodies are conjugated to a moiety, commonly Horseradish Peroxidase (HRP) that upon application of a chemical substrate (ECL, Amersham) will produce light. The light emitted by the reaction at the site of the protein of interest can be visualised as a band present when impressed on a sheet of auto-radiographic film in a dark room.

Procedure

Exponentially growing cells maintained in normal cell culture conditions were trypsinised and pelleted in a Falcon tube (10ml) by centrifugation at 1,300 g. Cells were then washed in ice cold phosphate buffered saline (PBS) and respun. To the resulting pellet RIPA buffer was added to lyse the cells, a flask containing $5x10^6$ cells required 100µl RIPA buffer. Lower cell amounts were treated accordingly, and protease inhibitor (Sigma Aldrich) was added at a volume of 1µl per million cells. The tube was then vortexed for 10 seconds to increase the extent of cell lysis and stored at -20°c for 30 minutes, this was then repeated four times to enhance the protein yield. Upon completion the protein lysates were centrifuged at 12,000g for 10 minutes at 4°c and supernatant was transferred into a new 1.5ml Eppendorf tube and stored at -80°c.

Quantification of proteins was required to ensure equal amounts were loaded between samples, unequal loading would influence interpretation of the resulting bands density. Using the Bio-Rad Protein Assay kit (Reagent A 500-0113, Reagent B 500-01114, Biorad) the concentration of proteins in a sample can be obtained. This process used the shift in colour change that was proportional to protein content within the reaction mix. Presence of the reaction shifts absorbance from 465nm to 595nm in conjunction with the stabilisation of the dye. This produced a visible colour change from yellow to blue. A standard solution containing Bovine serum albumin (BSA) in RIPA was produced at 10µg/µl and serial dilutions were performed in RIPA creating a standard curve. A volume of 5µl was loaded into duplicate wells of a clear bottom plastic 96-well plate (Costar), in addition 5µl of protein extracts were also added in duplicate. To each well Bradford reagent A (25ul) and Bradford reagent B (200µl) was added and the plate

left at room temperature for 10 minutes. The plate was then read using 1420 Multilabel Counter (Perkin Elmer) and resulting data transferred to a spreadsheet of the Excel program, determination of protein concentration occurred by the following method:

y = absorbance of well

a = slope of standard curve

x = concentration of sample

b = intercept

y = ax + b

Rearranging the equation gives x = (y-b)/a

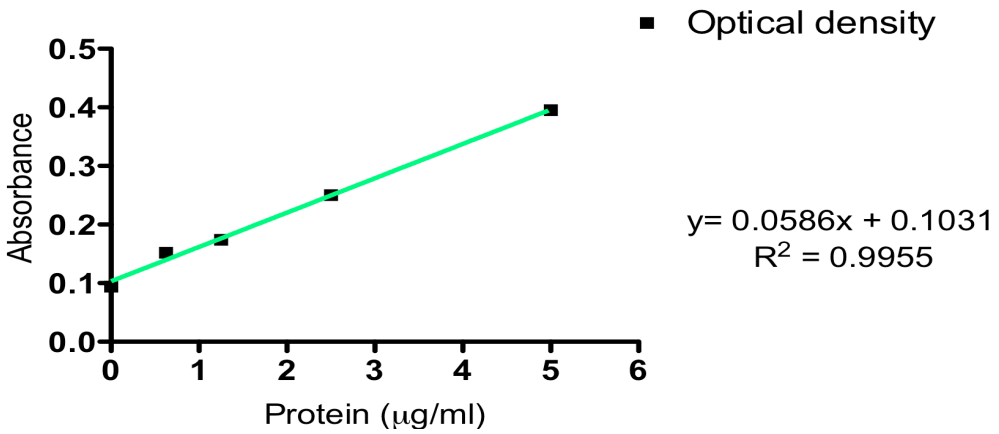

Figure 2.6 Linear regression curve obtained from running protein standards of BSA. This was used to calculate the protein concentration of the collected protein lysate samples. Absorbance is indicated along the y axis and protein concentration is along the x axis.

With the protein concentrations calculated, equal amounts (generally 30-40μg) were diluted into ddH20 and 2x Laemelli buffer (4% SDS, 10% β-mercaptoethanol, 20% Glycerol, 0.004% Bromophenol Blue & 0.125M Tris-HCL pH 6.8) to an equal volume. These were then boiled at 98^{o}c for 5 minutes to reduce secondary and tertiary structures

and coat the proteins in negatively charged SDS. Gels were cast with 12.5% acrylamide content using the following recipe:

Resolving gel:

Compound	Volume
Ammonium Persulphate (Sigma Aldrich)	Spatula tip
ddH_2O	1.9ml
Stock 2*	10ml
30% Bis-Acrylamide (Gene Flow)	8.1ml
Tetramethylethylenediamine (TEMED) (Sigma Aldrich)	6.2µl

* *STOCK2:* (500ml) - 0.75M TRIS 45.5g, 0.2% SDS 1g, pH 8.8, made up with ddH_2O

Table 2.7 Reagents and quantities used in the making of a resolving gel for western immunoblots.

Stacking (or loading) gel:

Compound	Volume
Ammonium Persulphate (Sigma Aldrich)	Spatula tip
ddH_2O	3.7ml
Stock 1*	5ml
30% Bis-Acrylamide (Gene Flow)	1.3ml
Tetramethylethylenediamine (TEMED) (Sigma Aldrich)	3.4µl

**STOCK1:* (500ml) - 0.2 M TRIS 15.15 g, 0.2%SDS 1 g, pH 6.8, made up with dH_2O

Table 2.8 Reagents and quantities used in the making of a stacking gel for western immunoblots.

The thickness of gels used was 1.5mm prepared by using 1.5mm plates (Biorad) and 1.5mm combs (Biorad) containing 10 wells. Once set gels were loaded into gel tanks (Biorad) and combs removed. Samples were loaded into the wells alongside a running ladder made up of marker proteins of a known molecular weight (Dual Colour Precision Ladder (Biorad)).

Gel tanks were filled with 1 litre 1X running buffer (1litre 10X: Glycine 141.1g (Sigma Aldrich), TRIS 30g (Sigma Aldrich), SDS 10g (Sigma Aldrich), made up 1L

dH_2O running buffer, the gels were run at a constant 120v for approximately 90 minutes or until the dye front passed through the bottom of the gel. Upon completion the apparatus was dismantled and gel removed for transfer to the PVDF (Millipore) membrane. This was prepared by immersion in methanol for 10 seconds to activate it, then placed in ddH_2O for 1 minute and then left to equilibrate in 1 litre 1X transfer buffer (1litre 10X: TRIS 30.28g, Glycine 144g, SDS 1g, made up 1L dH_2O – 1X: 100 ml 10X buffer, 700 ml dH_2O, 200 ml methanol) for 5 minutes. Using the appropriate apparatus (Biorad) the gel and PVDF membrane were set up between sponge and filter paper in the following order:

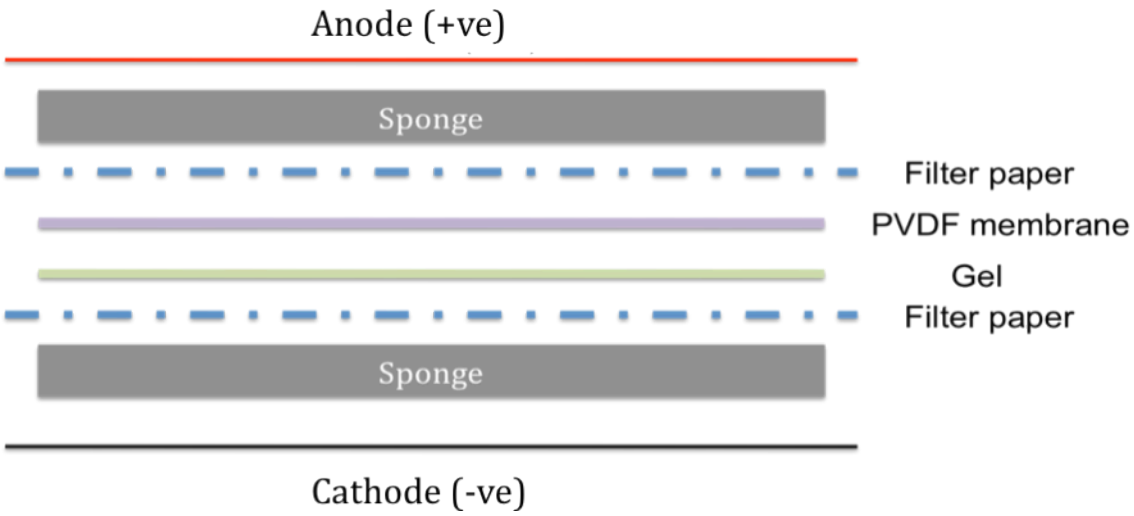

Figure 2.7 Arrangement of wet transfer protocol for protein transfer to PVDF membrane.

To ensure no air bubbles impeded protein transfer efficiency the sandwich was assembled in transfer buffer and each layer was rolled with a pipette to exclude air bubbles. The sandwich was enclosed in a cassette, immersed in transfer buffer containing an ice block and ran for 60 minutes at 80V at room temperature.

Upon completion the sandwich was removed and the PVDF membrane was stained with Ponceau S solution (Sigma Aldrich) for 5 minutes, this was then removed

and membrane washed in ddH_2O. Ponceau S stained present proteins and allowed visual assessment of the success of the transfer, successful transfers were then left in 5% milk dissolved in TBS-T (1litre 10X: 50 ml 1M Tris-HCl pH 7.6, NaCl 20g, Tween-80 0.625ml, dH_2O 2449.4 ml). Milk interacted and bound to the surface of the PVDF inhibiting any low affinity interactions with antibody, thus reducing non-specific binding signals. Blocking was conducted at room temperature on a rocking platform for at least 60 minutes. Upon completion the membrane was washed three times for 10 minutes in TBS-T to remove excess milk. Primary antibody was next added to a solution of 5% milk in TBS-T. Concentration of antibody used varies depending upon their efficiency. The membrane and antibody were incubated overnight on a rocking platform at 4^{o}c. The loading standard used in all western blots was for the β-actin gene and this was incubated at room temperature for 60 minutes. Below is a list of antibodies used in this work and their catalog number.

Antibody	Species	Catalogue number
VDR	Anti-Rabbit	Abcam Ab3508
COX-2	Anti-Rabbit	Cayman 160107
ALOX-5	Anti-Rabbit	Cayman 160402
MCM7	Anti-Mouse	Santa Cruz SC-9966
$P21^{(waf1/cip1)}$	Anti-Mouse	Abcam Ab-7960
β-actin	Anti-Rabbit	Abcam Ab-1801
AKR1C3	Anti-Mouse	Sigma Aldrich A6229

Table 2.9 List of primary antibodies used in Western immunoblotting.

The day after primary antibody incubation the membrane was washed three times for 15 minutes at room temperature. Secondary HRP linked antibody was added to the membrane diluted in 5% milk TBS-T and incubated for 60 minutes at room temperature on a rocking platform. The origin of the primary antibody specifies the secondary to be used and upon completion of the incubation stage it was washed four times for 15

minutes in TBS-T. Visualisation occurred using chemoluminesence (Pierce Super Signal Picostain). Equal volumes of solutions A and B were mixed and pipetted onto the PVDF membrane and left to incubate for 5 minutes. The excess was then removed from the membrane and the membrane was carefully wrapped in cling film and placed into a developing cassette. Exposure took place in a dark room using Kodak autoradiography film and was placed into a developer (Kodak) the exposure times varied depending upon the signal achieved after 1 minute.

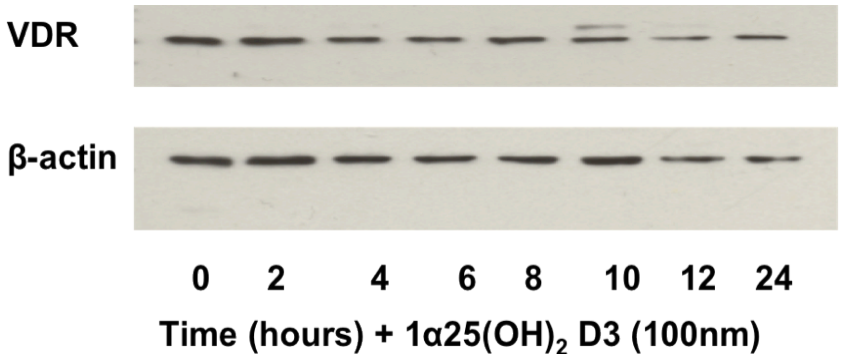

Figure 2.8 An image taken from Western immunoblot analysis probed for VDR and β-actin. The top section depicts bands obtained when probing with the VDR antibody and the lower picture shows bands from β-actin to show levels of protein loading.

2.1.10 Cross-linked Chromatin Immunoprecipitation (xChIP)

Principle

Chromatin immunoprecipitation has become a widely applied method used to detect the presence of proteins at specifically identified genomic loci.. Cells were fixed with formaldehyde, this compound is able to cross-link the protein-protein and even DNA-protein interactions. This created a stable but reversible bond between them. After fixation the cells were lysed and the genomic template sheared to render access to crosslinked DNA-protein. In addition the sheared DNA has to be of a suitable size for

interpretation and PCR analysis. The general chromatin size suggested is a shearing size of 100 to 1000bp (average 500bp). After shearing to a suitable size the soluble chromatin is aliquoted and subject to immunoprecipitation. Protein specific for the antibody is selected (along with bound crosslinked DNA) and washing the immunocomplexes in solutions of increasing salinity reduced unbound DNA impurities.

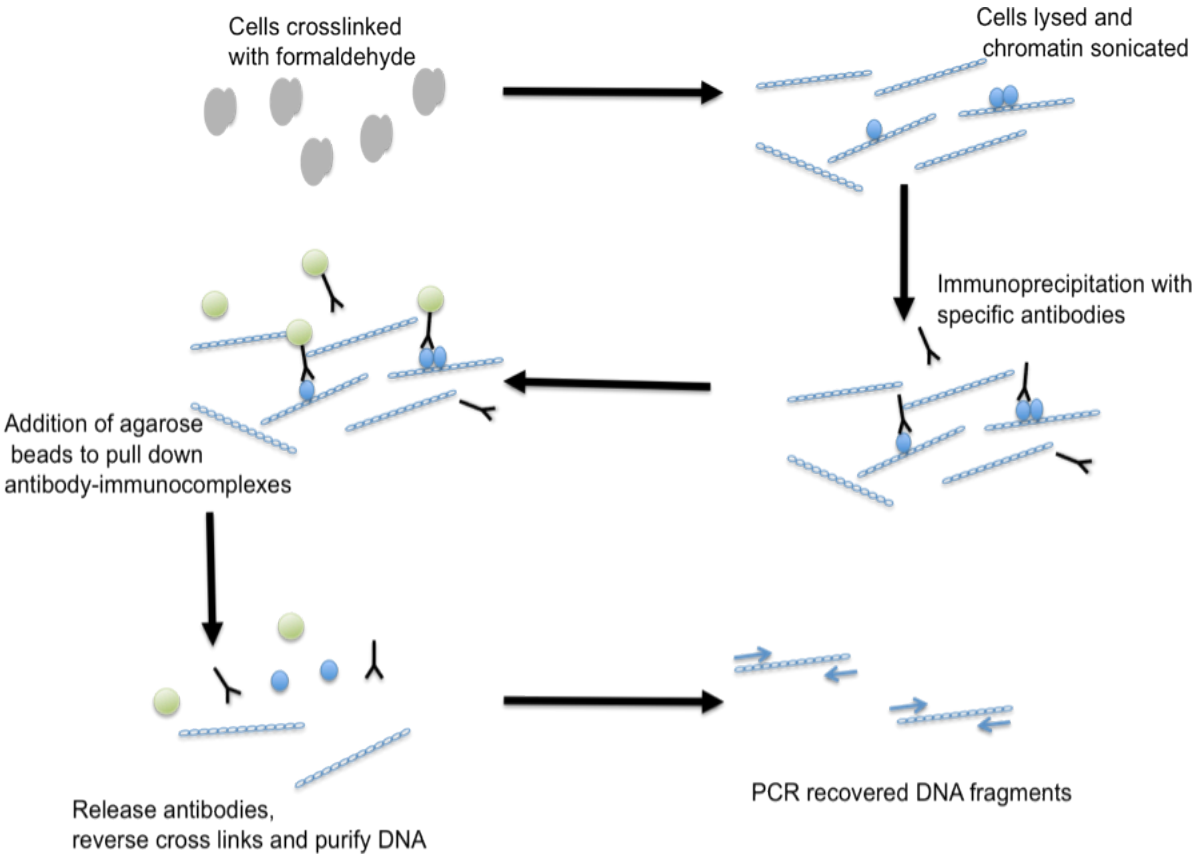

Figure 2.9 Chromatin immunoprecipitation for determining the association of proteins with specific genome sequences in vivo. Protein-DNA interactions are fixed with formaldehyde exposure. Cells are then lysed and soluble DNA sonicated. Specific antibody for the protein of interest is immunoprecipitated and pulled-down with agarose beads. Immunocomplexes are then removed and crosslinks are reversed by heating. Extracted DNA is isolated and used for PCR of specific genomic fragments.

The remaining antibody-Protein-DNA was then eluted to remove antibody. Reversal of the formaldehyde cross-links was conducted through heating and DNA phenol-chloroform extracted and ethanol precipitated.

Procedure

RWPE-1 and PC-3 cells were seeded and left overnight to adhere to the surface of the flasks. At approximately 60% confluence the cells were treated with $1\alpha,25(OH)_2D_3$ (100nm) or ethanol vehicle control. Upon cessation of the timecourse formaldehyde (Sigma Aldrich) was added to each flask to a concentration of 1% for 10 minutes at room temperature. To stop the crosslinking process glycine was added to a final concentration of 0.125M and left for 5 minutes at room temperature. Medium was poured out of the flasks and the cells were washed twice with ice cold PBS (5mls) containing protease inhibitor cocktail (Sigma Aldrich) (1µl per ml). Cells were scraped and harvested into 5mls ice cold PBS (containing protease inhibitor) and then spun at 1,200 g for 5 minutes at 4^oc. The resulting cell pellet was then suspended into SDS lysis buffer and left at room temperature for 5 minutes. Sonication was performed using a Diagenode Bioruptor specifically produced for chromatin shearing. Lysates were sonicated in ice cold water on a medium setting for 30 seconds on and 30 seconds off repeated with 5 cycles. Cellular debris was then removed by centrifugation at 12,000g for 10 minutes at 4^oc, and the supernatant containing the soluble chromatin fraction was transferred to new Eppendorfs. Aliquots of chromatin (200µl) were diluted to 500µl using dilution buffer (0.01%SDS, 1.1% Triton X-100, 1.2mM EDTA, 16.7mM Tris-HCl pH 8.1 and 167mM NaCl) and antibody added. This was then incubated on an end over end rotator (25 rotations per minute) overnight at 4^oc.

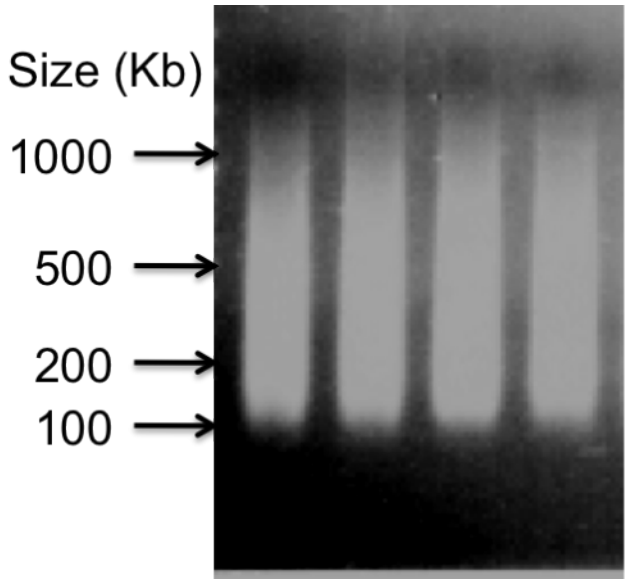

Figure 2.10 Chromatin fragments with an average shear size of 500bp. Chromatin has been sheared using the Bioruptor Sonicator. The sheared chromatin is analyzed on a 1.5% agarose gel.

Antibody	Catalogue number
VDR	Ab3508
p-POL II	Ab5131
NCOR1	Ab24552
NCOR-2/SMRT	Ab24551

Table 2.10 Antibodies used in the ChIP procedure and their respective catalogue numbers.

The following day protein A/G agarose slurry (Millipore) (60µls) was added to the sample and left to rotate for 1 hour. This collected the immunocomplexes formed over the previous night. Protein A (IgG binding protein) agarose beads have a porous sponge like structure that binds the antibodies immobilizing the protein-DNA bound fragments. The agarose pellets were spun 100g for 1 minute and washed sequentially on an end over end rotator with the following solutions: Low salt immune complex wash

buffer (0.1% SDS, 1%Triton X-100, 2mM EDTA, 20mM Tris-HCl pH8.1 and 150mM NaCl), high salt immune complex wash buffer (0.1% SDS, 1%Triton X-100, 2 mM EDTA, 20 mM Tris-HCl pH 8.1 and 500mM NaCl), LiCl immune complex wash buffer (0.25M LiCl, 1% NP40, 1% sodium deoxycholate, 10mM Tris-HCl pH 8.1 and 1mM EDTA) and twice with TE buffer (10mM Tris-HCl pH 8.0 and 1mM EDTA). Elution of immunocomplexes occurred within elution buffer (250µls) rotating for 30 minutes at room temperature. During this time Protein-DNA bound fragments were released from the agarose. This was repeated yielding 500µl of protein-DNA solution. Collected protein-DNA fragments present in the supernatant were subjected to 65^{o}c heating and NaCl (200mM) overnight to reverse the formaldehyde crosslinks. The following day proteinase K (40µg/µl) (Invitrogen) was added to the samples and incubated at 42^{o}c for at least 1 hour to digest proteins. This was conducted alongside a 200µl sample of stock chromatin made up to 500µl with dilution buffer (0.01%SDS, 1.1% Triton X-100, 1.2mM EDTA, 16.7mM Tris-HCl pH 8.1 and 167mM NaCl). This produced the input samples representing total DNA within the cell. DNA extraction, with the addition of phenol/chloroform/isoamyl alcohol (25:24:1) (500µl) (Ambion), was mixed well using a vortex mixer and spun for 5 minutes at 12,000g. This produced three phases and the clear top phase was collected taking care not to collect the intermediate white protein phase. The supernatant was re-extracted with chloroform (500µl) to remove excess phenol and mixed well before centrifugation at 12,000g for 5 minutes. Then clear supernatant was removed and added to ice-cold ethanol (1ml), glycogen (20µg/µl) (1µl) and sodium acetate (120µl) 3M pH5.2 and stored at -20^{o}c for at least 1 hour. The tubes were then spun for 15 minutes at 12,000g at 4^{o}c and the supernatant removed with care taken not to

disturb the DNA pellet. This was then washed with 70% ethanol and spun at 12,000g for 5 minutes and air dried before resuspension in nuclease free water (50μl). The resulting DNA is then stable for an indefinite period of time and stored at -20°c. DNA obtained from the chromatin immunoprecipitation (alongside the input samples of sonicated chromatin) was then be examined by PCR using primers design to amplify specific genomic regions the result of which is demonstrated below.

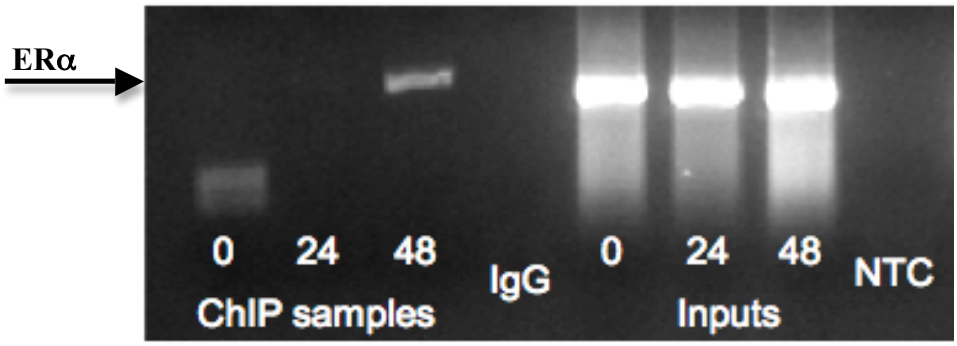

Figure 2.11 Example of semi-quantitative PCR from a ChIP experiment using the described protocol. The oestrogen receptor antibody (Santa Cruz) was used to pulldown crosslinked and sonicated chromatin in breast cancer cell line MCF-7 cells. This identified an ERα response element located proximal to the *PBF* gene and published in Watkins et al 2010 [168]. NTC= No template control.

However, as stated previously this process was semi-quantitative. Therefore, quantitative PCR analysis in real time with the double stranded DNA dye SYBR Green was preferred. This had a number of advantages over analysis by gel electrophoresis, not least was the high throughput approach increasing the number of samples used. Firstly, the product of PCR was quantified in the linear range and not an endpoint reaction. In addition to this reactions can be easily ran in triplicate wells preventing the drawing of conclusions from a single PCR reaction. SYBR Green is an intercalating dye able to

occupy double stranded DNA and was a financially viable alternative to using expensive FAM-TAMARA dyes used in q-RT-PCR reactions. The dyes level of fluorescence was measured at the annealing stage of each cycle allowing the PCR reaction to be visualized and quantified. The read out given was an amplification curve plotted on a graph of cycle time (Ct) and $\log_{10}$ fluorescence. As there was no specific probe used and SYBR Green was not selective all double stranded DNA will emit a fluorescent signal. A dissociation curve stage was carried out at the end of each PCR to ensure that the primers have formed a single product. Final measurements were an average of at least three independent experiments performed in triplicate wells for each timepoint. As with regular amplification of genomic DNA PCR with ChIP DNA used oligonucleotides approximately 20-22 bases in length with melting temperature of approximately 60^{o}c. However, in addition to these requirements primers for amplification of ChIP'ed DNA should yield a product no greater than 146 base pairs (the length of DNA wrapped around one nucleosome). To exclude binding non-specific target amplification and maintain primer efficiency sequences were validated for their optimum concentration and melting temperatures are shown below in Figure 2.12.

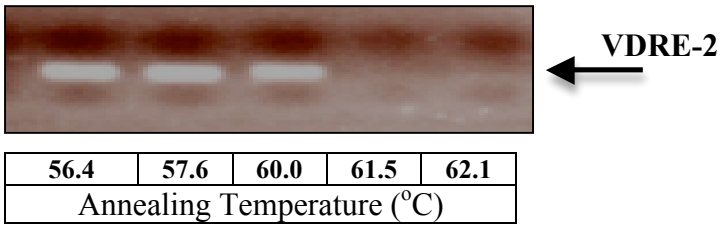

Figure 2.12 An example of a gradient PCR result examining optimum annealing temperatures for primer pairs. The above image demonstrates that primer pair VDRE-2 can be used with an annealing temperature between 56.4^{o}C and 60.0^{o}C.

Each primer set was subject to PCR reactions using a gradient PCR of five different annealing temperatures, products were then run on a 1.5% agarose gel containing ethidium bromide and visualised.

Region	Genomic location 5' – 3'	Forward	Reverse	Annealing Temp
TSS	-20 to +50	TATATCAGGGCCGCGCTG	GGCTCCACAAGGAACTGACTTC	60°C
VDRE1	-2146 to -2129	GAGGAAGGGGATGGTAGGAG	CTGGCAGATCACATACCCTGT	60°C
VDRE2	-4505 to -4489	TAGAGATGCTCAGGCTGCTG	AGAGCTTCACCGACATAGCC	60°C
VDRE3	-7056 to -7036	AGCAGCACTGAAGCCTAACC	GAGAGGCCTACCAGCTTCAG	60°C

Table 2.11 Forward and reverse primers used for p21$^{(waf1/cip1)}$ amplification in ChIP experiments, annealing temperature used and genomic location.

Reagent	Volume (µl)
PCR Master Mix dt (Quantace)	5.000
SYBR Green (Quantace)	0.200
Forward Primer (100µM)	0.125
Reverse Primer (100µM)	0.125
Nuclease Free Water	2.800
DNA	2.000

Table 2.12 Master mix reagents and volumes used for the q-RT PCR analysis of ChIP samples using SYBR Green.

For analysis of ChIP recovered DNA Q-RT PCR was performed using the following program.

Time	Temperature (°C)	Cycles
30 seconds	50	1
15 minutes	95	1
45 seconds	95	40
45 seconds	60	40
45 seconds	76	40

Table 2.13 PCR program for q-PCR analysis of ChIP recovered DNA.

SYBR Green is a nonspecific intercalating fluorescent dye it will emit a light signal upon interaction with double strand DNA. Therefore, it is important a dissociation study be performed on every PCR plate run. Triplicate wells were then examined for their dissociation curve, a single curve confirms that there is one specific product formed in the PCR well. Dissociation curves with more than one peak were excluded from the triplicate set (Figure 2.13).

Calculation for ChIP enrichment were as follows:

$$dCt\ (normalised\ ChIP) = (Ct_{(ChIP)} - (Ct_{(input)} - LOG^2\ (3.322^*))$$

$$\%\ Input = 2(-dCt(normalised\ ChIP))$$

*= Fraction of Input chromatin saved (1%)

Time	Temperature (°c)	Cycles
15 seconds	95	1
1 minute	60	1
15 seconds	95	1

Table 2.14 Dissociation curve program required to confirm single PCR product is formed within each wells reaction.

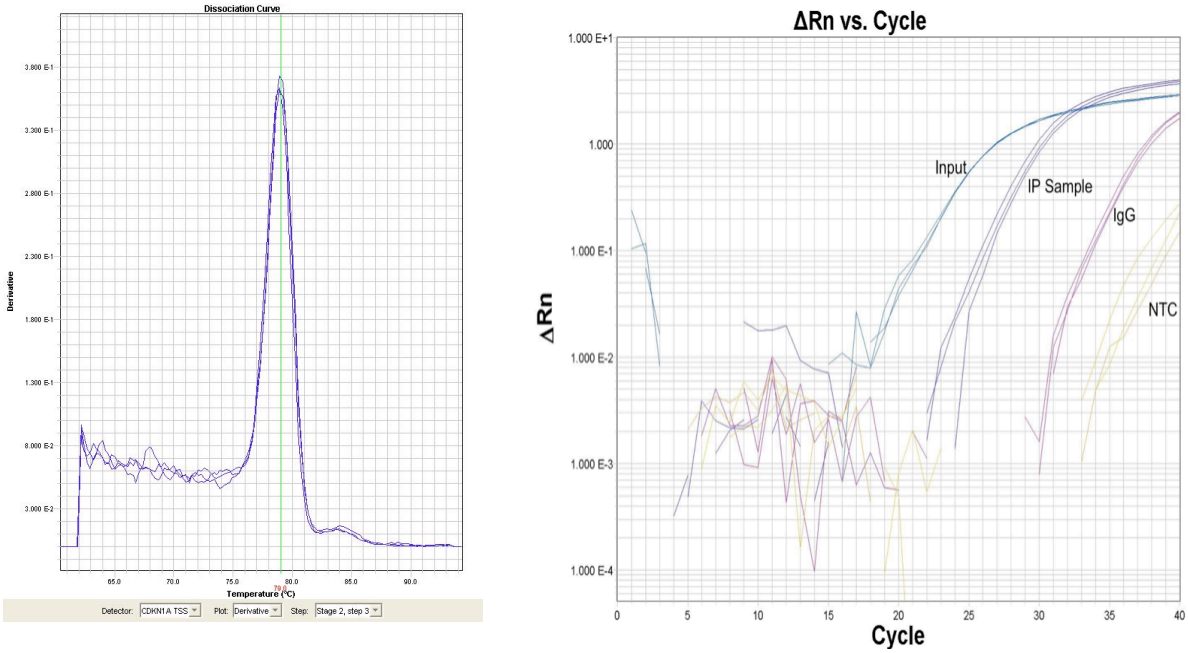

Figure 2.13 Image showing a dissociation curve peak and ChIP sample amplification curves demonstrating a single product formed in a PCR triplicate. Appearance of more than one peak indicates that non-specific product is also being formed and such wells are excluded from the analysis. q-Real-Time PCR amplification curves (right) from ChIP experiments. The IP sample produces a Ct higher than the Input chromatin and a Ct lower than that of the IgG negative control immunoprecipitation. An additional no template control well is depicted that arises above 35 cycles and therefore is discounted as it is due to fluorescence from primer dimers formed in the absence of DNA template.

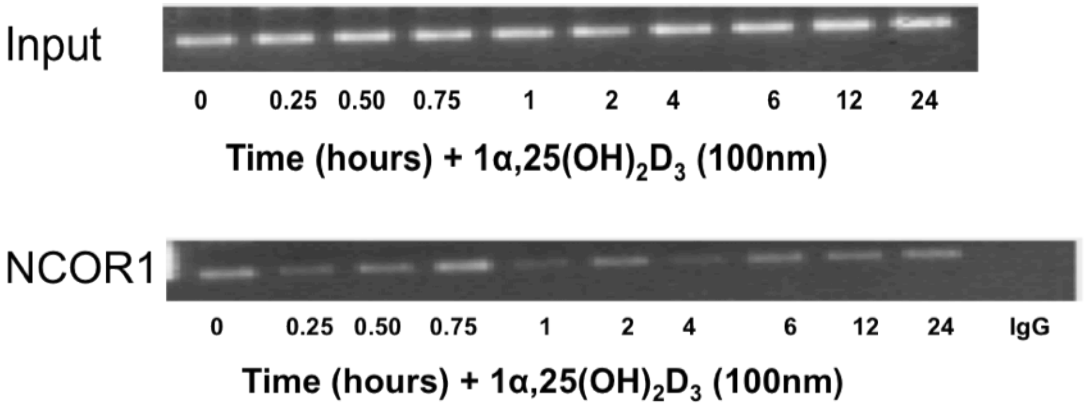

Figure 2.14 Image showing q-RT-PCR products from xChIP experiments using NCOR1 specific antibody ran out on a 1.5% agarose gel alongside Input samples. Crosslinked ChIP was conducted as described above. Recovered DNA was extracted and subject to Q-RT-PCR, upon completion the PCR product was removed from the well and ran on an ethidium bromide agarose gel at 100volts.

2.1.11 Re-ChIP

Re-ChIP was conducted as per xChIP with the addition of a further immunoprecipitation step. This is performed to examine the extent of co-occupancy of two proteins at the same genomic location. During the cross linking process protein-protein binding was fixed as well as protein-DNA binding. This means by performing Re-ChIP the relationship between two proteins can be observed. The experiments performed in this thesis investigated the levels of co-occupancy between VDR and NCOR1 and VDR and NCOR-2/SMRT. Therefore, the following antibodies were used:

Re-ChIP	First IP	Second IP
VDR-NCOR1	VDR (Ab3508)	NCOR1(Ab24552)
VDR-NCOR-2/SMRT	VDR (Ab3508)	NCOR-2/SMRT (Ab24551)

Table 2.15 Order of Re-ChIP antibody and their product identification.

Re-chip was performed as per the xChIP protocol with the addition of an incubation step in dilution buffer containing Dithiothreitol (DTT) (10mM) for 1hour. This is a strong reducing agent able to elute the first immunoprecipitant antibody (due to the high affinity for disulphide bonds) whilst leaving the formaldehyde crosslinks unaffected. The second round of immunoprecipitation took place and was washed as described in the xChIP procedure. Elution and extraction of immunoprecipitated DNA was performed as per above and q-RT PCR carried out using specific primers for the genomic region of interest.

2.1.12 Native chromatin Immunoprecipitation (nChIP)

Native chromatin immunoprecipitation is used for the analysis of histone modifications at specific genomic loci. The DNA from all nChIP samples used in this thesis were produced by Dr. James Thorne and used to examine the VDREs contained within the $p21^{(waf1/cip1)}$ promoter region in chapter 5. In addition to this the author of this thesis performed Q-RT-PCR for the following regions used the remaining DNA material from these samples:

Region	Genomic location 5' – 3'	Forward	Reverse	Annealing Temp
G0S2 TSS	+65 to -45	GGGGCCGCTTATATCTTTC	TTTTCCCCTCCTCTTCTTCC	60°C
ALOX5 TSS	+55 to -102	GCGTGAAGAGTGGGAGAGAA	CCAGGTGTCCGCATCTAGC	60°C
PTGS2 TSS	-22 to +58	GGAAGGTTCTCTCGGTTAGC	CTGCTGAGGAGTTCCTGGAC	60°C

Table 2.16 Forward and reverse primer sequences used for analysis of transcription start sites (TSS) using nChIP samples.

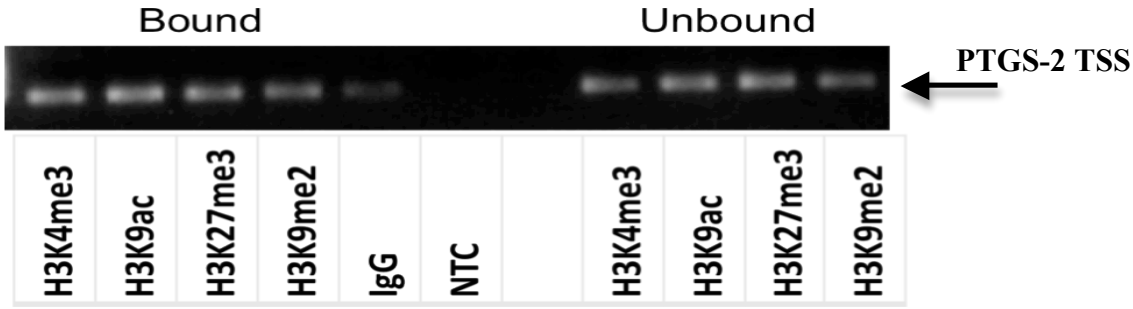

Figure 2.15 q-RT-PCR product performed on nChIP samples ran on an agarose gel (1.5%). Soluble chromatin was digested using micrococcal nuclease and immunoprecipitated with antibodies specific to histone tail modifications described above. Recovered DNA was extracted and subject to q-RT-PCR. Upon completion the PCR product was removed from the well and ran on an ethidium bromide agarose gel at 100volts.

Calculation for nChIP enrichment were as follows:

Normalised Fold Enrichment = $LOG^{2(Bound-Unbound)}$

2.1.13 Short hairpin RNA knockdown (ShRNA)

Principle

RNA interference is a naturally occurring mechanism used by cells to regulate translation of genes. In this way a gene can be transcribed but the genes active product (protein) is never formed. Responsible for the identification and breakdown of the gene transcript are short sequences of RNA approximately 22 nucleotides in length named small interfering RNAs (siRNA). These are made up of specific sequences complimentary to segments of the target genes mRNA. This gives siRNAs the ability to detect and bind to their corresponding targets marking them for degradation, and resulting in the functional protein not being translated. The first identification of this short sequences was found in plants and since has been identified in yeast all the way up to higher eukaryotes. This process has been utilized by molecular biology with the transfection of sequences into a cells genome able to produce siRNA effects. However, the transfection of siRNA into mammalian cells is not stable. As the cells divide it is lost due to a lack of the required RNA polymerases needed for their propagation. Therefore, molecular biology has had to develop a new technique specific for shRNA transfection stable across successive generations. Using a vector based system not only allows the incorporation of the polymerases required but also the sense and antisense sequences required to produce knockdown of a specific mRNA sequence. Furthermore, the vector also contains a resistance sequence (often to an antibiotic) producing drug resistance. This allows the use of a selective agent (such as Neomycin) that permits only cells expressing resistance to grow and those that do not carry the vector will die.

Procedure

To produce shRNA targeting AKR1C3 oligos containing the short hairpin sequence (Sigma Aldrich) were annealed and inserted in a pcDNA3.1 vector (Invitrogen). This has had the original CMV promoter substituted with the human H1 promoter. Both this and the establishment of the stable ShAKR1C3 cells was performed by Dr. Farhat Kahnim (University of Birmingham). Briefly, PC-3 cells were transfected with 2μg plasmid DNA and 6μl of lipofectamine 2000 transfection reagent. Transfection was ceased after 24 hours and RNA was extracted and subjected to reverse transcription and Q-RT-PCR using primers specific for 18s and AKR1C3.

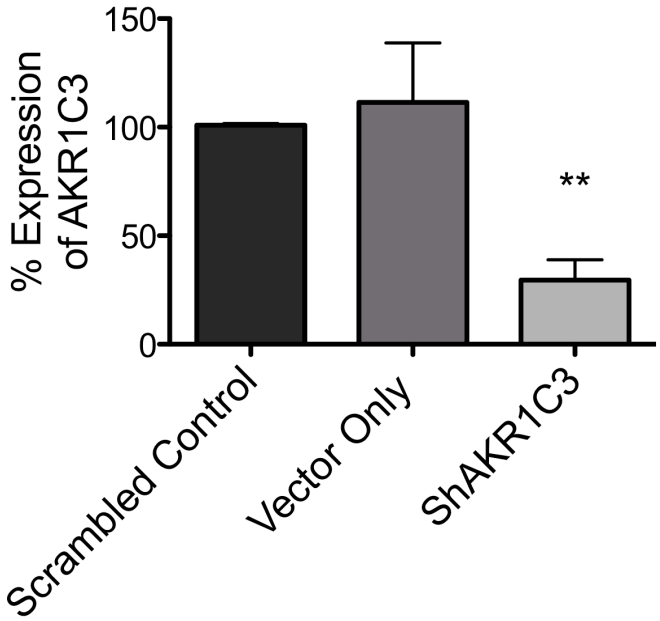

Figure 2.16 Validatory confirmation of scrambled control versus vector only and ShAKR1C3 sequences. PC-3 cells were seeded with of $5x10^5$ per well in a 6 well plate and left to adhere overnight. Cells were transfected with plasmid DNA and Lipofectamine 2000 for 24 hours. The following day mRNA was extracted, reverse transcribed and Q-RT-PCR performed. Each data point represents the mean of three separate mRNA isolates amplified in duplicate wells ±SEM. Statistical significance assessed using t-test (**=p-value <0.01).

2.1.14 MicroRNA isolation and extraction from TRAMP model serum samples

Principle

MicroRNAs are 19-24 base pairs in length and are highly abundant, currently there are approximately 800 microRNAs in observed in human cells [169]. However, the list has been rapidly expanding and their deregulation has also become apparent in many different cancers (reviewed in [170]) . However, more recent investigations demonstrated that serum and plasma samples are able to reflect levels of deregulated microRNAs found in disease states. This has propelled serum analysis for microRNAs to the forefront of diagnostic biomarker research.

Procedure

TRAMP mouse serum samples were collected from Roswell Park Cancer Institute Core Resource and extracted using the following protocol. Serum samples (100µl) were mixed with Trizol LS (300µl) (Invitrogen) and left to equilibrate at room temperature for 5 minutes. This allowed RNA extraction from a smaller number of cells or a sample that may have a low concentration of RNA such as serum. Chloroform (100µl) was added to the tube and vortexed for 10 seconds before leaving at room temperature for 10 minutes. The tubes were then centrifuged for 15 minutes at 12,000g. To the supernatant isopropanol (propan-2-ol) (200µl) was added and the tube inverted 5 times and kept at -20^{o}c for 30 minutes to ensure precipitation of RNA. The sample was then centrifuged for 10 minutes at 12,000g at 4^{o}c to collect a nucleic acid pellet at the bottom of the Eppendorf. The isopropanol was then removed and the pellet resuspended in 75% ethanol and centrifuged for 5 minutes at 12,000g at 4^{o}c. The 75% ethanol was then removed and the sample resuspended in nuclease free water (50µl) and stored at -80^{o}c. Reverse transcription of microRNA used an Applied Biosystems Reverse Transcription

microRNA kit. A master mix was produced for the specific microRNA of interest, alongside a second master mix. This second master mix was usedfor reverse transcription of the internal control used in the q-RT PCR reaction. The control most often used when investigating microRNAs in murine samples is snoRNA202, shown to be highly abundant in mouse tissue and so most commonly used. Therefore, two reverse transcription master mixes were produced. Upon completion of the reverse transcription protocol the samples are stored in -20^{o}c.

Component	(n=1) per 15 µl reaction
dNTP	0.15µl
RNase Inhibitor	0.19µl
Reverse Transcriptase enzyme	1.00µl
10x RT Buffer	1.50µl
Nuclease Free Water (NFW)	4.16µl
5x RT MiR106b Primers	3.00µl
RNA	10ng

Table 2.17 Components of the reverse transcription reaction required for miR106B.

Component	(n=1) per 15 µl reaction
dNTP	0.15µl
RNase Inhibitor	0.19µl
Reverse Transcriptase enzyme	1.00µl
10x RT Buffer	1.50µl
Nuclease Free Water (NFW)	4.16µl
5x RT SnoRNA202 Primers	3.00µl
RNA	10ng

Table 2.18 Components of the reverse transcription reaction required for the endogenous control SnoRNA202.

The reverse transcription of microRNAs was then conducted using the following thermal program:

Time	Temperature
30minutes	16°C
30minutes	42°C
5minutes	85°C
∞	4 °C

Table 2.19 Thermal profile for reverse transcription of microRNAs using Reverses Transcription microRNA kit (Applied Biosystems).

The q-RT PCR analysis of microRNAs in serum required the running of both the specific miR106B sample and SnoRNA202 in singleplex reactions. The MiR106B and SnoRNA202 reverse transcribed products were placed into a PCR reaction with their specific PCR primer and probe combinations (Applied Biosystems) in the quantities described below.

Component	(n=1) per 10 µl reaction
Master Mix	5µl
MiR106B Primer & Probe Mix	0.5µl
Nuclease Free Water (NFW)	3.5µl
cDNA MiR106B	1µl

Table 2.20 Components of the q-Real-Time PCR reaction required for miR106B.

Component	(n=1) per 10 µl reaction
Master Mix	5µl
SnoRNA202 Primer & Probe Mix	0.5µl
Nuclease Free Water (NFW)	3.5µl
cDNA SnoRNA202	1µl

Table 2.21 Components of the q-Real-Time PCR reaction required for the endogenous control SnoRNA202.

An ABI 7500 fast real time PCR system was used under the following cycle conditions:

Time	Temperature (°c)	Cycles
2 minutes	50	1
10 minutes	95	1
15 seconds	95	40
1 minute	60	40
30 seconds	72	40

Table 2.22 Thermocycling conditions for the amplification of MiR106B and the endogenous control SnoRNA202 .

Final measurements were an average of a minimum of three independent experiments, in triplicate wells for each condition. Assessment of statistical significance was performed using fold chances of gene expression was conducted by applying the unpaired t-test.

Upon analysis of the q-RT PCR data it was found that SnoRNA 202 was not present in the serum samples of TRAMP murine model. Therefore, it was necessary to explore alternative endogenous controls. The endogenous control used for analysis of human cell lines is the ribosomal 18s. Mouse 18s is homologous to human 18s and so it was decided that 18s levels of the TRAMP mouse cDNA should be assessed in serum. As shown in table 2.22 the levels of MiR-16 and MiR-143 were measured. Serum samples showed a high Ct of 18s and therefore two additional endogenous control alternatives were examined. These have been identified as potentially useful endogenous controls in serum analysis [171] and were assed for their level of expression. MiR-16 provided the highest level of expression (lowest Ct) and so was chosen as the endogenous control in serum q-RT PCR samples.

Endogenous control	SNO202	18s	MiR-16	MiR-143
Mean Ct	Undet.	27.37	25.46	31.61
STD Dev	Undet.	2.85	1.77	1.49
SEM	Undet.	0.42	0.26	0.22

Table 2.23 Comparison of the different endogenous controls used in the analysis of MiR-106B levels.

Chapter 3: Pre-receptor manipulation of PPARγ signalling

3.1 Introduction

Nuclear Receptors (NRs) regulate gene targets that control cell growth and differentiation in prostate epithelial cells. The ability of NRs to exert these gene regulatory effects is intimately controlled by numerous factors including epigenetic mechanisms (reviewed in [172, 173]). However, NR activity is also governed by ligand availability.

Targeting of the AR by androgen deprivation therapy (ADT) forms the current treatment mainstay for CaP that has escaped the local prostate environment. However, recurrence of CaP in a castrate recurrent form, so called ADT-R CaP is predominantly lethal [174]. CaP in both early and late stage disease remains an attractive target for anticancer therapies that target NRs such as VDR, RARs/RXRs and PPARα/γ. However*, de novo* and acquired receptor resistance has limited these applications.

Expression of PPARγ is sustained in CaP and is able to exert a range of tumour repressive effects. Through induction of anti-proliferative and pro-differentiating gene targets PPARγ receptor has been the target of a phase II clinical study with Troglitazone, suggesting that this NR is a promising potential target for prostate cancer therapy [175]. Deregulated co-repressor functions appear to be an important component for this resistance [176] with similar events disrupting AR signalling [177, 178] (reviewed in [85]). In an attempt to restore and enhance growth restraint a number of studies have targeted enzymes involved in androgen synthesis.

As a mechanism to restore PPARγ signaling we have considered the regulatory actions of aldoketoreductase 1C3 (AKR1C3), a type 2 3α-Hydroxysteroid dehydrogenase or 17-beta-HSD type 5. This is involved in the metabolism of androgen, converting androstenedione to testosterone [139]. However, AKR1C3 is a highly promiscuous, multi-functioning enzyme

that is able to convert many different substrates. The lack of primary substrate may result in the enzyme acting on alternative substrates, among which are the arachadonate derived prostaglandins that act as *de novo* ligands for PPARγ. Perhaps reflecting this ambiguity the other substrate choice for AKR1C3 is overexpressed in prostate cancer tissue samples and cell lines [179], but also is detected in cell lines with absent or low levels of AR. These findings suggest that 5α-Dihydrotestosterone may not be the primary substrate of AKR1C3 [137, 138].

AKR1C3 may therefore utilise prostaglandin D_2 (PGD_2), converting it into the 9α,11β prostaglandin F_2 [141] and preventing the generation of PGJ_2 which is a potent, endogenous PPARγ ligand. Medroxyprogesterone acetate (MPA) is a sex hormone that has been demonstrated to be a potent inhibitor of AKR1C3 and other metabolic enzymes [180]. In leukemic systems a synergistic effect on cell death occurs in combination with PPARγ ligand bezafibrate, as a result of elevation of PGD_2 concentrations [181]. Combinatorial treatments of MPA and PGD_2 have been shown in other cancer disease models and samples to induce apoptosis and cell cycle arrest through PPARγ mediated activation pathways [182]. These findings suggest that elevated AKR1C3 may provide two key CaP benefits; namely to promote AR signalling and to limit anti-proliferative actions of PPARγ signalling. This study examined the effect of reducing AKR1C3 levels in prostate cell lines and thus elucidating its role in ADT-R CaP. ADT-R CaP cells stably expressing a short hairpin RNA sequence to AKR1C3 were investigated for the impact of the response to treatment with PGD_2.

3.2 Results

3.2.1 Characterisation of ShAKR1C3 clones.

The transfected short hairpin mRNA sequence is processed in the nucleus by DROSHA and exported into the cytoplasm where it is bound by the RISC complex and cleaved. The resulting short nucleotide sequence, complementary to *AKR1C3* mRNA (shAKR1C3) is able to detect AKR1C3 transcript targeting it for degradation. Thus cell lines stably expressing reduced *AKR1C3* mRNA and protein are produced. The clones transfected with shAKR1C3 sequence were measured against an empty vector control.

PC-3 and DU 145 cells containing the short hairpin sequences showed significant reduction in AKR1C3 mRNA in comparison to the vector only (VO) control transfection data (shown in Figure 3.1).

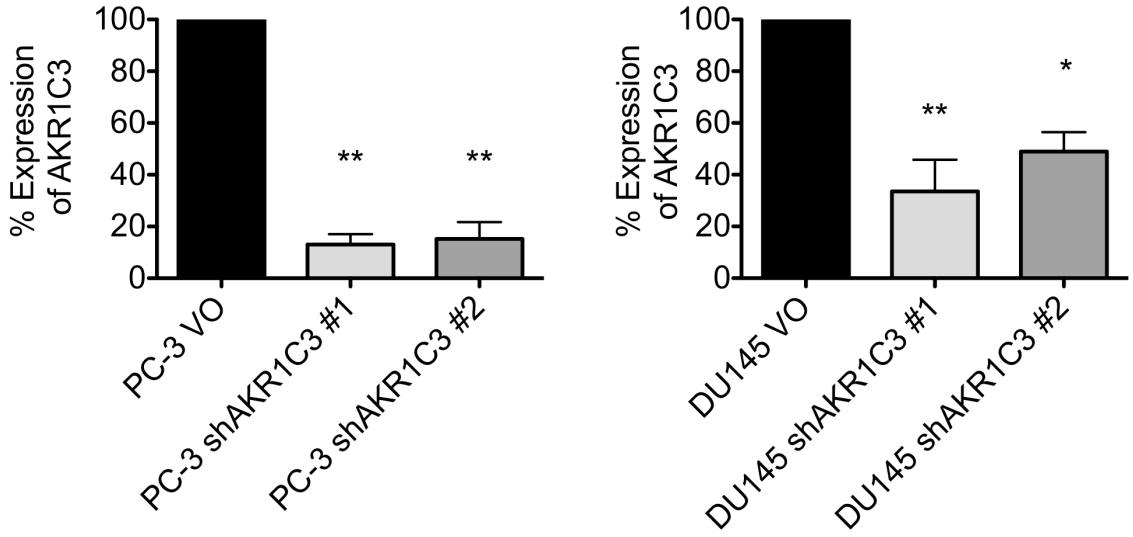

Figure 3.1 Stably expressing shAKR1C3 achieved significant AKR1C3 knock-down in prostate cancer cell lines. PC-3 and DU 145 cells were seeded with of $5x10^5$ per well in a 6 well plate and left to adhere overnight. The following day mRNA was extracted, reverse transcribed and Q-RT-PCR performed. VO = Vector only. Each data point represents the mean of four separate mRNA isolates amplified in triplicate wells ±SEM. Statistical significance assessed using t-test (*=p-value <0.05, **=p-value <0.01).

PC-3 short hairpin clone #1 demonstrated 13.08% (±4.00 SEM) and clone #2 demonstrated 15.21% (±6.50 SEM) expression in comparison to the vector only control. DU 145 shAKR1C3 also show reduced transcript measured at (33.56% (±12.21 SEM) and 48.91% (±7.52 SEM) for clone #1 and clone #2 respectively.)

To examine further the extent of AKR1C3 knockdown Western immunoblot analysis was conducted using an antibody specific for the AKR1C3 protein. The shAKR1C3 transfected cell lines demonstrated reduced AKR1C3 at a protein level (Figure 3.2).

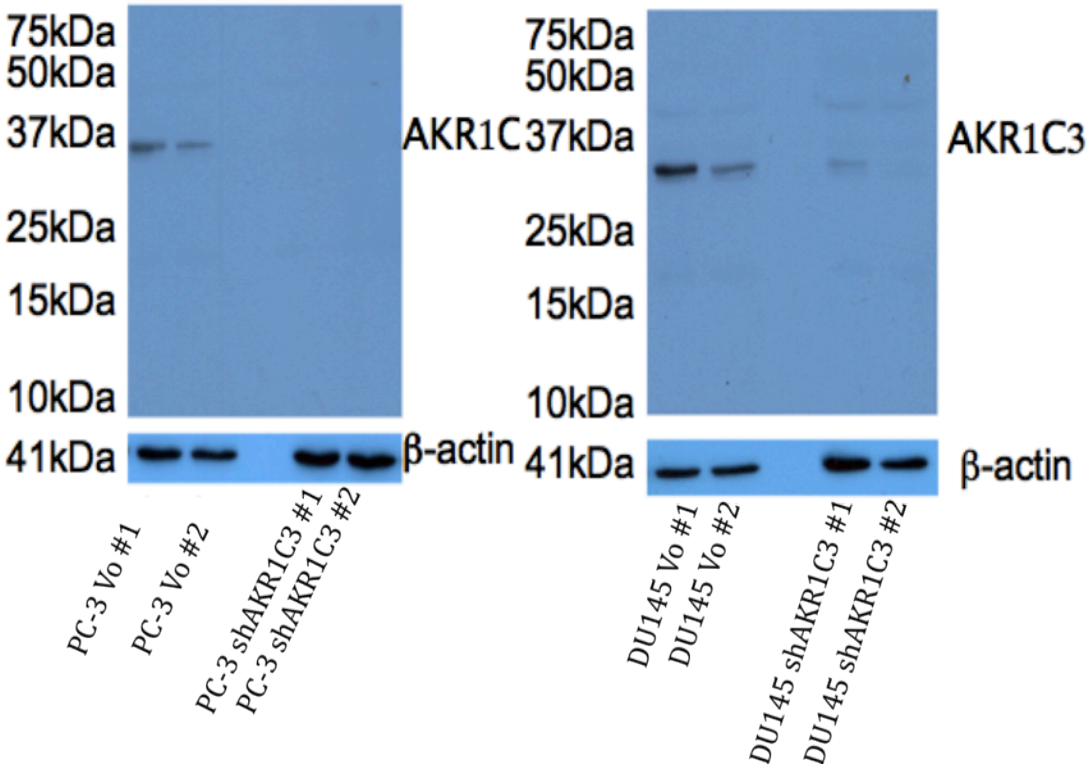

Figure 3.2 Protein levels in ShRNA AKR1C3 Clones. PC-3 and DU 145 cells (two Vector only (VO) and two shAKR1C3 clones) were plated at $1x10^6$ into T75 flask and left overnight to adhere. The following day cells were harvested and proteins extracted. Analysis of AKR1C3 was determined using Western immunoblot. Representative image shown of three independent experiments. β-actin used as a loading control.

To examine the functional consequence of reduced AKR1C3 mRNA and protein and to test the hypothesis that AKR1C3 contributes to impaired PPARγ activity the actions of PPARγ in the absence of AKR1C3 were investigated.

3.2.2 Effect of PGD_2 addition on growth rate in the reduced AKR1C3 environment.

Given that prostaglandin D_2 is the biological precursor of PGJ_2, exogenous addition would prompt either the conversion into PGF_2 or hypothetically in the shAKR1C3 cells permit non-enzymatic conversion to the PPARγ ligand PGJ_2. Therefore a dose response of PGD_2 was conducted to establish any dose dependent effect that varies between the two cell lines. Data obtained from this experiment are shown in Figure 3.3. Exposure to PGD_2 (5.0μM) in PC-3 shAKR1C3 clone 1 produced no significant decrease in proliferation, an effect similar to that seen in DU 145 knockdown cells. In addition, lower concentrations of PGD_2 (2.50μM, 1.25μM and 0.625μM) also produced no significant change in proliferation response in comparison to vector only controls.

Therefore, exogenous addition of PGD_2 did not induce a significant decrease in proliferation. In an attempt to enhance to action of PPARγ treatment in the presence of the HDAC inhibitor Suberoylanilide hydroxamic acid (SAHA) was conducted. It was hypothesized that the use of SAHA in this study would overcome aberrant levels of HDAC activity present in malignant cell lines that may limit PGD_2 signalling via PPARγ.

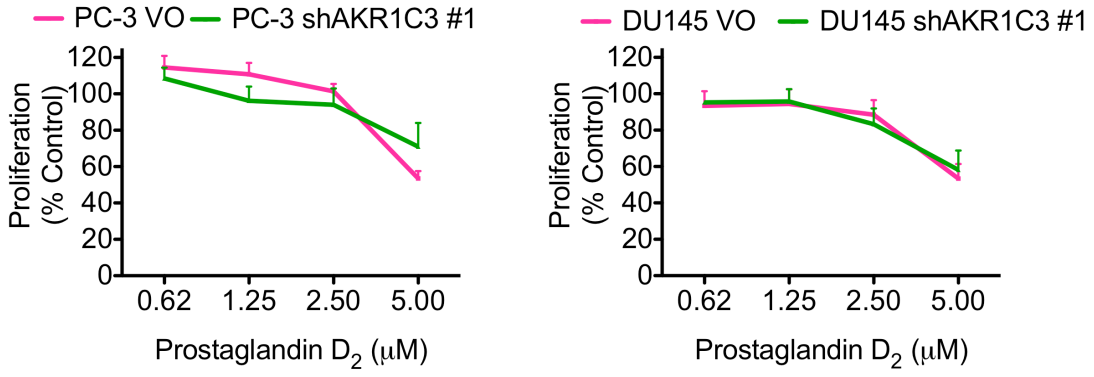

Figure 3.3 Cell proliferation is not altered in cells with AKR1C3 knockdown in response to PGD_2. Cells were plated in a 96-well plate at $2x10^3$ cells per well. PC-3 shAK1C3 #1 and DU 145 shAKR1C3 #1 dose response to PGD_2 was measured. Ligand exposure time was 96 hours with retreatment at 48 hours. VO=Vector only. Each data point represents the mean of four independent experiments each in triplicate wells ± SEM.

3.2.3 Cell proliferation in response to the HDACi SAHA in PC-3 and DU 145 ShAKR1C3 transfected cells.

Prostate cancer tissue and cell lines have been shown previously to have a decreased level of acetylated lysine residues in their core histones [151, 183]. A reduction in the overall level of HDAC activity is proposed to increase in lysine acetylation and induce an open chromatin context. In agreement with this, previous studies have shown this to facilitate PPARγ mediated actions [181, 184]. Therefore, it was hypothesized that HDACi in combination with the exogenous PGD_2 may activate PPARγ target genes within ShAKR1C3 cells.

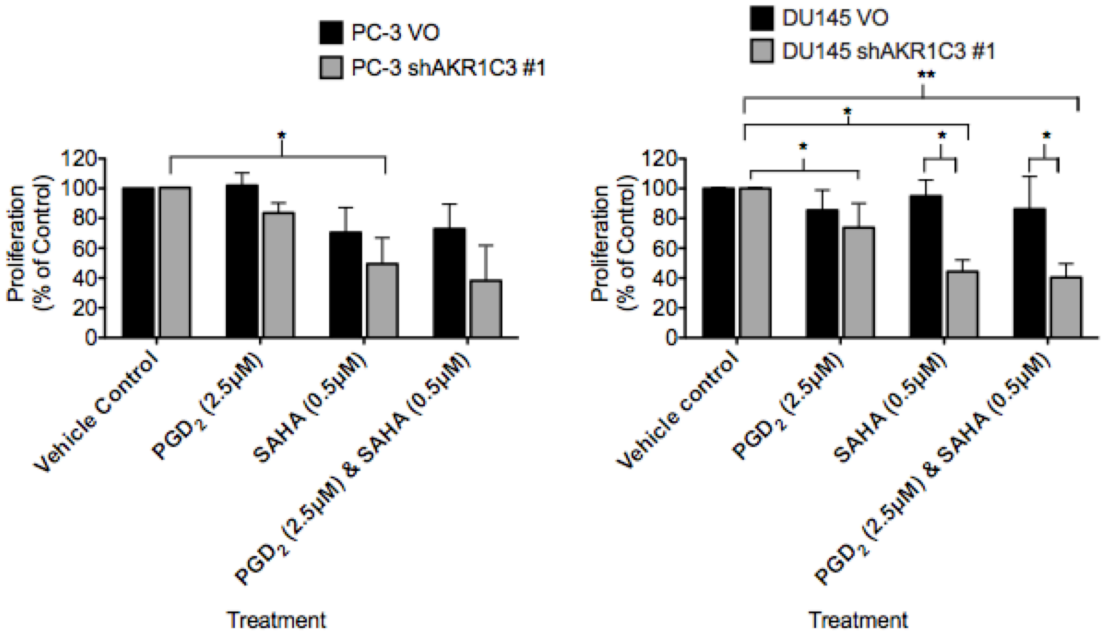

Figure 3.4 PC-3 and DU 145 proliferation response of malignant prostate cell lines in response to the PGJ_2 precursor (PGD_2) alone and in combination with the HDAC inhibitor SAHA. Cells were plated in a 96-well plate at $2x10^3$ cells per well and left overnight to adhere to the plate. Treatments commenced the following day and wells were retreated after 48 hours, total treatment time was 96 hours. Each data point represents the mean of three separate mRNA isolates amplified in triplicate wells ±SEM. VO=Vector only. Statistical significance assessed using t-test in comparison to vehicle treated controls (*=p-value <0.05, **=p-value <0.01).

Figure 3.4 shows PC-3 shAKR1C3 #1, DU 145 shAKR1C3 #1 and empty vector control responses to SAHA (0.5μM), PGD_2 (2.50μM) alone and both in combination. SAHA inhibited proliferation in PC-3 and DU 145 cells containing the shAKR1C3 sequence. PC-3 shAKR1C3 #1 showed no additive response when under the co-treatment conditions. Surprisingly, this experiment suggests that attenuating the level of AKR1C3 may increase the sensitivity of the cell to HDAC inhibitors. The effect was measured in DU 145 shAKR1C3 #1 when compared to the empty vector control of the same treatment and trended toward to same response in PC-3 shAKR1C3 #1.

3.2.4 Cell proliferation in response to PPARγ antagonist GW9662 in PC-3 and DU 145 ShAKR1C3 transfected cells.

To investigate if this effect is mediated by PPARγ, a potent antagonist (GW9662) was used. This experiment was designed to investigate whether inhibition of PPARγ alone and in combination with SAHA will impact the proliferation rate of cells with reduced AKR1C3.

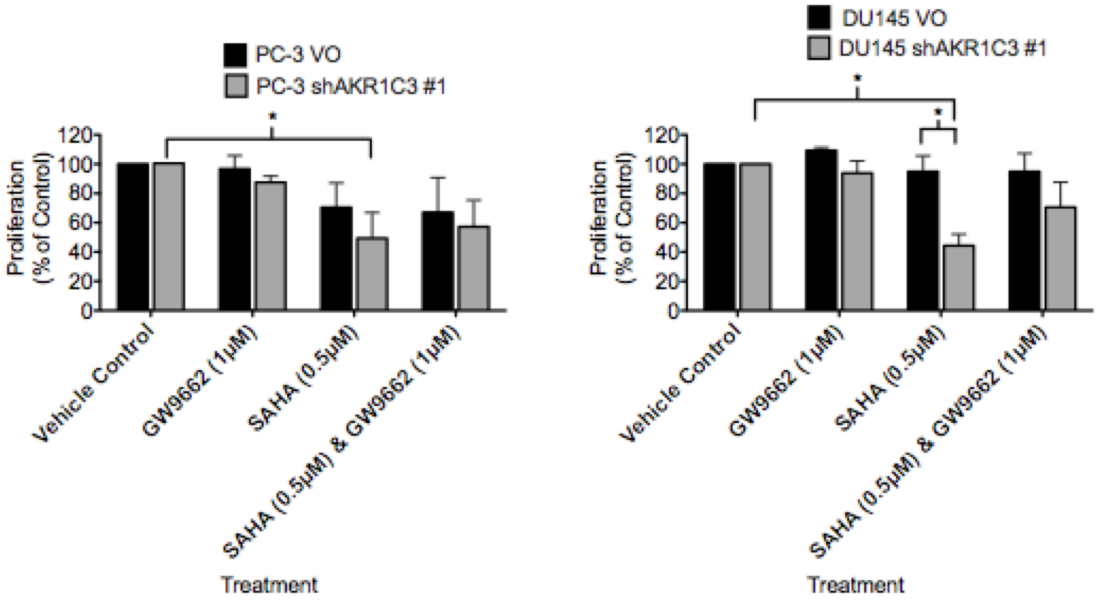

Figure 3.5 Proliferation response of malignant prostate cancer cell lines in response to the PPARγ antagonist GW9662 and the HDAC inhibitor. Cells were plated in a 96-well plate at $2x10^3$ cells per well and left overnight to adhere to the plate. Treatments commenced the following day and wells were retreated after 48 hours, total treatment time was 96 hours. Each data point represent s the mean of three separate mRNA isolates amplified in triplicate wells ±SEM. Statistical significance assessed using t-test in comparison to vehicle treated controls (*=p-value <0.05).

Figure 3.5 shows response of shAKR1C3 transfected clones and empty vector controls treated with SAHA, GW9662 and both in combination. DU 145 cells showed an increased sensitivity to SAHA in the presence of reduced AKR1C3 levels. Demonstrated also is that the potency of this response is diminished upon combined treatment with

GW9662, though this was not statistically significant. These experiments indicate that PPARγ maybe exerting minimal anti-proliferative responses upon cells with reduced AKR1C3 levels.

3.2.5 Multi-targeted micro-fluidic Q-RT-PCR analysis of shAKR1C3 PC-3 cells.

A microfluidic Q-RT-PCR approach was used to further this study and examine the impact of reduced AKR1C3 levels. Gene targets on the micro-fluidic card were selected to reflect the nuclear receptor role in the prostate environment including fatty acid regulatory factors, nuclear receptors (broad and low affinity), cell surface transporters, cell cycle regulators, and transcriptional coregulators.

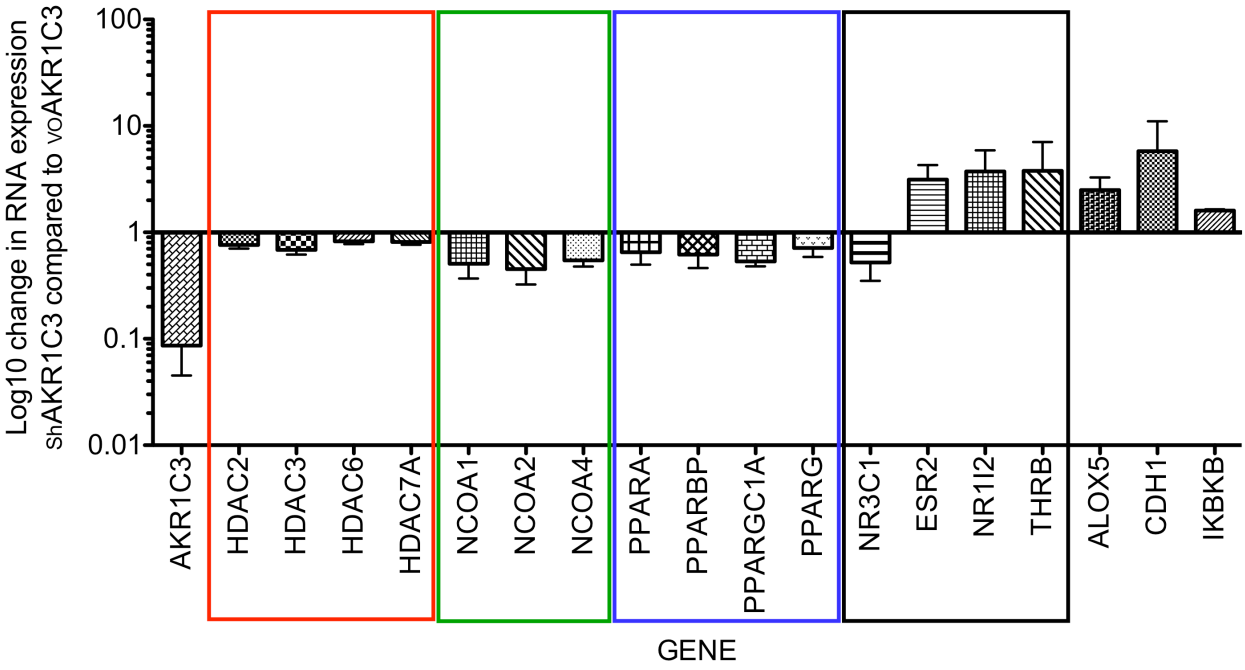

Figure 3.6 AKR1C3 knockdown influences a network of genes involved in transcriptional regulation. Untreated PC-3 vector only controls and untreated shAKR1C3 PC-3 Clone #1 samples were used. Total mRNA was added to the micro-fluidic reverse transcription Q-RT-PCR two step reaction. Primer sets on the card were selected for their nuclear receptor prostate specific context consisting of nine groups listed in the materials and methods section. Downregulated genes were grouped according to their cellular actions. Histone deactylases (red box), NR CoAs (green box), (PPAR and PPAR specific CoAs) (blue box) and NRs (black box). Data are the mean of three biological experiments performed in technical duplicate.

The data shown in Figure 3.6 illustrates the genes with deregulated basal levels in PC-3 shAKR1C3 clone #1. These were then grouped according to their biological function. Reduction in AKR1C3 levels was able to decrease the levels of expression of histone deactylases, nuclear receptor coactivators and PPARα and PPARγ. Importantly, the shAKR1C3 environment not only reduced the levels of these PPARs but also their specific coactivator PPARGC1A. A reduction of AKR1C3 levels was found to increase the basal expression of other nuclear receptors including ESR2 and THRβ.

3.3 Discussion

Previous studies show elevated AKR1C3 deprives the cell of J-series prostaglandins that are responsible for multiple cascade signals and ligands for NR mediated transcription. Further, it has recently been demonstrated [185] that stable expression of AKR1C3 in hormone dependent MCF-7 breast cancer cell lines has a negative impact upon the anti-proliferative actions of PGD_2. It has been therefore hypothesised that silencing AKR1C3 within hormone independent disease may result in the pathway reverting to the non-enzymatic conversion to 15-PGJ_2 a ligand for PPARγ initiating potentially apoptotic and differentiating actions.

PPARγ ligands have been investigated for the treatment of various cancer types for example neuroblastomas [186], colorectal [187] breast and prostate cancers [188, 189]. Metastatic prostate cancer cells overexpressing AKR1C3 have been suggested to deprive PPARγ of its natural ligand 15Δ-PGJ_2, driving the available PGD_2 towards the formation of the proliferative 9α,11β-PGF_2.

Some CaP cell lines overexpress AKR1C3 mRNA and primary prostate tissue tumours are shown to have significantly increased AKR1C3 levels. Successful knockdown of AKR1C3 in PC-3 and DU 145 cells has been demonstrated using short hairpin sequences. Examination of the shAKR1C3 cells response to PGD_2 was assessed as found not to produce significant changes in comparison to control (Vector only) cells. NR resistance has been previously measured in many CaP cells and is demonstrated herein. Epigenetically enforced repression of NR target genes has been previously demonstrated. In this study SAHA was utilised to increase levels of acetylation at PPARγ target genesin an attempt to reinitiate PPARγ functioning. Treatment of DU 145 shAKR1C3 #1 cells with a combination of PGD_2 and SAHA significantly reduced proliferation to a similar extent of SAHA alone. This suggests that overexpression of AKR1C3 maybe not be responsible for the maintenance of increased proliferation.

PC-3 and DU 145 are ADT-R CaP cell lines exposed to PPARγ antagonist GW9662 both isolated and in combination with PGD_2 were not found to produce any significant response in proliferation. This indicates that the role of PPARγ signalling in cancer cell growth in these cell lines may be minimal, indeed the physiological relevance and consequence of the achieved AKR1C3 knockdown in ADT-R cells remain ambiguous.

Analysis of NR prostate specific gene alterations using the Q-RT-PCR indicates that reducing AKR1C3 level produces marginal changes within the NR networks. Down regulation of HDACs supports the hypothesis that AKR1C3 mediates repression of anti-proliferative genes. Further, downregulation of coactivators and the NCOR1 corepressor (not shown) shows AKR1C3 may have some influence upon gene regulatory

mechanisms. Interestingly, the upregulation of IKBKB correlates with previous findings suggesting a link between AKR1C3 and regulation of NF-kB signalling pathways. The actions of elevated AKR1C3 in cancer have been classified in a cancer contributory context in many cell types such as leukaemia, CLL. By depriving the anti-proliferative PPARγ nuclear receptor of a high affinity ligand it can induce the pro-growth actions of 9α,11β prostaglandin F_2. The role of AKR1C3 overexpression in ADT-R CaP remains unclear. However, an epigenetic mis-regulation previously observed in NR signalling is recapitulated here. Furthermore, this is shown to be more susceptible to HDAC inhibition in the reduced AKR1C3 environment. Therefore, AKR1C3 is implicated in the mechanism of NR resistance observed in cancer from various tissue types. Perhaps most importantly the levels of both PPARγ and PPARGC1A are down regulated with AKR1C3. PARGC1A is a specific coactivator to PPARγ that facilitates the recruitment of factors such as the CREB (cAMP Response Element Binding Protein) and its transcriptional response. Thus a decreased level of not only PPARγ but also its specific coactivator may have impinged on the NRs activation. The molecular pathways by which reduced AKR1C3 impact upon PPAR expression levels are unclear. However, it is clear that this promiscuous steroid converting enzyme is linked to many process involved in the regulation of NR transcription.

Chapter 4: Targeting sirtuins to enhance NR signalling

4.1 Introduction

Sirtuins are nicotinamide adenine dinucleotide (NAD^+)-dependent deacetylases that have become heavily researched with respect to both ageing and cancer. They are unique in their HDAC activity, as they require NAD^+ for their action.

Several NRs have been demonstrated to be regulated by sirtuin mediated deactlyation and additionally NR coregulators have also been shown to alter their activity in the presence of sirtuins. Sirtuin 1 (SIRT1) has been demonstrated to enhance transcriptional repressive activity shown by NCOR1 when inhibiting the PPARγ [190]. The direct interaction of sirtuins has also been shown to affect other NRs such as the AR whose activity is inhibited by its deacetylation [155]. In addition the ER has been impaired by SIRT1 action [191]. Though not prostate orientated these findings demonstrate that the sirtuins act as both direct and indirect regulators of NR activity.

Previous studies have indicated that there is an overexpression in the level of sirtuins within the malignant environment. Their reduction may also be associated with decreased tumour growth [146, 192, 193]. However, the action of sirtuins within the prostate is poorly understood with a publication indicated SIRT1 is overexpressed in CaP patients compared to healthy controls [146].

Therefore, the expression levels of selected sirtuin family members will be examined and the effect of a selective chemical inhibitor upon their ability to impair nuclear receptor signaling will be investigated. Current understanding suggests sirtuin overexpression may mediate epigenetic silencing of NR target genes. Therefore inhibition of their action may restore NR signaling capability.

4.2 Results

4.2.1 Examination of *Sirt2* and *Sirt6* levels within CaP cell lines.

To investigate if sirtuins are overexpressed in CaP mRNA was extracted from a panel of prostate cancer cell lines and subjected to traditional q-RT-PCR using specific primers for *SIRT2* and *SIRT6*. These members of the family have been previously indicated to be elevated in malignant CaP models (data not shown). RWPE-2, PC-3 cells, LNCaP and LNCaP C-42s were also utilized to establish how sirtuin expression changes in malignancy. Amplification of *SIRT2* and *SIRT6* was compared to those in RWPE-1 cells. Figure 4.1 shows significant elevation in *SIRT2* levels occur in PC-3 and LNCaP prostate cells (2.39 ± 0.36 SEM and 3.27 ± 0.60 SEM respectively), whereas *SIRT6* levels did not significantly vary when compared to RWPE-1.

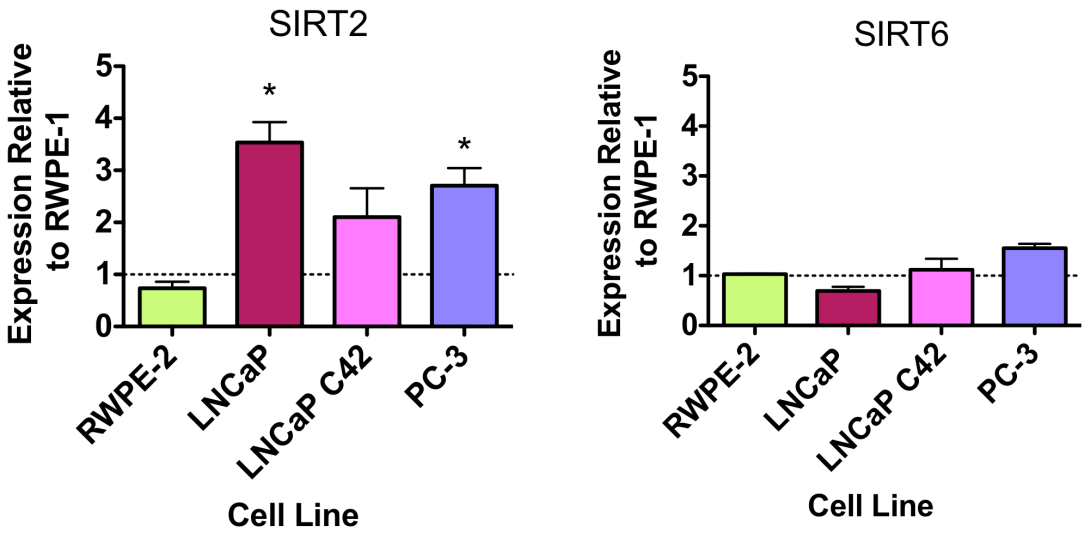

Figure 4.1 Assessment of mRNA levels of *SIRT2* and *SIRT6* in prostate cell lines. Reverse transcription and Q-RT-PCR was conducted using primers specific for *SIRT2* and *SIRT6*. All results shown are the mean of three independent experiments performed in triplicate ± SEM. Statistical significance was assessed using t-test where *=p-value <0.05.

Q-RT-PCR indicated that *SIRT2* was elevated in PC-3 cells. Western immunoblot analysis revealed the increased SIRT2 protein levels in the malignant PC-3 cells (Figure 4.2). Therefore, malignant cells often overexpress the SIRT2 protein, this may contribute to the increased proliferative activity of CaP cells.

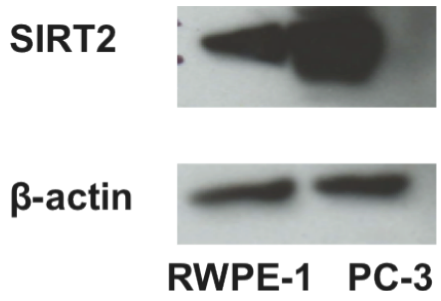

Figure 4.2 PC-3 show basaly elevated SIRT2 in comparison to RWPE-1 cells. Analysis of SIRT2 protein levels were detected using Western analysis, β-actin levels are shown as a loading control.

4.2.2 Impact of the sirtuin inhibitor Sirtinol upon proliferation of RWPE-1 and PC-3 cells

To examine the impact of elevated SIRT2 a sirtuin inhibitor (Sirtinol) was used to produce a dose response curve in RWPE-1 and PC-3 cells. This assay was performed to find an effective dose for treatment of cells with Sirtinol. Figure 4.3 shows PC-3 cells to be more resistant to the actions of Sirtinol in comparison to RWPE-1 cells. RWPE-1 cells showed a significant decrease in proliferation at 0.01μM (89.94% ±3.0% of controls), 10μM 58.88% (±9.62 SEM) and 50μM 8.86 (±4.12 SEM). PC-3 cells are more resistant to the inhibitory effects with only 50μM achieving significant decrease in proliferation (59.34 (± 29.23 SEM). RWPE-1 exposure to Sirtinol at 10μM produced close to ED_{50} response and the ED_{50} for PC3 was approximately 50μM.

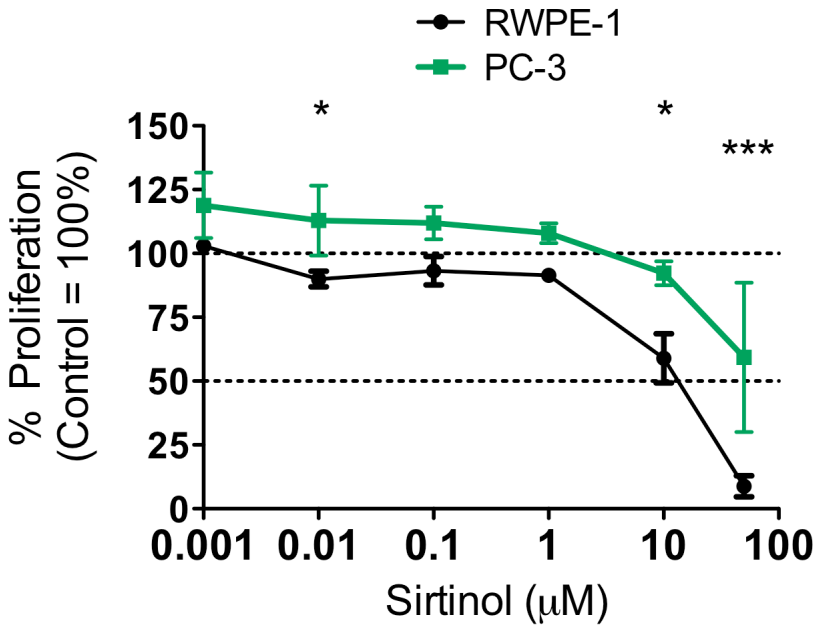

Figure 4.3 Resistance to sirtuin inihbitor Sirtinol. Cells were plated into 96 well plates and left overnight to adhere. Treatments comenced the following day. All points are mean of three independent experiments performed in triplicate wells shown ± SEM. Statistical analysis was performed using t-test. *=p-value 0.05, **=p-value 0.01, ***=p-value 0.001.

4.2.3 Response of RWPE-1 cells treated with Sirtinol and Bezafibrate alone and in combination.

In order to establish the mechanism behind RWPE-1 growth inhibition and PC-3 resistance to Sirtinol cells were exposed the sirtuin inhibitor (10μM) alone and in combination with the PPARγ ligand Bezafibrate (0.5μM & 5.0μM). Cells were treated for 0.5 and 4 hours before mRNA collection. Reverse transcription was performed and cDNA analysed by Q-RT-PCR for the *PTGS2* and *CDKN1A* transcript levels. Bezafibrate has been demonstrated to decrease the levels of *PTGS2* whilst also increasing the level of *CDKN1A* [176].

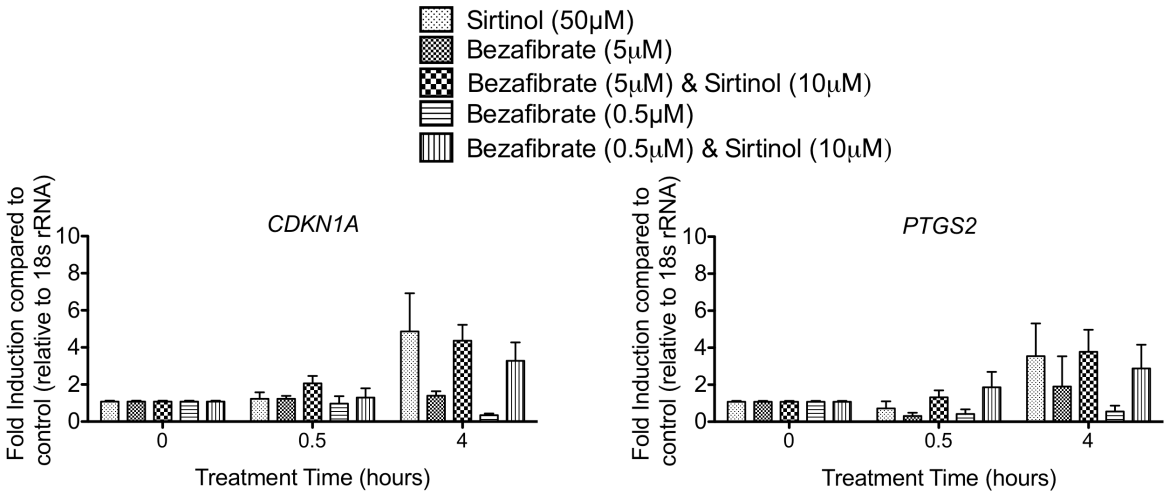

Figure 4.4 Sirtinol alone and in combination with the PPARγ ligand Bezafibrate in RWPE-1 cells. RWPE-1 cells were plated at $1x10^5$ left overnight before treatment with Sirtinol, Bezafibrate or both in combination. Control cells were normalised to 1.0. All bars are the mean of three independent experiments performed in triplicate PCR wells ± SEM.

Figure 4.4 illustrates the RWPE-1 response to Bezafibrate and Sirtinol alone and in combination. Sirtinol treatment in RWPE-1 cells was able to induce expression of the *CDKN1A* and *PTGS2* mRNA after 4 hours of exposure. These data suggest sirtuins have some role in suppressing PPARγ mediated expression and their inhibition can partially restore sensitivity. To investigate how this role is altered in malignancy the same experiment was conducted using sirtinol resistant PC-3 cells.

4.2.4 Response of PC-3 cells treated with Sirtinol and Bezafibrate alone and in combination.

Figure 4.5 Sirtinol alone and in combination with the PPARγ ligand Bezafibrate in PC-3 cells. PC-3 cells were plated at $5x10^4$ left overnight before treatment with Sirtinol, Bezafibrate or both in combination. Control cells were normalised to 1.0. All bars are the mean of three independent experiments performed in triplicate PCR wells ± SEM.

Figure 4.5 shows the response of PC-3 cells to the Sirtinol and Bezafibrate treatment conditions. Bezafibrate exposure was unable to induce *CDKN1A* but in combination with Sirtinol produce an upward trend greater than Sirtinol alone. Combination of Bezafibrate (0.5μM) and Sirtinol produced significant mRNA accumulation. Again PC-3 cells demonstrate a level of resistance toward Sirtinol with pronounced induction. In addition, expression of CDKN1A is not restored with combined treatment.

4.3 Discussion

Restoration of NR signaling remains a key target for cancer research. The prospect of therapy that can overcome the phenomenon of NRs resistance and restore activation is compelling. Sirtuin mediated deregulation of NR signaling has been demonstrated to occur both at a direct (deacetylation of the estrogen receptor enhances its transcriptional activity) [194] and an epigenetic level (histone deacetylation reduces that transcriptional output of target genes) [195]. Currently the impact of sirtuins upon NR activity within CaP is ambiguous. This study attempts to reveal the extent of silencing mediated through Sirtuins in ART-R CaP.

A previous study compared the prostate gene expression network during the cell cycle and showed *SIRT2* and *SIRT6* to be continually upregulated [195]. Analysis of a panel of CaP cell lines demonstrated that *SIRT2* is elevated in PC-3 and LNCaP cells when compared to RWPE-1 cells. Therefore, to challenge the NR silencing activity of sirtuins cells were exposed to a range of concentrations of Sirtinol. This revealed PC-3 cells have increased resistance to Sirtinol in comparison to RWPE-1 cells.

The reduced activity of PC-3 cells to NR stimulation compared to RWPE-1 is in correlation with previous studies [68, 74, 196]. In addition, selective loss of PPARγ target gene mediated through NCOR1 action has been investigated [176], this study adds further insight to the loss of NR actions. The data herein find an upregulation of SIRT2 in malignancy to play a contributory role in PPARγ silencing with particular respect to the target gene *CDKN1A*. Ongoing studies should target both the action of SIRT2 and possible interaction with NCOR1 in an attempt to achieve sustained NR potency.

Chapter 5: Regulation of VDR target genes in non-malignant and malignant prostate cells

5.1 Introduction

Published findings have demonstrated a loss in anti-proliferative response to vitamin D receptor (VDR) ligands [197, 198] in many malignancies including CaP. The mechanisms behind this loss of sensitivity have been previously investigated in PC-3 and DU 145 cells. These studies have demonstrated that elevated levels of NCOR1 and NCOR2/SMRT are able to contribute to gene repression via increased HDAC3 recruitment [131]. This mechanism results in aberrant deactylation at the local chromatin environment repressing transcription.

In addition, studies have also demonstrated NR mediated gene transcription to occur in a cyclical fashion. This process involves sequential recruitment and release of both CoR and CoA complexes bound to the NR. Consequently changes in the chromatin PTMs placed around the gene affect its level of transcription. However, these studies have not examined how the VDR regulates target genes within the normal epithelial state. All previous studies have used derivations of breast or prostate cancer cell lines to examine transcriptional regulatory events. Therefore, the following work examined the ability of VDR to regulate genes in the normal prostate epithelial model RWPE-1. By using a non-malignant cell system this work investigated a transcriptional response that equates to *in-situ* epithelial prostate cells. This served to establish a baseline of VDR mediated activity in the non-transformed state. Bulk cell populations were treated with vitamin D receptor ligand ($1\alpha,25(OH)_2D_3$) and VDR target gene dynamics were observed over 24 hours.

It was hypothesized that comparison of RWPE-1 VDR target gene expression to transformed malignant cell lines PC-3 and the isogenic RWPE-2 these experiments may unveil the extent of misregulation underlying the progression of CaP.

Many NRs including AR have also been demonstrated to influence expression of microRNAs (miRNAs) as a regulatory components of their transcription networks [199]. Genome wide analysis of malignant tissues has revealed the full extent of miRNA deregulation within tumours [200, 201]. Altered miRNA levels have been associated with many hormonally mediated malignancies including the CaP [202, 203]. Previous work by this laboratory (unpublished data) has identified that $1\alpha,25(OH)_2D_3$ activation of VDR induced the DNA replicative helicase *MCM7*. The *MCM7* gene sequence contains a miRNA sequence within the 3'UTR located on intron 13 that produces the miRNA named MiR106b [204]. MiR106b has been shown previously to target *CDKN1A* transcript for degradation [205]. Therefore, VDR regulation of MiR106b produces a negative feedforward loop, and further distortion of this loop may be a key contributory factor to NR resistance often observed in CaP.

To test this hypothesis the levels of MCM7 and MiR106b expression were observed in both RWPE-1 and PC-3 cell lines. In addition the VDR feedforward loop containing MiR106b was examined for its relationship to tumour progression within the TRAMP murine model.

5.2 Results

5.2.1 The effect of growth media upon VDR target genes in CaP cell lines.

The RWPE-1, RWPE-2 and PC-3 cell lines used in this experiment were maintained in different media conditions. RWPE-2 cells were a derivative of RWPE-1 and were maintained in the KSF complete medium. However, PC-3 cells were maintained in RPMI1640 complete medium. Therefore, to investigate the effect of each media and its supplements upon each cell line the following experiment was conducted using variations in the growth conditions. RWPE-1 cells were plated in three conditions to examine the impact of the components on cell growth:

1) KSF complete (including BPE and EGF)

2) KSF and BPE without EGF

3) KSF complete overnight and replaced with RMPI (+FBS).

The malignant cell line model PC-3 was also investigated for the influence of their recommended media upon the transcription of the VDR target genes (*CYP24A1* and *CDKN1A*). PC-3 cells are grown in RPMI 1640 medium supplemented with Fetal Bovine Serum (FBS). Since FBS contains many growth factors that may influence the transcriptional outcome of these two VDR genes it was important to assess their effect. PC-3 cells were plated in either:

1) RPMI 1640 (+FBS)

2) RPMI 1640 (+FBS) + EGF

3) KSF complete

Upon completion of treatment, the cells mRNA was isolated, extracted, reverse transcribed and Q-RT-PCR performed for VDR target genes *CYP24A1* and *CDKN1A*.

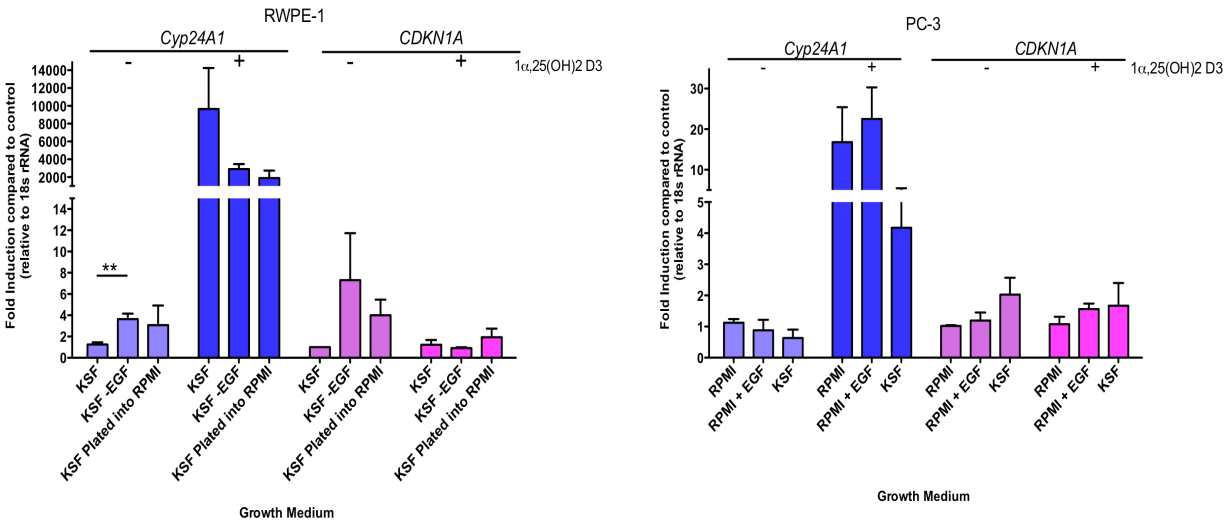

Figure 5.1 Variations in medium componants have minimal impact upon VDR target gene expression. RWPE-1 ($1x10^5$) and PC-3 ($5x10^4$) cells were plated in to 6 well plates and treated with either vehicle control or $1\alpha,25(OH)_2D_3$ (100nm) for 6 hours. mRNA was assessed for *CDKN1A* and *CYP24A1* transcript levels. All results are mean of at least three independent experiments ± SEM. Statistical analysis was performed using t-test, **=p-value 0.01.

Exposure to $1\alpha,25(OH)_2D_3$ (100nm) for 6 hours induced expression of the *CYP24A1* gene in both RWPE-1 and PC-3 cells. However, the PC-3 cells showed a lower level of induction (approximately 10 fold) than that observed in RWPE-1 cells (1000 fold). In addition *CYP24A1* remained inducible in the cell populations plated in alternative media conditions. The data showed a lack of induction of *CDKN1A* in both RWPE-1 and PC-3 cells that in RWPE-1 maybe due to the selected treatment time (6 hours). Such a selection provides evidence of the importance in timepoint used to measure ligand response. Withdrawal of EGF from RWPE-1 cells causes a statistically significant basal increase (3.64 ± 0.51% fold change) in the *CYP24A1* transcript level. All other media modifications used produced no statistical change in either *CYP24A1* or *CDKN1A* transcript levels. Interestingly, treatment of RWPE-1 cells with $1\alpha,25(OH)_2D_3$ (100nm) for 6 hours produced a downward trend in *CYP24A1* induction. *CDKN1A*

mRNA response in either untreated, or 1α,25$(OH)_2D_3$ (100nm) treated cells was not significantly altered by the media variations examined in this experiment.

Changing the media PC-3 cells are grown in also had little effect upon the VDR target gene expression as there was no statistical significance between treated or untreated controls. This supported the use of the recommended media as it shows their gene expression is not altered its absence.

5.2.2 Comparison of the effect of 1α,25$(OH)_2D_3$ upon the cell cycle in non-malignant and malignant CaP cells.

Inhibition of the cell cycle contributes to anti-tumourigenic action of 1α,25$(OH)_2D_3$ and was investigated by FACS analysis. To investigate the response VDR stimulation has upon the cell cycle RWPE-1 and PC-3 cells were treated with two different doses of 1α,25$(OH)_2D_3$ (10nm and 100nm) for 24 hours before FACS analysis. Figure 5.2 demonstrates exposure over 24 hours was able to induce cell cycle arrest in RWPE-1 cells. This response appeared to be dose-dependent as 1α,25$(OH)_2D_3$ (10nm) induced a marginal but statistical increase in G1 phase (73.8 ±0.8% fold change) where as 100nm treatment lead to an increase in G1 phase of the cell cycle (87.9 ±0.5% fold change) with a corresponding decrease of cells in S phase and G2/M.

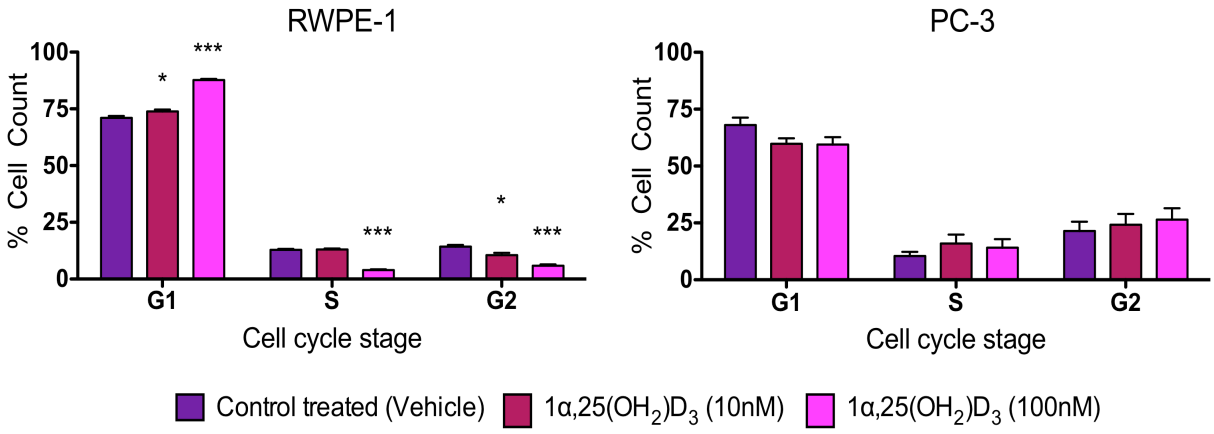

Figure 5.2 Cell cycle arrest induced by 1α,25(OH)$_2$D$_3$ in RWPE-1 cells is lost in PC-3 cells. RWPE-1 and PC-3 cells were seeded at 1x10^6 and 5x10^5 cells per well respectively. Treatment was with 1α,25(OH)$_2$D$_3$ (10nm) and (100nm) for 24 hours. Cells were stained with propidium idodide and analysed for cell cycle status by FACS. Each data bar represents the mean (± SEM) of at least three independent experiments. Statistical analysis was performed using t-test. *=p-value 0.05, **=p-value 0.01, ***=p-value 0.001.

These results are in agreement with previously published data [206, 207]. Similar FACS analysis of PC-3 cells in response to 1α,25(OH)$_2$D$_3$ (10nm and 100nm) failed to produce cell cycle arrest as observed in RWPE-1 cells. Interestingly, treatment of PC-3 cells produced marginal increases of cells in S and G2 phase, although this is not found to be significant when challenged with t-test assessment.

5.2.3 VDR target gene dynamics within RWPE-1 cells.

Vitamin D response elements (VDREs) are found within gene promoters of the VDR target genes. Past studies within this group have examined established target genes of the VDR and a panel of these were selected for further study.

The *ALOX5* gene produces the 5-lipoxygenase enzyme. This is responsible for the conversion of cholesterol-derived phospholipids into the pro-inflammatory mediators called leukotrienes. Although *ALOX5* expression has some correlation with tumour

tissues the first identification of *ALOX5* being upregulated by $1\alpha,25(OH)_2D_3$ came in 1995 [208].

More recently, investigations of the *ALOX5* gene demonstrated that although there are various VDREs within its promoter these are non-functional when analysed using reporter gene constructs. Furthermore, it was hypothesised that the VDREs within the 10kb promoter required VDREs at more distal sequence to exert significant transcriptional regulation [209]. In correlation, detailed analysis by the same research group showed that VDREs outside of the *ALOX5* promoter region are strongly influenced by VDR ligand exposure. From the 84kb surrounding the *ALOX5* gene it was discovered that the most potent VDRE was approximately 42kb upstream of the transcription start site of the gene [210].

Thus, VDR activation is able to produce activation of the *ALOX5* gene, contributing to the regulation of the inflammatory response. In conjunction with this action are reports indicating that VDR also has the *PTGS2* gene as a target [184]. *PTGS2* encodes the Cyclooxygenase 2 (COX-2) protein and has a strong association with pro-tumourigenic inflammatory effects within the prostate. Upregulation of COX-2 promotes prostagladin catabolism contributing to inflammation.

Additional to this, VDR target genes for study were selected including the G1-G0 switch gene (G0S2). This gene is thought to regulate the movement of cells in and out of the cell cycle thus controlling the cells rate of division. Since the discovery of *G0S2* it has exhibited regulation through the PPAR and the RAR nuclear receptor families [211, 212]. Also identified in previous work by this group to be a VDR target gene [184] and was

chosen alongside the ESR1 (encodes ERα) and MAPK4 that were also identified being VDR regulated.

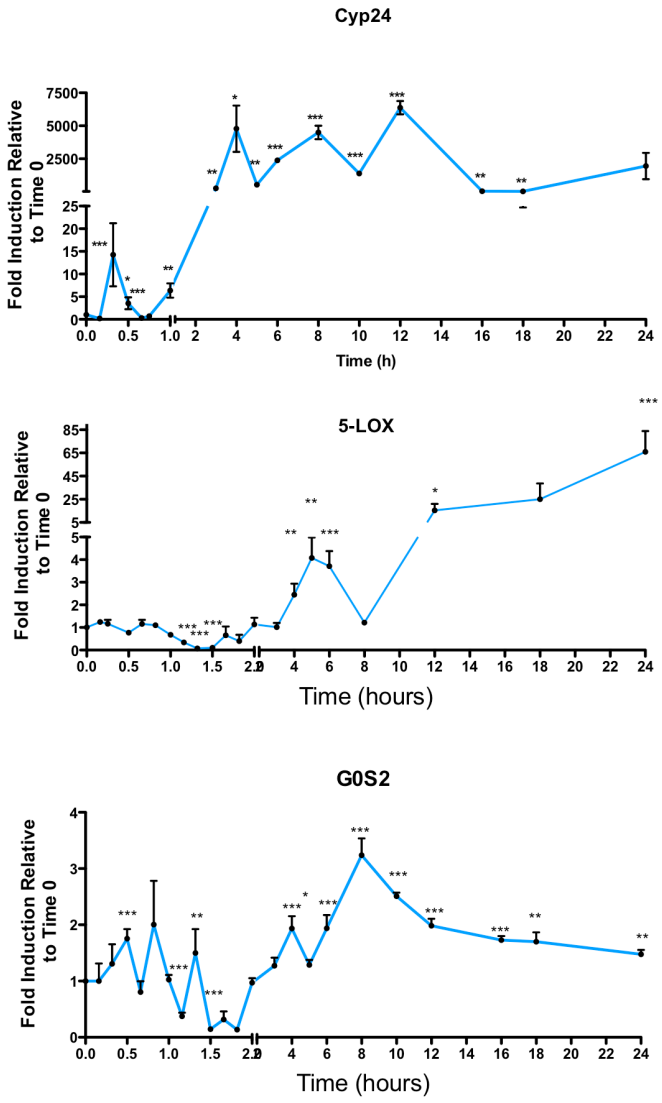

Figure 5.3 VDR regulates target genes with sustained mRNA output*. RWPE-1 cells were plated into 6 well plates at a density of 1x10^5 and treated with 1α25(OH)$_2$D$_3$ (100nm). mRNA was isolated and reverse transcribed. Levels of transcript were analysed by Q-RT-PCR. Each data bar represents the mean (± SEM) of at least three independent experiments. *=p-value 0.05, **=p-value 0.01, ***=p-value 0.001.*

Figure 5.3 illustrates that the kinetics of *CYP24A1, G0S2* and *ALOX5* show similar aspects. For example, these all displayed a common significant mRNA accumulation throughout the timecourse. However, their magnitude of response varied.

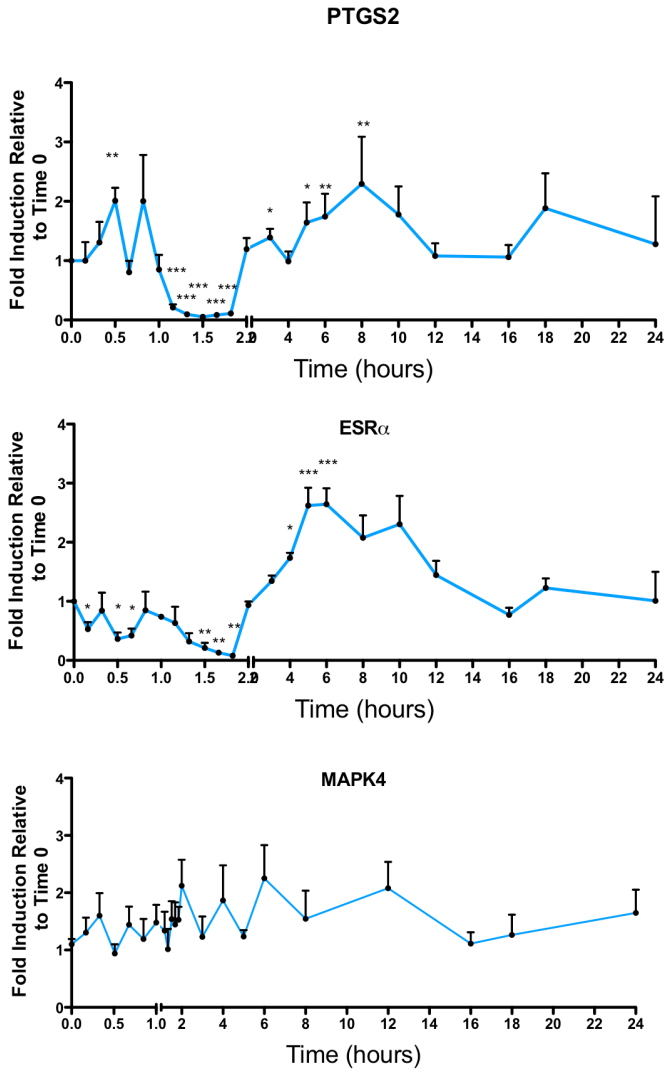

Figure 5.4 VDR selectively regulates ESR1 and PTGS2 target genes with short term mRNA output. RWPE-1 cells were plated into 6 well plates at 1x10^5 cells per well and treated with 1α25$(OH)_2D_3$ (100nm). mRNA was isolated and reverse transcribed. Total mRNA levels were analysed by Q-RT-PCR. Each data bar represents the mean (± SEM) of at least three independent experiments. *=p-value 0.05, **=p-value 0.01, ***=p-value 0.001.

The kinetic profile produced by *PTGS2, ESR1* and *MAPK4* (Figure 5.4) did not resemble the initial fluctuation and sustained increased mRNA transcription observed

with the previous genes (*CYP24A1*, *ALOX5* or *G0S2*). There were no statistically significant increases in mRNA production beyond 8 hours treatment. Similar to those previously observed in *ALOX5* and *G0S2* there is a sustained repressive period that in *PTGS2* is extended and runs from 70 minutes to 110 minutes. This is followed by an increase at 8 hours. In a comparable manner to that of *PTGS2*, *ESR1* shows fluctuation in mRNA followed by upregulated gene expression. This elevation was not sustained but terminates at 6 hours.

To investigate how VDR regulated epigenetic events control target gene expression histone modifications associated with active or repressive roles in gene transcription were measured at target gene transcription start sites. Illustrated in Figure 5.5 are the data from analysis of the *G0S2*, *ALOX5* and *PTGS2* TSS and the fold changes of selected histone marks present. From the mRNA expression profiles both *G0S2* and *ALOX5* were shown to produce sustained transcriptional output over the 24 hour time-period. In contrast the *PTGS2* gene produced significant mRNA accumulation up until 8 hours post VDR activation. Therefore, analysis of differential histone modification recruitment between genes TSS may reveal a 'short term' histone code that retains instructions for gene expression dynamics observed in Figures 5.3 and 5.4.

H3K27me3 was shown to be higher at the TSS of sustained expression genes (*ALOX5* and *G0S2*) upon treatment with $1\alpha,25(OH)_2D_3$ (100nm). G0S2 TSS has a significantly reduced level of H3K27me3 mark at 0.5, 1, 4 and 24 hours post treatment. ALOX5 demonstrated a loss of H3K27me3 that remained significantly reduced throughout, with high levels but declining at 0.5, 4, 12 and 24 hours treatment $1\alpha,25(OH)_2D_3$ (100nm).

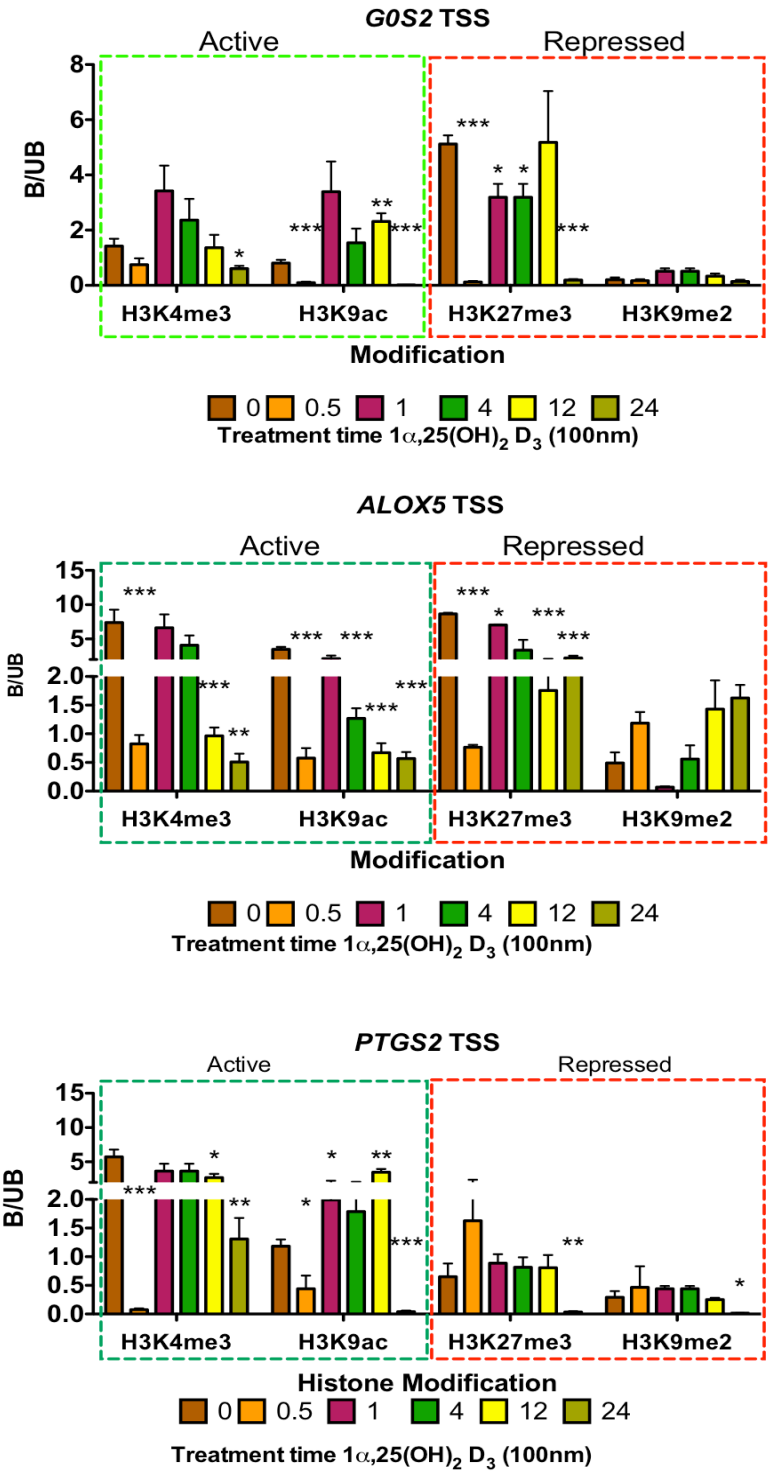

Figure 5.5 Oscillation of activating and repressing histone modifications during gene transcription. RWPE-1 DNA recovered by nChIP was analysed by q-RT-PCR. H3K4me3 and H3K9ac are activation marks (contained within a green box) and H3K27me3 ad K3K9me2 are assicated with repressed gene expression (contained within red box). Each data bar represents the mean (± SEM) of three independent experiments. *=p-value 0.05, **=p-value 0.01, ***=p-value 0.001.

PTGS2 shows no significant change in the enrichment levels of H3K27me3 until 24 hours post treatment (0.036 ±0.182% fold enrichment). H3K9me2 is also associated with repression of transcription. Observation of this mark over the TSS of *ALOX5*, *G0S2* and *PTGS2* resulted in significant changes in *ALOX5* (1.62 ± 0.22% fold enrichment) and *PTGS2* treatment at 24 hours (0.016 ±0.002% fold enrichment).

H3K4me3 became enriched at genomic regions containing active genes. This study compared the changes in this histone mark in response to VDR activation and found the TSS of different genes show differential levels of H3K4me3. The *G0S2* gene shows a significantly reduced level after 24 hours $1\alpha,25(OH)_2D_3$ (100nm). However, the TSS of *ALOX5* demonstrates rapid loss and restoration of this mark in response to activation. Therefore, genes exhibiting sustained mRNA expression may utilise H3K4me3 release to induce transcription. Furthermore, the level of this mark may influence the rate of transcription. H3K9ac was significantly reduced at 0.5 h at the TSS of G0S2, ALOX5 and PTGS2. Later time points demonstrated that H3K9ac levels were upregulated on all three genes reflecting the positive mRNA regulation. Together these findings suggest that H3K9ac enrichment at the TSS and mRNA accumulation were closely coordinated. This is the first time these histone modifications have been shown to fluctuate with VDR target gene activation, in addition it is also demonstrated that these post translational marks have levels of accumulation unique to each target gene.

5.2.4 Protein production in response to 1α,25(OH)$_2$D$_3$ (100nm) over time.

To examine the productivity of the mRNA kinetics observed Western immunoblotting was conducted and Figure 5.6 shows the response of ALOX5 in RWPE-1 cells treated with 1α,25(OH)$_2$D$_3$ (100nm). This revealed a fluctuating protein response, indicating dynamic regulation of ALOX5 in response to VDR activity.

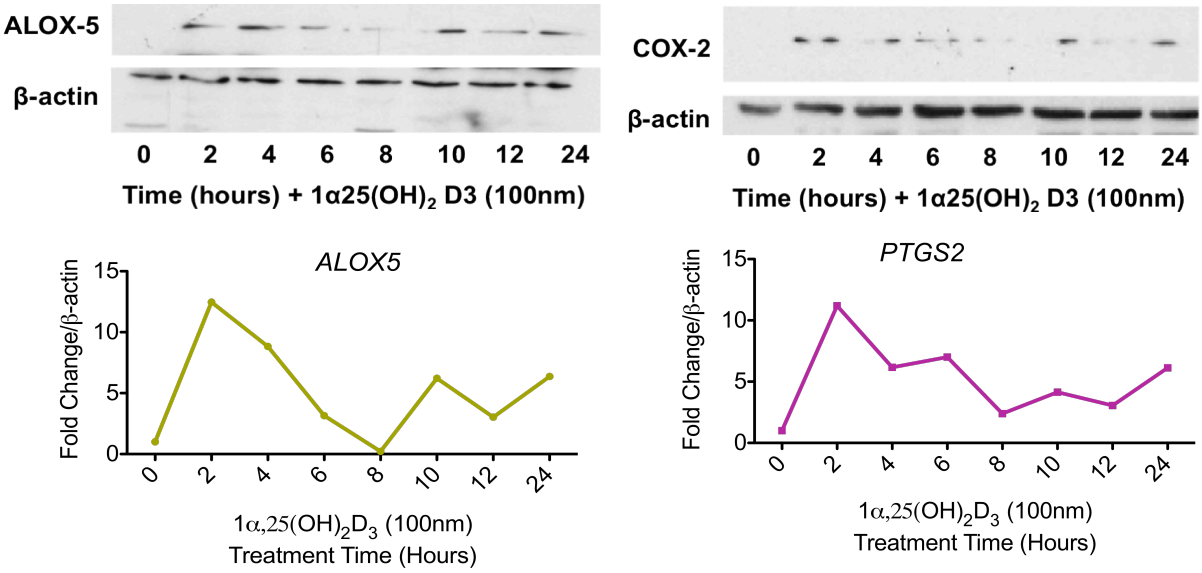

Figure 5.6 1α,25(OH)$_2$D$_3$ periodically induces ALOX5 and COX-2 protein in RWPE-1 cells. RWPE-1 cells were plated into T75 flasks at a density of 1x10^6 and treated with 1α,25(OH)$_2$D$_3$ (100nm). Cells were harvested and protein lysates recovered and subject to western imunnobloting. Quantification was by Image-J software and relative to β-actin (n=1).

Analysis at the protein level (Figure 5.6) showed elevated protein levels of COX-2 reached a maximum two hours after treatment, this then decreased but remains above basal levels for the duration of the timecourse. Therefore, the activation of VDR is producing productive transcriptional variations that are translated into protein. Further, these two target genes exhibit similar protein dynamics in comparison to differing mRNA kinetics.

5.2.5 Basal levels of novel and established VDR target genes within RWPE-1 and PC-3 cells.

As discussed previously mis-regulation of NR signaling capacity in malignancy is frequently reported [68, 213-216]. Disturbance of the VDR activity in CaP has also been established. Observation of the basal expression of VDR target genes relative to basal VDR expression itself may suggest the target genes ability to respond to activation. Furthermore, comparing the basal levels of these genes between normal and malignant cells may provide further elucidation of VDR signaling network deregulation in prostate carcinogenesis.

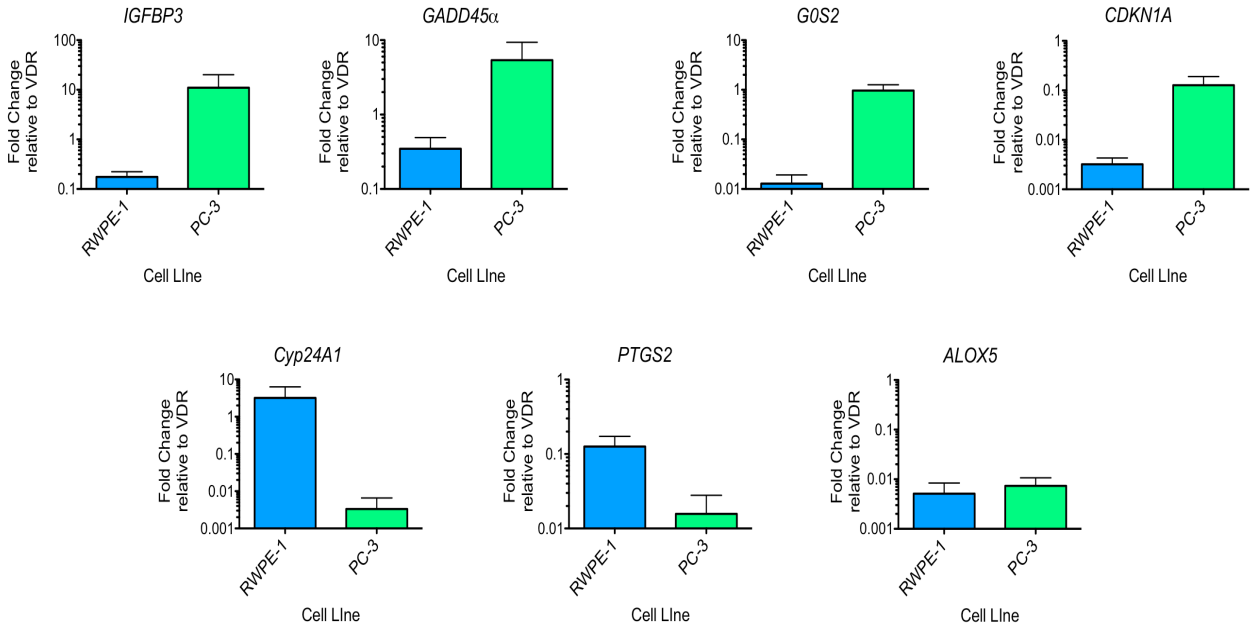

Figure 5.7 Basal expression of VDR target genes suggests their responsive capacity to 1α,25(OH)$_2$D$_3$. *Untreated RWPE-1 (1x10^5) and PC-3 cells (5x10^4) were plated and left overnight. The following day mRNA was isolated and reverse transcribed. Basal gene levels were assessed using Q-RT-PCR and normalised to the VDR from each cell line. Bars shown are mean of at least two independent experiments (± SEM) and performed in triplicate.*

CYP24A1 showed a basal level of expression not significantly different from that of VDR (3.21 (±3.12 SEM) fold change), this is an example of how normal prostate epithelium is enriched for $1\alpha,25(OH)_2D_3$ response genes. Genes that respond rapidly to VDR stimulation (*such as PTGS2*) have levels of basal expression approximately 10 fold below that of VDR. This was in comparison to the late responding genes (Figure 5.7) *G0S2* and *ALOX5* have levels of enrichment approximately 100 fold lower than VDR. However, the expression of ALOX5 is not altered in PC-3 cells.

Conducting a similar experiment in PC-3 cells unveils a skewed relationship between the level of basal VDR expression and its target genes. These data show the enrichment of VDR was lost in PC-3 cells and this distortion in basal expression may contribute to NR resistance.

5.2.6 VDR target gene expression in PC-3 cells

To reveal the extent of VDR signaling deregulation in ADT-R CaP detailed timecourse investigations were conducted in PC-3 cells. Figure 5.8 demonstrates that the VDR target gene *CDKN1A* became unresponsive to ligand stimulation.

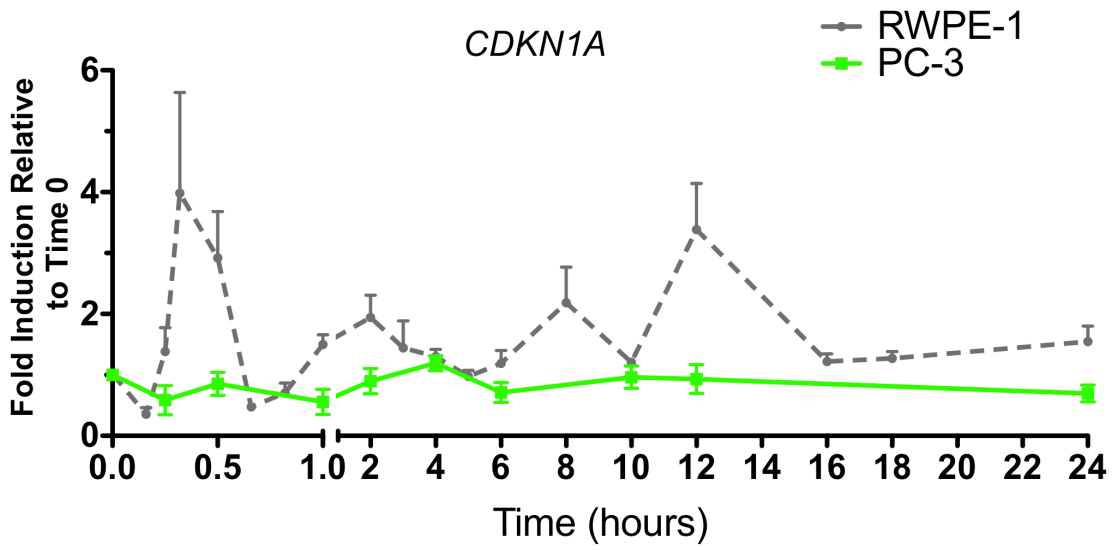

Figure 5.8 VDR mediated response of CDKN1A mRNA is lost in prostate cancer cell line PC-3. Cells were plated into 6 well plates at a number of $5x10^4$ cells per well and left overnight. Treatment commenced the following day $1\alpha,25(OH)_2D_3$ (100nm). mRNA was isolated and expression levels were determined using q-RT-CPR. Each data bar represents the mean (± SEM) of at least three independent experiments.

Analysis of the total mRNA for the *CDKN1A* transcript reveled that these cells are insensitive to the action of the VDR. There was no statistically significant change in the mRNA output in comparison to the vehicle only controls.

CDKN1A mRNA is processed and translated into the protein $p21^{(waf1/cip1)}$. This protein contributes directly to the cell cycle arrest through inhibition of cyclin dependent kinases (CDKs), an effect measured in RWPE-1 cell by G1 cell cycle arrest (Figure 5.2).

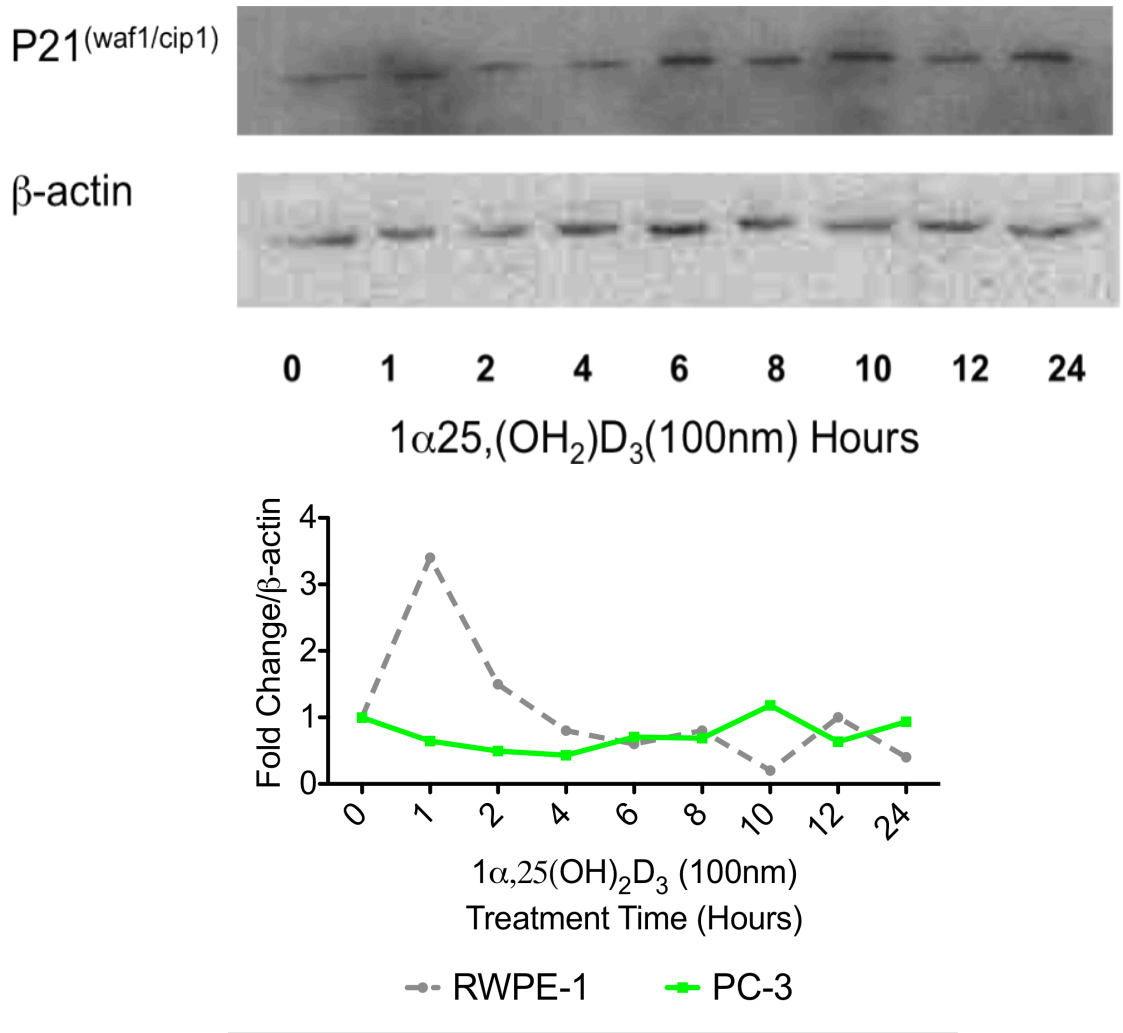

Figure 5.9 VDR stimulation is unable to induce p21$^{(waf1/cip1)}$ protein levels in PC-3 cells. PC-3 cells were plated into T75 flasks at a density of 5x10^5 and treated with 1α,25(OH)$_2$D$_3$ (100nm). Cells were harvested and protein lysates recovered and subject to western immunobloting. Quantification was by Image-J software and relative to β-actin. *=p-value 0.05, **=p-value 0.01, ***=p-value 0.001.

The loss of VDR sensitivity shown by the PC-3 cells was also measured at a protein level (Figure 5.9). Quantification of the image demonstrated the p21$^{(waf1/cip1)}$ protein was not induced upon addition of 1α,25(OH)$_2$D$_3$ (100nm).Whether the specificity of NR insensitivity was limited to growth regulatory genes or global targets of the NR in question had not been addressed. Therefore, to establish the extent of VDR signaling deregulation a panel of target genes was examined. Each gene has previously

demonstrated to be responsive in the non-malignant model (RWPE-1), but was shown to be transcriptionally unresponsive in ADT-R CaP (Figure 5.10). There were visible fluctuations in the kinetics of *PTGS2* and *ALOX5* mRNA of PC-3 cells. However, these were not statistically significant when subjected to t-test.

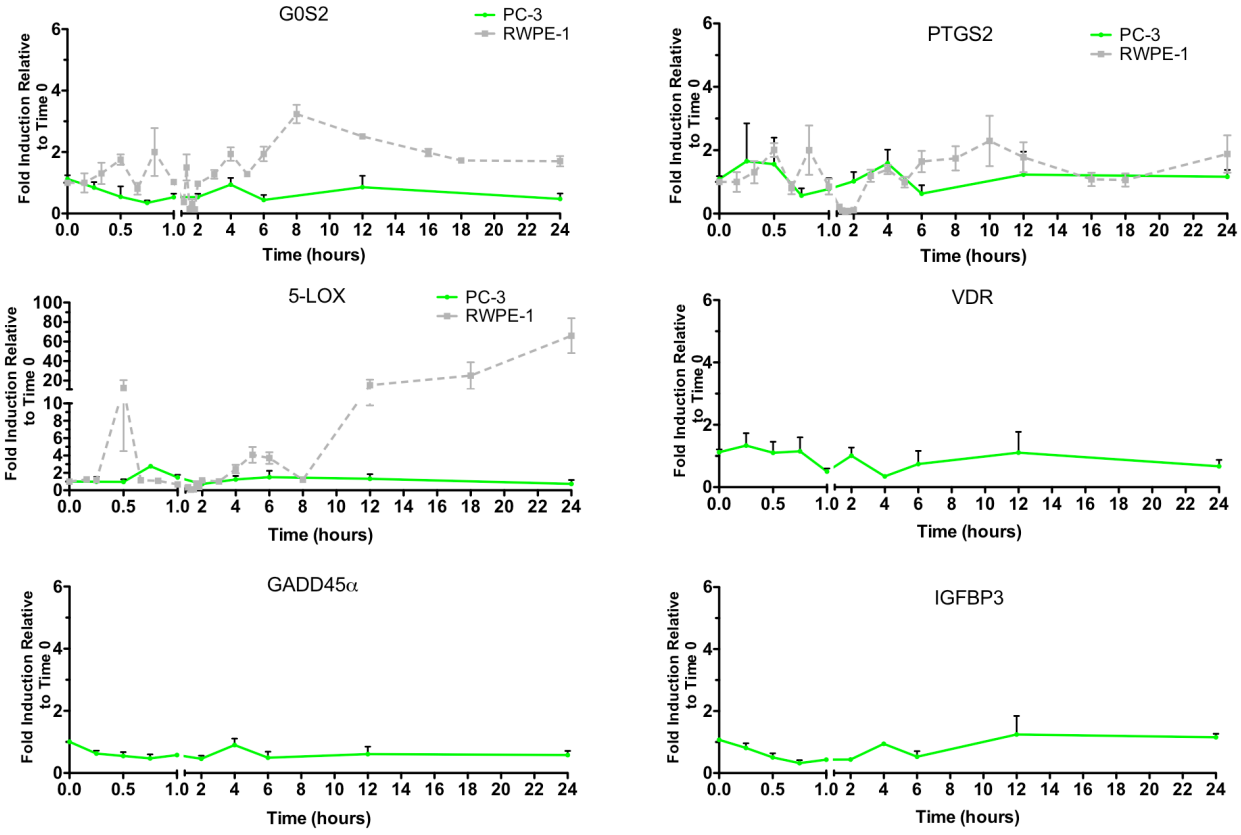

Figure 5.10 VDR regulated genes are unresponsive to ligand treatment in PC-3 cell line. PC-3 cells were plated into 6 well plates at $5x10^4$ cells per well and treated with $1\alpha25(OH)_2D_3$ (100nm). RNA was isolated and reverse transcribed. mRNA levels were analysed by Q-RT-PCR. Each data bar represents the mean (± SEM) of at least three independent experiments. *=p-value 0.05, **=p-value 0.01, ***=p-value 0.001.

5.2.7 Distortion of VDR signalling within an isogenic cell line.

How or when cells acquire NR resistance is not known but VDR insensitivity has been demonstrated in ADT-R CaP. The following experiment used RWPE-2 cells to assess the progression of VDR deregulation within a genetic background similar to RWPE-1. Figure 5.11 illustrates the data obtained from Q-RT-PCR analysis of the *CDKN1A* gene within RWPE-2 cells. Though there is an initial peak of mRNA occurring at 0.5 hours it is not statistically significant and throughout the timecourse there was no significant accumulation of *CDKN1A* mRNA.

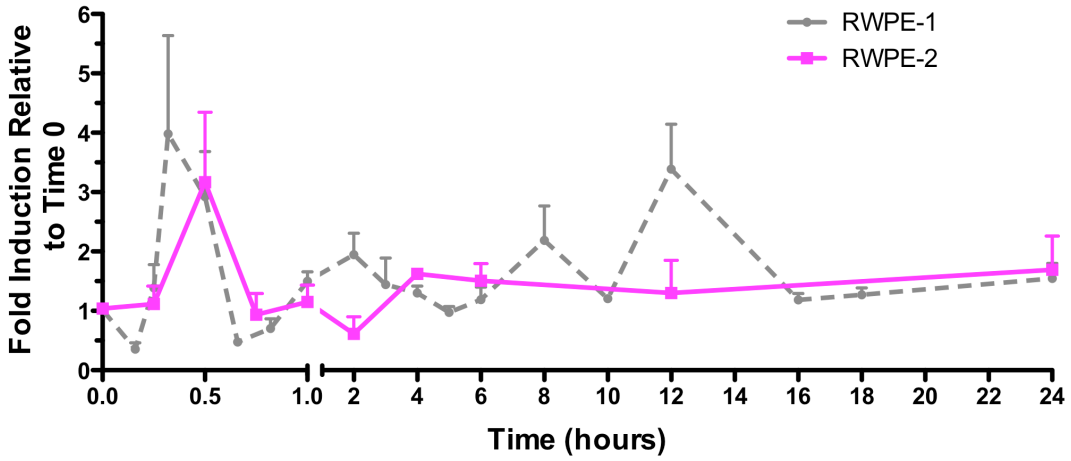

Figure 5.11 RWPE-2 cells exhibit differential VDR target gene regulation in response to 1α,25(OH)$_2$D$_3$ (100nm). *Total mRNA was collected from cells (1x10^5 per well) and reverse transcribed Q-RT-PCR analysis of cells exposed to 1α,25(OH)$_2$D$_3$ (100nm) over time using primers specific for CDKN1A. The fold change to vehicle only control was calculated. Points shown are the mean of at least three independent experiments ± SEM. Data was subject to t-test using Welch Correction to account for unequal population variances. *=p-value 0.05, **=p-value 0.01, ***=p-value 0.001.*

As insensitivity was demonstrated in the *CDKN1A* gene in RWPE-2 other VDR regulated genes were examined. Figure 5.12 shows the *CYP24A1*, *PTGS2*, *VDR* and *GADD45α* genes. *PTGS2*, *VDR* and *GADD45α* show no significant induction in response

to ligand. RWPE-2 cells produce a similar of *CYP24A1* induction in comparison to RWPE-1.

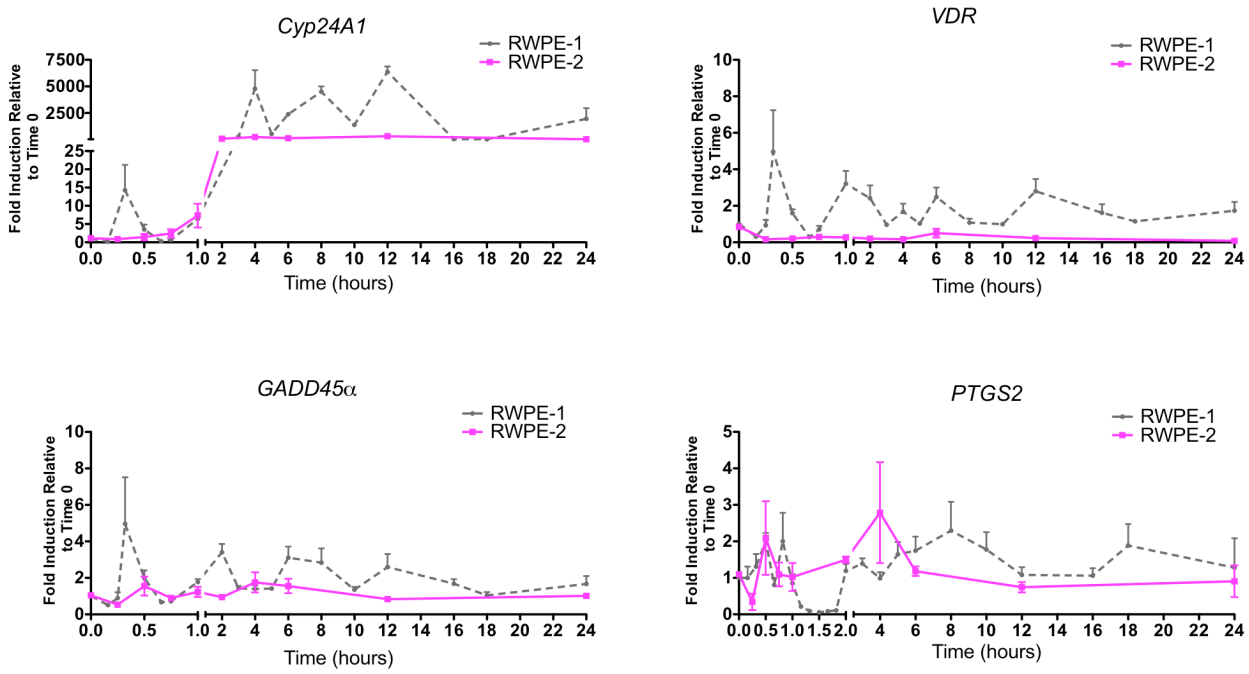

Figure 5.12 RWPE-2 cells exhibit selective VDR insensitivity in response to 1α,25(OH)$_2$D$_3$. *Total mRNA was collected from cells (1x10^5 per well) and reverse transcribed Q-RT-PCR analysis of cells exposed to 1α,25(OH)$_2$D$_3$ (100nm) over time. mRNA was measured and the fold change to vehicle only control was calculated. Points shown are the mean of at least three independent experiments ± SEM.*

5.2.8 MCM7 expression in response to 1α,25(OH)$_2$D$_3$ in RWPE-1 and PC-3 cells.

To further understand VDR regulation within a physiological signaling response the MCM7 gene, a target of S-phase transcription factors was examined. RWPE-1 cells treated with 1α,25(OH)$_2$D$_3$ (100nM) produced a down regulation of the MCM7 protein.

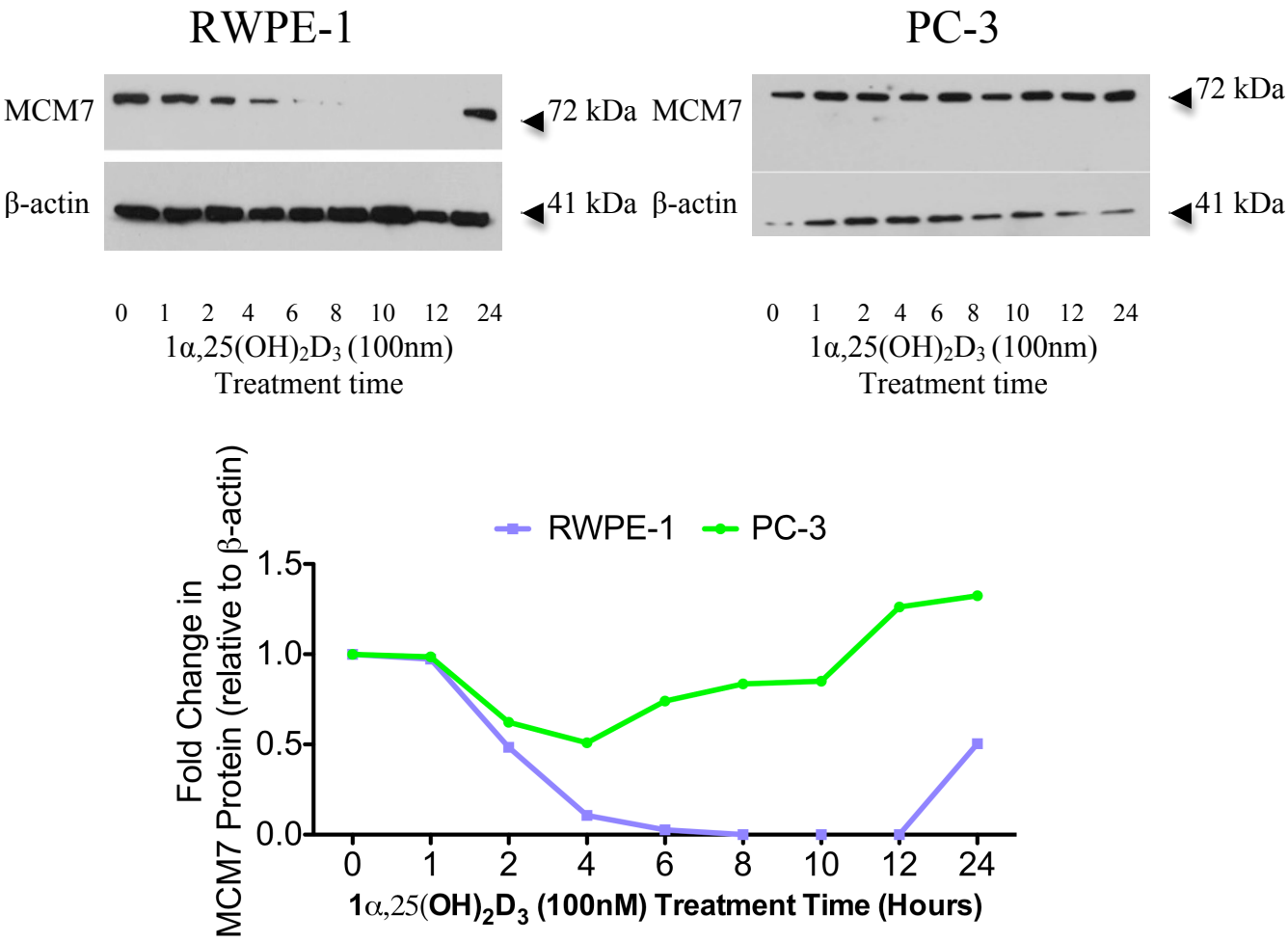

Figure 5.13 1α,25(OH)$_2$D$_3$ induced MCM7 protein level changes in RWPE-1 and PC-3 cells. RWPE-1 and PC-3 cells were plated in T75 flasks at 1x10^6 and 5x10^5 cells per well respectively. Treatment commenced the following day with 1α,25(OH)$_2$D$_3$ (100nm) controls were treated with ethanol vehicle only. Protein lysates were harvested and analysed by Western with MCM7 specific antibody. Quantification conducted by Image-J software and MCM7 bands were normalized to respective β-actin loading controls.

Conducting the same experiment in PC-3 cells showed that the magnitude of this response is diminished in ADT-R CaP. This demonstrates that VDR insensitivity may enhance the replicative potential of the malignant cell (Figure 5.13). Elevated MCM7 expression is associated with an increased cellular proliferation potential within the cell and it has been shown that this protein is overexpressed in ADT-R CaP [217]. Analysis of basal protein levels in RWPE-1 and PC-3 cells shown in Figure 5.14 showed PC-3 cells overexpress MCM7 protein with a 3.6 fold increase in levels in comparison to RWPE-1 cells.

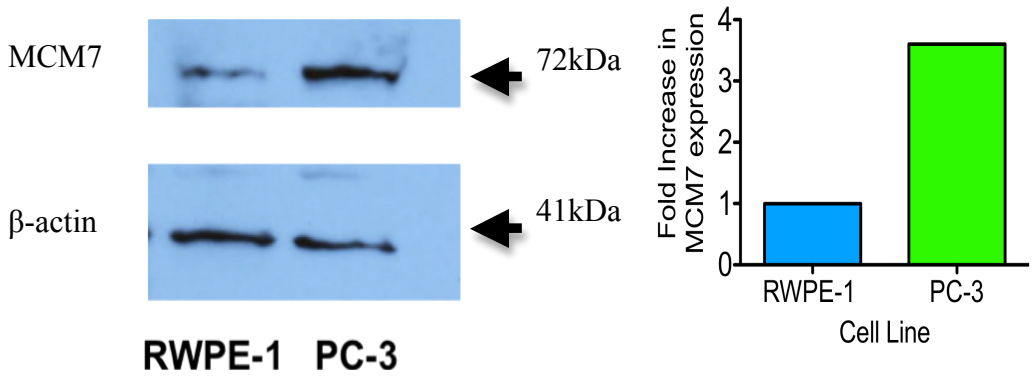

Figure 5.14 Replicative helicase MCM7 is overexpressed in PC-3 cells. RWPE-1 and PC-3 cells were plated in T75 flasks at $1x10^6$ and $5x10^5$ cells per well respectively. Protein lysates were harvested and analysed by Western Immunoblot with MCM7 specific antibody. Quantification conducted by Image-J software and MCM7 bands were normalized to respective β-actin loading controls.

Elevation in the level of the MCM7 protein suggested that the levels of MiR106b are also elevated within malignancy. Such accumulation would lead to increased targeting of CDKN1A transcript reducing protein levels within transformed cells. This may establish a novel VDR dependent mechanism that becomes deregulated in CaP. Therefore to understand this response during prostate tumourigenesis TRAMP mouse

model mRNA at differing stages of tumour growth was examined for differential expression within the VDR-MCM7-CDKN1A feedforward loop.

5.2.9 Disruption of a VDR feed forward loop in CaP.

Components of the VDR feed forward loop become significantly altered within the TRAMP model of CaP (Figure 5.15). Primary TRAMP tumours show significant increases in cdkn1a mRNA (197.20 fold ± 30.99 SEM) levels. Analysis of metastatic tissue also demonstrated a significant increase in cdkn1a message (91.55 fold increase ±6.47 SEM). TRAMP levels of mcm7 were found to be elevated in comparison to wild type with both primary and metastatic tumours showing a significant elevation in message (168.30 ±34.63 SEM and 417.9 ±103.3 SEM respectively). Furthermore, comparison between the two tumour types shows that metastatic tumours have a higher level of mcm7 than primary tumours (p-value 0.009).

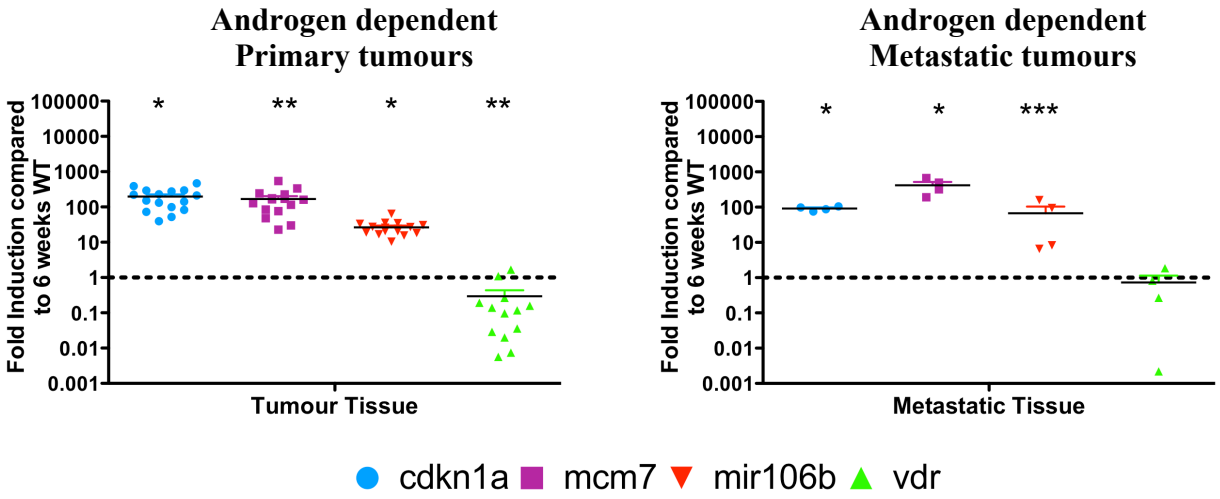

Figure 5.15 cdkn1a, mcm7 and mir106b are elevated in primary and metastatic TRAMP tissue in comparison to wild type tissue. Tissue samples were taken from the TRAMP model and mRNA analysed for cdkn1a, mcm7, vdr and mir106b transcripts. Each points represents a tumour taken from an individual mouse (N=at least 3) ± SEM. Data was subject to t-test. *=p-value 0.05, **=p-value 0.01, ***=p-value 0.001.

The mir106b transcript was also found to be overexpressed in both primary and metastatic tumours (26.50 ± 3.09 SEM and 67.02 ± 36.80 SEM respectively). In conjunction with metastatic tumours demonstrating increased mcm7 there is a statistically higher expression of mir106b in comparison to the primary tissue tumours (p-value 0.036). Expression of VDR within primary tumours was shown to be significantly lower in comparison to wild type mice with a fold reduction of 0.29 (± 0.13 SEM). There was no significant change in the VDR transcript abundance in the metastatic TRAMP tissue samples (0.73 ± 0.47% fold change of VDR). From these data is it evident the governing nuclear receptor, VDR and the motifs within the feedforward loop become deregulated. Furthermore, both mcm7 and mir106b were significantly elevated in the metastatic samples in comparison to primary tumours, suggesting a differential modulation of the feed forward circuitry.

To examine this further TRAMP tumour samples from castrated mice were selected for analysis. These represent an ADT-R model of prostate disease and were extracted and analysed alongside the androgen dependent tissue samples. Such hormone refractory tumours have been previously demonstrated to exhibit NR deregulation. Analysis of the manner of deregulation may reveal the role of androgen sensitivity as being a key mechanism by which malignancy produces a VDR insensitive phenotype, and facilitating a bypass of the $p21^{(waf1/cip1)}$ cell cycle arrest response between the two diseases.

The data presented in Figure 5.16 show that elements of the VDR-MCM7-CDKN1A feed-forward loop are deregulated within ADT-R disease but are also altered in prostate malignancy that is not representative of recurrent disease. Elevation of

Cdkn1a was observed in both the primary tumour and malignant tumour samples from the castrated mice (3482.05 fold change ±1894.00 SEM and 315.04 fold change ±83.02 SEM respectively.

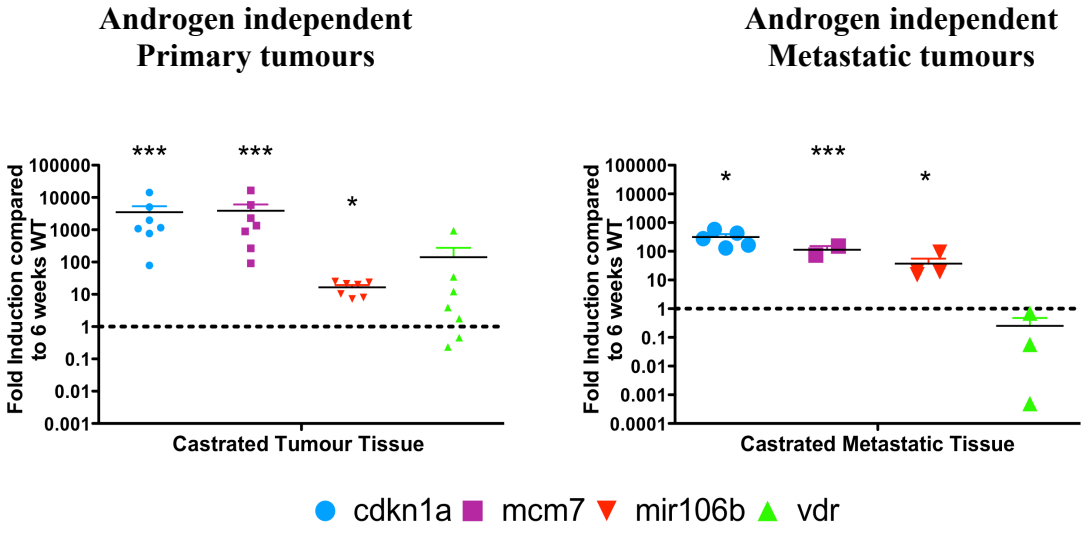

Figure 5.16 cdkn1a, mcm7 and mir106b are elevated in primary and metastatic TRAMP tissue taken from castrated mice in comparison to wild type tissue. Tissue samples were taken from the TRAMP mice. mRNA was analysed for cdkn1a, mcm7, vdr and mir106b transcripts. Each point represents a tumour taken from an individual mouse (N= at least 3) ± SEM. Data was subject to t-test. *=p-value 0.05, **=p-value 0.01, ***=p-value 0.001.

Reflective of the findings in the non-castrated samples (both primary and metastiatic) both mcm7 and mir106b transcripts are also elevated in TRAMP based malignancy. Furthermore, the vdr transcript abundance was not altered in castrated tumour tissue in comparison to wild type. This suggests that the mechanism of deregulation of the incoherent feedforward loop in androgen independent primary tissue may be similar to metastatic disease.

The disruption of miR106b within CaP is in corroboration with many studies that conclude miR expression is important in tumourigenesis (reviewed in [218]). Emerging literature also supports the hypothesis that miRNA overexpression can be detected within

the serum of patients [219]. This has potential to become a new area of diagnostic biomarkers for cancer. Therefore, it was hypothesised that elevated miR106b within the circulating serum of individuals may be an important indicator of VDR responsiveness and of tumour progression. The test this serum was collected from TRAMP mice used in the tissue mRNA study and the level of miR106b were assessed.

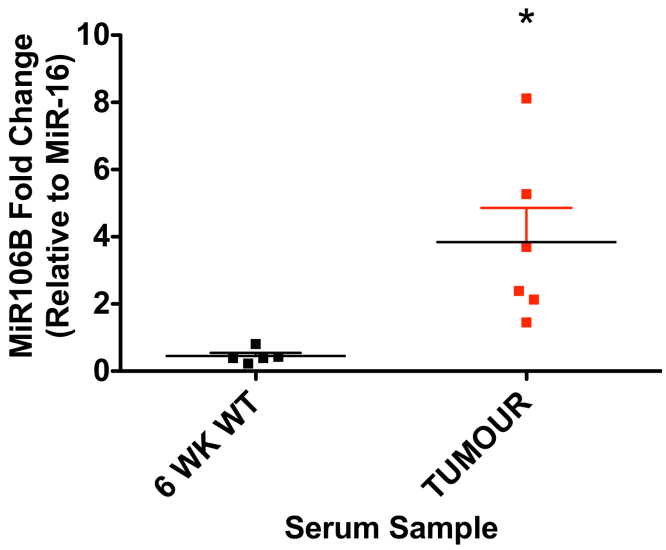

Figure 5.17 mir106b is elevated in the serum of TRAMP mice in comparison to wild type tissue. Serum samples were taken from the TRAMP model core facility in Roswell Park Cancer Institute and mRNA was extracted, reverse transcribed and analysed for mir106b transcripts and made relative to miR-16 as an endogenous control. Each points represents a tumour taken from an individual mouse (N= at least 3) ± SEM. Data was subject to t-test. *=p-value 0.05, **=p-value 0.01, ***=p-value 0.001.

The data illustrated in Figure 5.17 shows miR106b was significantly elevated in the serum of TRAMP tumour mouse models (3.84 fold change ±1.01 SEM). This finding supports the hypothesis that serum expression of VDR regulated microRNA within cancer may be useful to define molecular phenotypes such as aggressiveness or resistance to VDR ligands.

5.3 Discussion

This investigation addressed the dynamic regulation of the VDR within a non-transformed prostate epithelial cell line (RWPE-1). Using this model of prostate epithelial cell status the functional role of NR target genes was observed. Data showing the regulation of VDR target genes was compared to models of prostate malignancy (PC-3 and RWPE-2). Both isogenic and non-derivative cell lines showed levels of VDR insensitivity, however, the corruption of VDR signaling is pronounced in PC-3 cells. Before studying gene expression within the VDR network it was also critical to evaluate the effects of media components upon the cells growth characteristics. This study found that the addition of growth stimulatory EGF to medium of RWPE-1 cells had no significant impact upon the levels of VDR target gene expression. This demonstrated VDR regulated actions are suitably observed within the RWPE-1 and PC-3 cell lines.

Activation of VDR was able to induce varying mRNA dynamic profiles within RWPE-1 cells. The kinetics of these responses allowed genes to be divided into two groups of sustained elevated mRNA (*CYP24A1*, *ALOX-5*, *G0S2*) or short-term induction over the first 8 hours treatment (*ESR1* and *PTGS2*).

Non-transformed prostate cells were shown to exhibit enriched VDR and basal levels of target genes that are proportional to their VDR responsiveness. Further, the malignant cells lose their enriched basal levels of VDR in comparison to VDR target genes. This may reflect the inability of these cells to respond to VDR in the presence of ligand.

Studies have demonstrated that an epigenetic lesion within malignant disease contributes to loss of VDR sensitivity [129]. In particular, deregulated NCOR1 has been shown to play are role in this process [176].

From the data herein it is proposed that the prostate VDR network contains an incoherent feedforward loop (FFL) that modulates the expression of *CDKN1A* mRNA. Activation of VDR directly induces *CDKN1A* expression, in addition there is activation of MiR106B that is able to target and degrade the *CDKN1A* message thus producing an incoherent FFL.

Both coherent and incoherant FFLs have been implicated in temporal waves of response [220] and serve to regulate the level of mRNA output modulating signal strength and preventing inappropriate mRNA accumulation whilst at the same time permitting accumulation of message at levels greater than background noise. However, we observe that malignancy renders the prostate cells selectively unresponsive to VDR ligand mediated activation. The presence of $1\alpha,25(OH)_2D_3$ in PC-3 cells does not activate the *CDKN1A* response but does activate MCM7 and MiR106B (although there is observable change in magnitude and timing). This suggests that the present incoherent FFL becomes altered in disease allowing accumulation of the *CDKN1A* repressive element whilst impeding the *CDKN1A* activating element. Such selective aberrance is not uncommon in cancer and has been observed in other FFLs of both a coherent [221] and incoherent [222] nature.

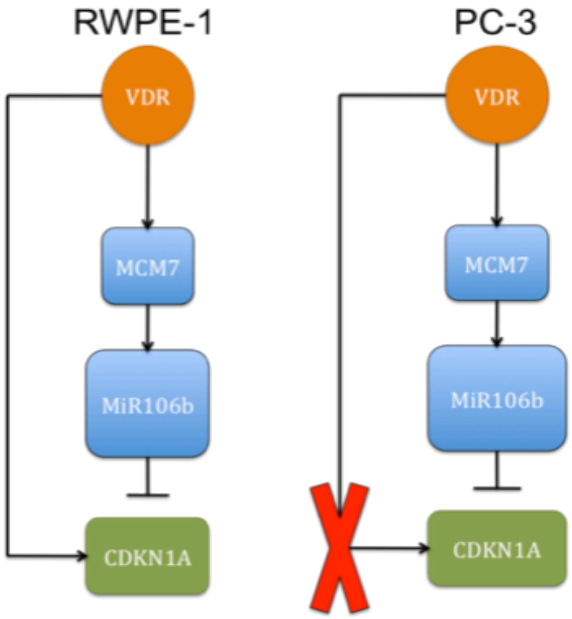

Figure 5.18 Incoherent feedforward loop (IFFL) implemented by VDR activation becomes deregulated in cancer models. Demonstrated above in non-transformed cells VDR activation stimulates CDKN1A but in combination is able to indirectly decrease $p21^{(waf1/cip1)}$ levels through MiR-106B induction. Deregulation of the IFFL in prostate cancer models is shown only at the direct level, indirect regulation by MiR106B induction remains unaltered.

Of further interest is the deregulation of MCM7 at the protein level observed in the malignant disease model, VDR ligand was successful at inducing the degradation of the MCM7 protein levels not previously observed (however, the molecular mechanism behind this response is unclear). However, in disease the effect of VDR activation upon MCM7 level is not replicated and MCM7 levels were sustained.

Members of the MCM family have been demonstrated previously to be targeted and degraded by the MiR-1296 [223], in addition it has been shown that the miRNA MiR-1296 is lost in CaP. Therefore, it is hypothesised that during CaP development the cell loses the ability to express MiR-1296 resulting in aberrant and sustained activation of MCM7. This demonstrates another level of transcriptional deregulation present in

malignant disease. Additionally, the MiR-1296 sequence is located on chromosome 10 within the second intron of the histone demethylase JMJD1c (originally named TRIP8) suggesting that activation of VDR is responsible for up-regulation of both a histone modifying demethylase and a microRNA. Upon validation this would exemplify the existence of another incoherent feedforward loop that becomes deregulated in CaP.

This study found detectable levels of MiR106b present within the serum samples from TRAMP model mice. Furthermore, the study demonstrated elevated levels of MiR106B present in CaP serum samples. Current screening for prostate cancer utilises the expression levels of PSA that are linked to androgen receptor levels. Indeed, since the introduction of the PSA test 25 million are performed yearly in the USA [224]. Current guidelines state a PSA concentration of greater than 4.0ng/ml indicates the presence of cancer. However, there are many reported cases of prostate cancer occurring in patients with a PSA lower than the 4.0ng/ml cut off limit. Therefore, it is clear that whilst the PSA test has produced an increase in the levels of detection of prostate cancer, it is unable to distinguish between associated prostatic conditions such as benign prostate hyperplasia (BPH) and prostatic inflammation. The search for new biomarkers of prostate cancer is continuing with any potential serum biomarkers being of great value. Elevation of MiR106B in comparison to normal serum samples in TRAMP mice indicates that this miRNA is released into the serum and may be a new novel biomarker of prostate cancer pathology. In order to validate this finding further, serum samples from humans with differing grades of prostate cancer development should be assessed for their MiR106B content.

Chapter 6: VDR governed control of gene transcription and epigenetic components within *CDKN1A* expression

6.1 Introduction

Investigations into the mechanisms of inappropriate gene repression have demonstrated that epigenetic lesions are induced by elevated recruitment of CoRs and HDACs to target gene promoters [131]. Using RWPE-1 and PC-3 cells the following investigation examined how ligand stimulation of VDR governs the recruitment of nuclear corepressors (NCOR1, NCOR2/SMRT) and activated polymerase II (phosphorylated polymerase II) to the promoter of *CDKN1A*. Previous publications have focused on the significant role of the CoRs, and both NCOR1 and NCOR2/SMRT can interact with VDR to negatively regulate transcriptional responses [225, 226]. Specifically, CaP cells have been demonstrated to upregulate the expression and activity of the NCOR1 and NCOR2/SMRT proteins [213] that contribute to transcription silencing.

Analysis to examine the extent of CoR release and recapture by the VDR has not yet been conducted. Also not fully elucidated are the levels of preference (if any) that the VDR demonstrates either towards NCOR1 or NCOR2/SMRT. Earlier investigations indicate that the VDR uses both NCOR1 and NCOR2/SMRT to modulate of mRNA production. Repression of transcriptional response through the interaction of corepressors may produce variations in mRNA kinetics. Therefore, it was hypothesised that their analysis may reveal the rate of interaction of NRs with CoRs and how they work in tandem with epigenetic marks to facilitate polymerase activation. In addition to this the binding status of the same elements in the malignant prostate cell line PC-3 was also investigated. This may allow identification of molecular deregulations present in ADT-R forms of CaP.

6.2 Results

6.2.1 Re-ChIP in RWPE-1 cells to reveal VDR-CoR interactions.

To understand how corepressors influence the action of $1\alpha25(OH)_2D_3$ treated VDR in normal prostate environment re-chip studies were conducted. In response to ligand activation VDR bound NCOR1 and VDR bound NCOR2/SMRT were immunoprecipitated to examine the role of corepressor recapture and release upon *CDKN1A* transcription. Measurement of VDR in the presence of NCOR1 unveiled significant release of this CoR at each response element and the TSS 0.5 hours post treatment in comparison to vehicle only controls (VDRE-3 0.191 ± 0.058 SEM, VDRE-2 0.317 ±0.137 SEM, VDRE-1 0.273 ±0.092 and TSS 0.156 ± 0.081 SEM) (Figure 6.1). These events occurred at 1 and 4 hours post $1\alpha,25(OH)_2D_3$ (100nm) exposure. VDRE-2 showed a 3.199 fold change (±0.659 SEM) in NCOR1 bound VDR at 1 hour and 3.971 (±0.804 SEM) at 4 hours. These indicated significant enrichment of NCOR1 associating with the ligand activated VDR at 1 and 4 hours at VDRE-2. There was no statistically significant change in the level of NCOR2/SMRT associated with VDR. However, there were trends shown at VDRE-2 at 0.5, 1 and 4 hours treatment. In addition there were increases in the level of NCOR2/SMRT found bound to VDR at the TSS at 4 and 12 hours, suggesting some recruitment for this CoR. Thus, as found previously VDR can interact with both NCOR1 and NCOR2/SMRT. However, here it has been demonstrated that ligand stimulation produced significant shifts in the enrichment of VDR bound to NCOR1. These data therefore suggest that NCOR1 holds a greater influence over VDR target gene regulation than NCOR2/SMRT.

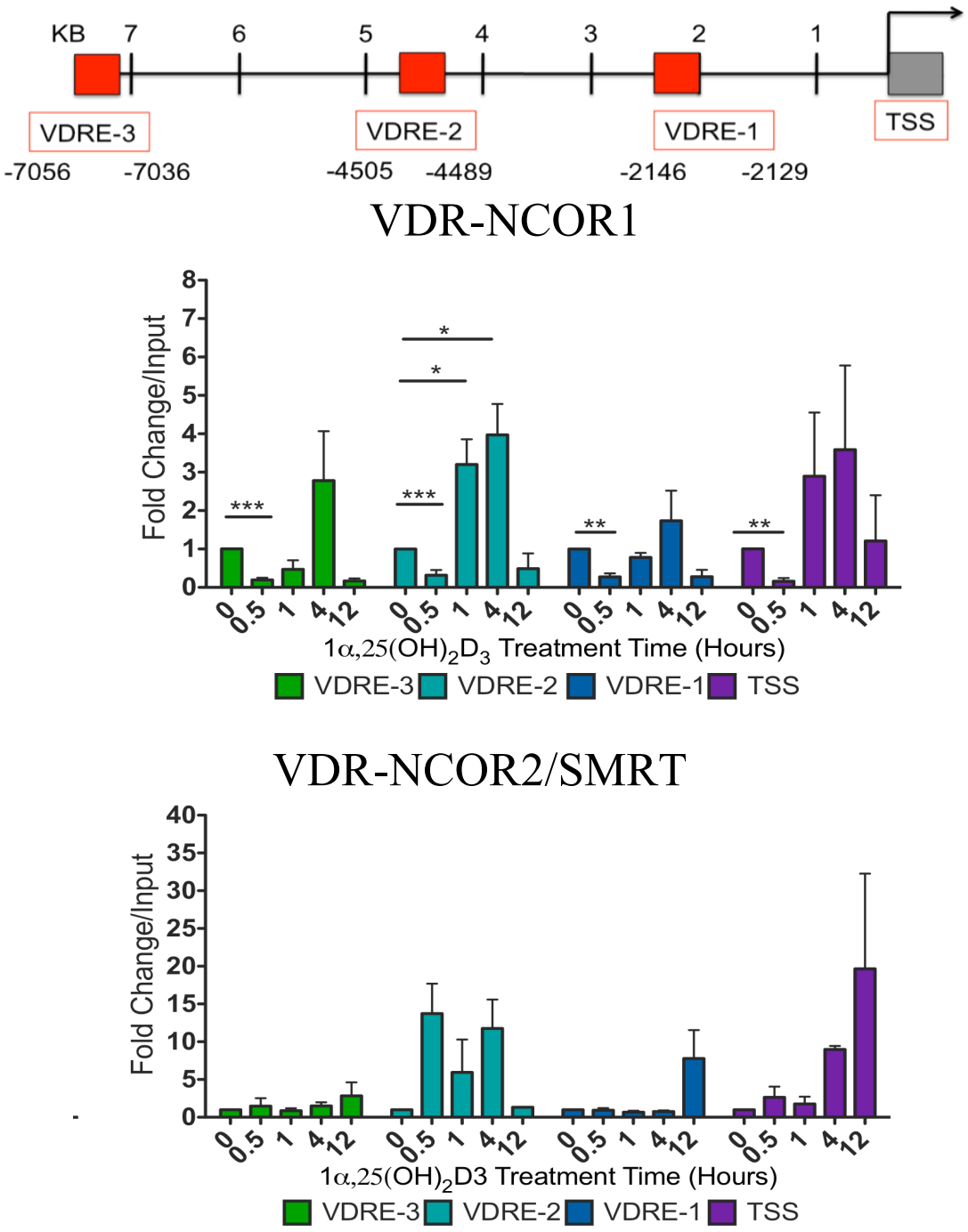

Figure 6.1 Interactions of VDR with transcriptional corepressors on the *CDKN1A* gene promoter. RWPE-1 cells were treated with 1α,25(OH)$_2$D$_3$ (100nm) for 0.5, 1, 4 or 12 hours, chromatin was extracted and subject to Re-Chip analysis with either VDR and NCOR1 antibodies or VDR and SMRT antibodies. Levels of DNA recovered from the sequential ChIP experiments at the VDREs and TSS of CDKN1A were analysed. Data was normalized and calculated as fold enrichment over input. Experiments were performed on three independent occasions and statistical significance was assessed using t-test analysis. *=p-value 0.05, **=p-value 0.01, ***=p-value 0.001.

6.2.2 VDR regulated binding events on the CDKN1A promoter in RWPE-1 and PC-3 cells.

Current consensus on the procedure of gene transcription is that it is a highly dynamic process conducted by numerous interacting factors. To help reveal how factors interact with a single gene upon transcriptional activation, recruitment of VDR, NCOR1 and phosphorylated polymerase 2 (p-POL II) was measured for their presence at the *CDKN1A* promoter and TSS in RWPE-1 cells. Additionally, to identify deregulation contributing to transcriptional resistance exhibited in ADT-R CaP PC-3 cells were analysed for their *CDKN1A* recruitment dynamics and compared to the RWPE-1 findings.

The response element most distal from the CDKN1A TSS is located -7056 to -7036 base pairs upstream VDRE3 (Figure 1.15). Examination by xChIP suggested a higher level of VDR enrichment within RWPE-1 cells and significant increases over PC-3 cells were measured at 2 and 12 hours post treatment (Figure 6.2). Generally there is a depletion of VDR binding at this VDRE demonstrating eviction of the VDR in PC-3 cells upon ligand addition. This is in opposition to the sustained levels measured in RWPE-1 cells. NCOR1 association at this region indicates that there was CoR depletion of the RWPE-1 cells, with a sustained level of NCOR1 in the PC-3 cells. There was clear early enrichment in both cell types (0.25 hours for RWPE-1 and 0.50 hours for PC-3 cells) of CoR. However this was followed a protracted loss in levels that was greater in the RWPE-1 cells again demonstrating elevated CoR presence in PC-3. There were no significant changes in the level of phosphorylated polymerase 2 recorded in either cell line. This indicated that transcriptional machinery has limited role upon gene activity at this distal location.

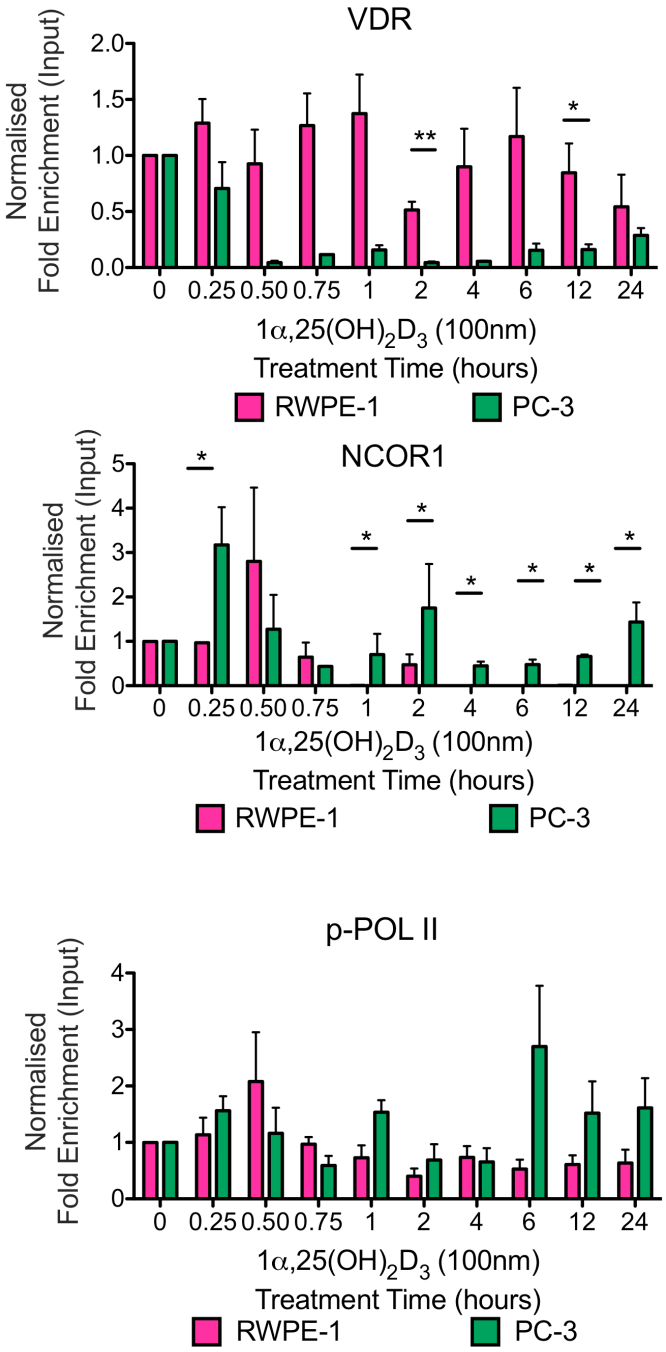

Figure 6.2 Recruitment and loss of factors at VDRE3. RWPE-1 and PC-3 cells were plated at $1x10^7$ and $5x10^6$ cells per flask respectively. Treatment was with $1\alpha,25(OH)_2D_3$ (100nm) for the described time periods. Crosslinked chromatin was harvested and sonicated to an average of 500bp in length. Specific antibodies were used to pull down proteins bound to DNA. Levels of immunoprecipitated DNA were measured using Q-RT-PCR. Data was normalized and calculate as fold enrichment over input. Bars indicate the mean of at least three independent experiments analysed in triplicate PCR well ± SEM. *=p-value 0.05, **=p-value 0.01, ***=p-value 0.001.

Figure 6.3 shows the data from the VDRE located -4505 to -4489 base pairs upstream of the *CDKN1A* TSS. These data indicate there was accumulation of NCOR1 at specific times post treatment. Furthermore, NCOR1 was found to become significantly enriched in the PC-3 cells at 0.5 hours. This supports the hypothesis that aberrant corepressor recruitment may act as a molecular brake upon transcriptional activation. Levels of VDR and p-POL II enrichment between the two cell lines showed little significant variation. Only enrichment of VDR at 1 hour was shown in RWPE-1 cells indicating some activity at this region. Taking into consideration the histone modification changes occurring upon VDR activation revealed parallel epigenetic regulation. The enrichment of VDR shown at 0.5 and 1 hour not only occurred with a release of NCOR1 but also correlated to increases in H3K9ac and depletion of the repressive H3K9me2 mark. However, the modifications at H3K9 reverted back to a repressive signature by 1 hour (Figure 1.18). This suggests a tightly controlled response to ligand addition programmed to activate transcription.

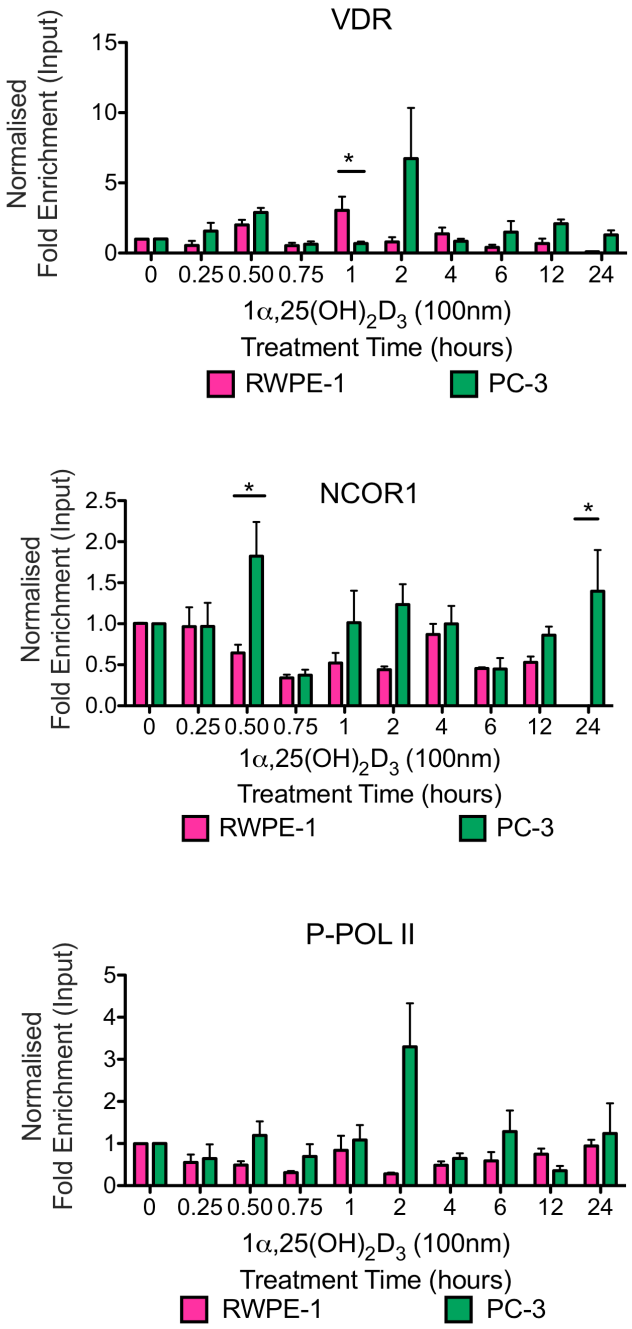

Figure 6.3 Recruitment and loss of factors at the VDRE2. RWPE-1 and PC-3 cells were plated at $1x10^7$ and $5x10^6$ cells per flask respectively. Treatment was with $1\alpha,25(OH)_2D_3$ (100nm) for the described time periods. Crosslinked chromatin was harvested and sonicated to an average of 500bp in length. Specific antibodies were used to pull down proteins bound to DNA. Levels of immunoprecipitated DNA were measured using Q-RT-PCR. Data was normalized and calculate as fold enrichment over input. Bars indicate the mean of at least three independent experiments analysed in triplicate PCR well ± SEM. *=p-value 0.05, **=p-value 0.01, ***=p-value 0.001.

Located 2146–2129 base pairs upstream of the *CDKN1A* TSS is a VDRE (VDRE1). Binding characteristics in both RWPE-1 and PC-3 cells at this functioning VDRE were measured in response to ligand and are shown in Figure 6.4.

VDR enrichment at VDRE1 was demonstrated to be more persistent in RWPE-1 cells with significantly higher levels at 1 and 24 hours in comparison to PC-3 cells. These data suggest a depletion of VDR presence in PC-3 cells. Measurement of NCOR1 activity showed no statistically significant difference between the two cell lines. However, there was an upward trend of NCOR1 within PC-3 cells at 4 and 6 hours suggesting a role in 'late' transcriptional events. Accumulation of p-POL II was highly active in the RWPE-1 cells and is significantly elevated above PC-3 cells. This was consistent with the regions proximity to the TSS of an active gene in comparison the CDKN1A in PC-3 cells demonstrated not to be activated by VDR stimulation. Analysis using phosphorylated POL II antibody serves as an indication for transcriptional activity, and p-POL II levels were significantly enriched in RWPE-1 cells compared to PC-3 cells. This finding alludes to the lack of transcriptional response in malignant cells, prevention of VDR recruitment to this region inturn impacts upon the enrichment of p-POL II.

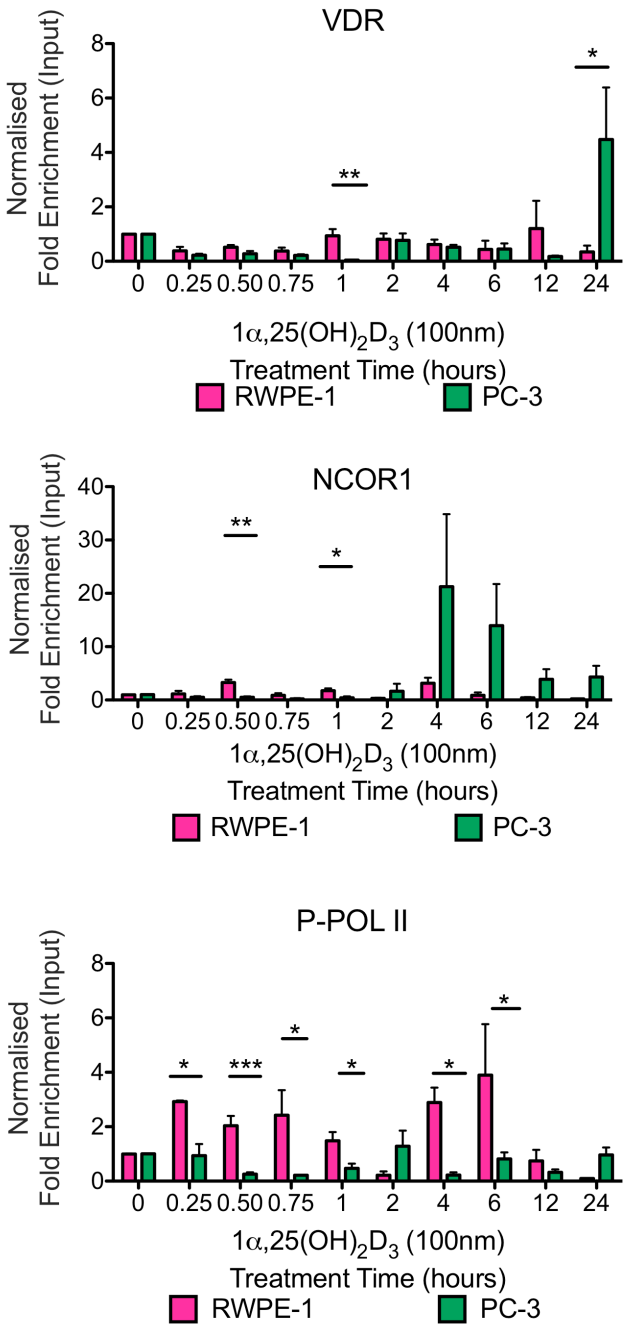

Figure 6.4 Recruitment and loss of factors at the VDRE1. RWPE-1 and PC-3 cells were plated at $1x10^7$ and $5x10^6$ cells per flask respectively. Treatment was with $1\alpha,25(OH)_2D_3$ (100nm) for the described time periods. Crosslinked chromatin was harvested and sonicated to an average of 500bp in length. Specific antibodies were used to pull down proteins bound to DNA. Levels of immunoprecipitated DNA were measured using Q-RT-PCR. Data was normalized and calculate as fold enrichment over input. Bars indicate the mean of at least three independent experiments analysed in triplicate PCR well ± SEM. *=p-value 0.05, **=p-value 0.01, ***=p-value 0.001.

Recruitment at the *CDKN1A* TSS is shown in Figure 6.5. VDR binding at the TSS showed significant enrichment in RWPE-1 cells at 0.75 hours (1.75 fold change ±0.21 SEM) when compared to PC-3 cells (0.30 fold change ±0.04 SEM).

Furthermore, PC-3 cells demonstrated an elevation of NCOR1 levels to the *CDKN1A* TSS in response to VDR activation. This is in contrast to RWPE-1 cells, which show a rapid depletion of NCOR1 upon VDR activation. These become statistically significant at 0.75, 1, 4, 6 and 24 hours suggesting that VDR in untransformed prostate epithelial cells are able to release NCOR1 upon ligand binding. Moreover, these data also suggest that this becomes corrupt in malignancy preventing the release of NCOR1 from the TSS. The analysis of p-POL II levels indicates PC-3 cells show enrichment greater than RWPE-1 cells with significant accumulations measured at 0.75 and 2 hours post treatment.

Taken together, the xChIP analysis confirms that RWPE-1 and PC-3 cells exhibit differential recruitment of factors to the VDREs encoded within the *CDKN1A* promoter. Furthermore, the enrichment of the factors observed varied in a time dependent fashion and each region demonstrates individual binding patterns of VDR, NCOR1 and p-POL II. This establishment of recruitment and loss of these factors in non-transformed cell lines provides integral understanding of the mechanisms behind transcriptional activation. For example, $1\alpha,25(OH)_2D_3$ treatment induced depletion of NCOR1 from the TSS, presumably to allow CoA recruitment. An additional key finding shown at the TSS the persistent NCOR1 levels at the TSS in PC-3 cells in contrast to the accumulation of p-POL II.

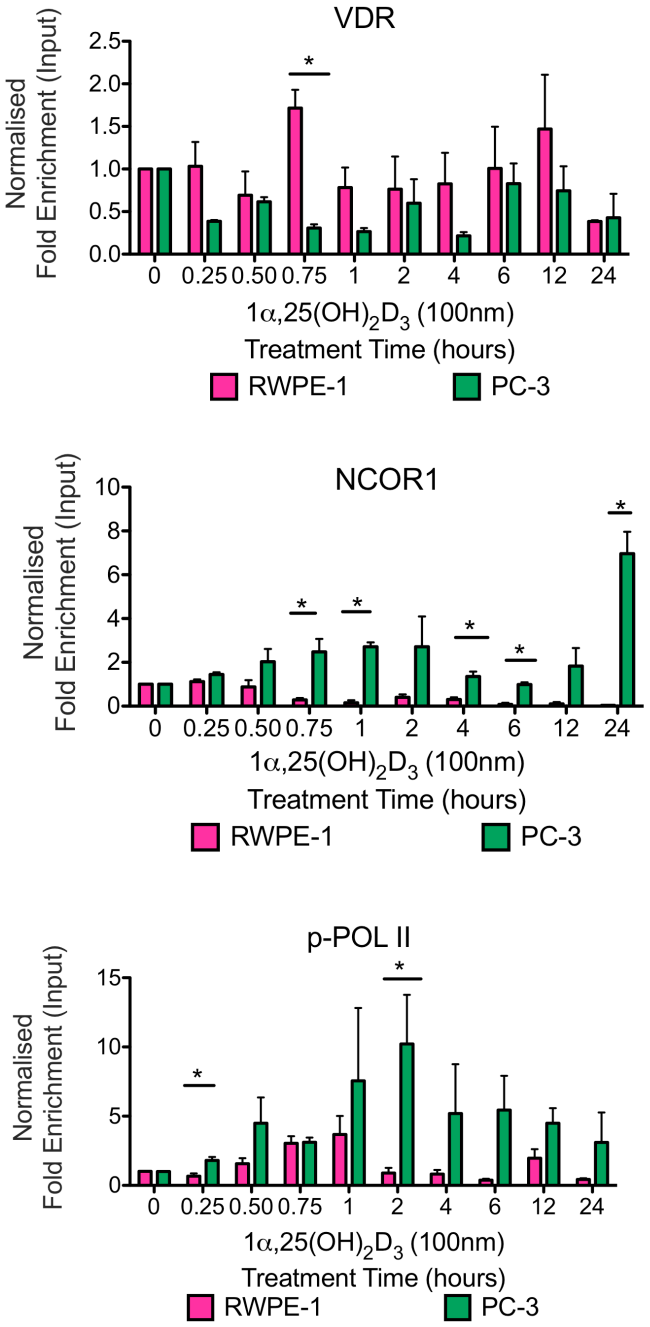

Figure 6.5. Recruitment and loss of factors at the CDKN1A transcription start site (TSS). RWPE-1 and PC-3 cells were plated at $1x10^7$ and $5x10^6$ cells per flask respectively. Treatment was with $1\alpha,25(OH)_2D_3$ (100nm) for the described time periods. Crosslinked chromatin was harvested and sonicated to an average of 500bp in length. Specific antibodies were used to pull down proteins bound to DNA. Levels of immunoprecipitated DNA were measured using Q-RT-PCR. Data was normalized and calculate as fold enrichment over input. Bars indicate the mean of at least three independent experiments analysed in triplicate PCR well ± SEM. *=p-value 0.05, **=p-value 0.01, ***=p-value 0.001.

6.3 Discussion

These data established that the VDR target gene CDKN1A exhibits fluctuations in the dynamics of NR and CoR exchanges that occur in a unique manner at each response element. These changes have been reflected further by the recently demonstrated chromatin looping of these VDREs toward the CDKN1A TSS [126].

As previously discussed this laboratory and others have purported NCOR1 as the pertinent corepressor in VDR mediated target gene regulation [129, 131, 227]. However, the importance of NCOR2/SMRT within VDR activation until now had not been fully investigated. To address this Re-ChIP analysis of VDR bound with NCOR2/SMRT and VDR bound with NCOR1 was conducted. Analysis by Re-ChIP demonstrated that VDR favorably interacts with NCOR1 in preference to NCOR2/SMRT (Figure 6.1). The significant release of NCOR1 observed at 0.5 hours from VDR also suggests this may be a major contributor early mRNA peak observed in Chapter 1 Figure 1.16. Furthermore, an increased level of NCOR1 associated with VDR at the VDRE1 at 1 and 4 hours and this may serve to temper the transcriptional output of the *CDKN1A* gene. Therefore, this demonstrated this VDRE to have a specific role in the transcriptional regulation of *CDKN1A*.

Through xChIP analysis of the *CDKN1A* promoter it was found that RWPE-1 cells recruit VDR to the TSS upon ligand activation. In addition TSS bound VDR was found to be depleted for NCOR1 in a time dependent manner. This loss of CoR is in corroboration with the classical view of transcriptional studies and a reduction in NCOR1 indicates there may be enrichment of CoAs (such as CBP, SRC and TRAP220 which have been previously shown to become enriched at the *CDKN1A* VDREs [75]).

Concordant with these findings there is a general increase in the levels of p-POL II at the TSS emphasising transcriptional activation.

Characterisation of the binding patterns in RWPE-1 at the VDREs showed individual accumulation and loss patterns isolated to each region. It is hypothesised that each region contributes through DNA bound VDR looping of the response element to the TSS (Reviewed in [228, 229]). These events can occur regardless of their physical proximity and investigations conducted that show the looping of VDREs to exhibit an irregular cyclical quality [126].

Therefore, it is postulated that cyclical looping of VDREs to the *CDKN1A* TSS maybe reflected by the recruitment of VDR, coeffectors and phosphorylation of Polymerase II in order to drive transcriptional activation. This yields a specific mRNA profile characteristic of the gene's VDREs and epigenetic status.

The altered VDR target gene expression patterns in Chapter 5 were reflected by changes in the patterns of NCOR1 recruitment in RWPE-1 and PC-3 cells. Also both CoRs associate on the *CDKN1A* promoter in a highly dynamic manner in response to VDR activation, however, only NCOR1 was able to show statistical significance. These data also show NCOR1 clearly associated on the *CDKN1A* promoter in PC-3 in a more dominant manner in comparison to RWPE-1 cells. Thus, instead of inducing co-repressor release, NCOR1 was actively enriched at all three response elements and reflected the transcriptional repression. The molecular mechanisms behind vitamin D insensitivity in PC-3 cells in Chapter 5 is not fully clear. This study finds in PC-3 cells there are differential recruitment patterns most notably resulting in accumulation of NCOR1 at the TSS. This represents deregulation of the switch model leading to corepressor/activator

exchange [230]. In PC-3 cells there is an inability of VDR to release the NCOR1 leading to maintenance of transcriptional status, preventing activation. Future studies should be conducted into the molecular basis regulating NCOR1 binding, including its ubiquination that governs its clearance from ligand bound NR complexes [231].

Chapter 7: Conclusions and future work

Identifying the mechanisms behind dietary and hormone signaling and their impact upon cancer progression is an important goal of research. Nuclear receptors respond directly and indirectly to modulate target gene expression producing essential physiological process such as differentiation and cellular growth. However, their activity appears impeded in various malignancies. Furthermore, this NR resistance is heavily implicated within breast and prostate cancer progression (reviewed by [232]).

7.1 Pre-receptor regulation of NR activity in ADT-R CaP.

Prereceptor ligand metabolism has been previously demonstrated as an important factor in the regulation of nuclear receptor activity. Networks of signaling pathways can therefore influence the levels of NR ligand available to the receptor. During progression, CaP cells acquire the ability to upregulate the formation of AKR1C3 [233]. This enzyme is able to convert the naturally occurring ligand for PPARγ into a compound with pro-growth effects of PGF_2, thus hypothetically depriving the anti-proliferative pathways normally activated by PPARγ. This study attempted to restore the actions of this anti-tumourigenic nuclear receptor through reduction in the levels of AKR1C3. This may increase the levels of ligand available for PPARγ activation. Such experiments have previously shown knocking down AKR1C3 has proved successful in various leukemic and breast cell lines [185, 234]. Therefore, this investigation used PC-3 and DU 145 (both models of ADT-R disease) and found that reducing the levels of AKR1C3 and co-treatment with PGD_2 and SAHA was unable to restore activation of this NR. To address these findings further it is suggested that interventionist studies of the following nature should be conducted; Upregulation of HAT enzymes may enhance the responsiveness shown by these results. It is hypothesized that exogenous exposure of HATs would aid

the placement of acetyl groups increasing expression. Knocking down AKR1C3 is shown to have a profound effect upon various elements important to transcriptional activation. These effects may be specific to ADT-R CaP cells and inhibiting any elevation in PPARγ activity. In addition quantification in the levels of PGJ_2 being produced within shAKR1C3 cells would serve to verify increased presence of NR ligand.

7.2 Elevated sirtuin levels produce aberrant HDAC activity

Insensitivity toward VDR and PPARγ ligands in CaP has been associated with increased CoR and HDAC expression. Furthermore, inhibition of HDACs has been demonstrated to enhance to responsiveness of NR ligands [184]. Here investigations found a member of the sirtuin family SIRT2 to be overexpressed in some but not all CaP cell lines. Thus, the hypothesis was formed that increased levels of SIRT2 led to targeting histone hypoacetylation, and repression of NR target gene expression. To test this RWPE-1 and PC-3 cell lines were exposed to a sirtuin inhibitor (Sirtinol) in an attempt to reduce levels of deacetylation. It was found PC-3 cells were resistant to the inhibitory effects of Sirtinol in comparison with RWPE-1 cells.

Previous work has also shown that knocking down NCOR1 reduced the ED_{50} of HDAC inhibitors needed to reduce PC-3 growth [184]. Therefore, it is suggested that NR target gene repression is maintained through CoRs. As there is minimal evidence for sirtuins interacting directly with the CoRs this possibility was explored through observation of NR target gene activity. Therefore, combined treatment of Sirtinol in conjunction with NR activation was performed. Addition of both VDR and PPARγ ligands in the presence of sirtinol were found to be unable to restore signaling of the nuclear receptors within the malignant cell environment. These findings indicate that

although prostate cancer cells contain upregulated levels of SIRT2 these have limited significance upon the NR silencing response observed within the PC-3 cell line which is a model of prostate malignancy.

7.3 VDR gene regulation within CaP progression

Regulation of genes in response to hormonal and dietary signals manifests from NRs, these activate networks of genes producing a physiological response. The VDR has been demonstrated to activate anti-tumourigeneic genes capable of slowing growth rates of cells. This work finds sub-sets of VDR regulated genes hold similarities in their pattern of expression independent of the physiological action they are associated with. This thesis, consistent with previous findings describes malignant metastatic prostate tumour cell lines to be insensitive to the biologically active form of vitamin D [235]. Several genes regulated by VDR in RWPE-1 cells become unresponsive in the PC-3 malignant cell line. Furthermore, the disruption is also shown to be present in the isogenic RWPE-2 cell line suggesting that deregulation occurs prior to ADT-R in NR activity. This study also demonstrated that the regulation of VDR regulated genes is highly dynamic and the magnitude of target gene expression varies in timing and magnitude. Furthermore, these genes can be grouped according to the kinetics and level of transcriptional response to $1\alpha,25(OH)_2D_3$.

During cancer development cells become increasingly aggressive in their growth characteristics and develop insensitivity to the vitamin D ligand. Insensitivity is shown in Chapter 5 of this work with PC-3 cells unable to be regulated by the nuclear receptor VDR. In accordance with this the basal levels of the VDR in PC-3 cells become altered.

Levels of VDR expression is lost in correlation to its target genes, this reflects the ability of VDR to exert its actions in cells which have become transformed.

The incoherent feedforward reponse observed within VDR-MCM7 signalling contains a microRNA (MiR106b) whose activity becomes disrupted in cancer. Therefore, it is evident that selective upregulation of the MCM7 promoter provides a growth advantage to the transformed cell. Not only does the proliferative MCM7 protein become upregulated but also the miR106b that targets *CDKN1A* transcript becomes upregulated. Similar deregulations of microRNAs in CaP are common (reviewed in [236]), the microRNA identified here not only is regulated by VDR but also targets a VDR target gene essential to growth control for degradation. Therefore, the hypothesis is put forward that MiR106b is a proto-oncogene capable of indicating the VDR resistant status of CaP. In relation, strong evidence is now emerging that microRNA expression of tumours are related to their levels of serum expression [237]. This makes them an exciting potential biomarker for the responses which they are involved in. To continue this work it is suggested that the serum analysis of human patients with various stages of prostate disease should be analysed and compared alongside normal control groups. The nature and consequence of the elevated MCM7 protein levels observed in malignancy are not clear. The hypothesis that increased MCM7 directly contributes in increased DNA replication of these cells needs to be further examined. In parallel the mechanism by which $1\alpha,25(OH)_2D_3$ is able to profoundly downregulate MCM7 protein levels in RWPE-1 and the loss of this in PC-3 needs deeper analysis.

Furthermore, previous evidence has suggested that the elevated expression of CoR and their increased deacetylation effect is able to selectively target specific genes.

For example partial correlation analysis showed NCOR1, PPARγ, C/EBPα, PTGS2 and ALOX5 cluster together separately from NCOR2/SMRT, AR and CDH1 [184]. This reveals that each CoR plays distinct roles in gene regulation for different subsets of target genes.

7.4 Regulation of CDKN1A transcription

Within the VDR network the nuclear corepressor NCOR1 has been shown to be a key regulator of transcriptional repression. Furthermore, previous studies have shown various cancer cells lines and tissues to contain elevated levels of corepressors [184]. ReChIP analysis in this work demonstrated that VDR bound to the CDKN1A gene promoter contains either NCOR1 or NCOR2/SMRT. This is in line with previous findings that have shown inducible knockdown models of NCOR1 to increase NR mediated gene expression [184]. However, not shown previously was the level of interaction over time in response to ligand. Additionally, although ADT-R CaP disease shows elevated CoR levels, examination of NCOR1 and NCOR2/SMRT activity at bound NRs within non-transformed cells has not been studied. This thesis reveals that fluctuations occur in the levels of NCOR1 and NCOR2/SMRT bound to VDR upon ligand stimulation. However, these changes only become significantly altered when measuring the VDR-NCOR1 levels. Such findings show that although VDR-NCOR2/SMRT is present at the CDKN1A VDREs and TSS they appear to play a minimal role in regulating transcription. The level of VDR-NCOR1 interaction is has been demonstrated to dramatically change over time. The rapid decrease in NCOR1 levels associated with VDR demonstrates a coordinated release of this CoR. Furthermore, there is recruitment of NCOR1 occurring over the later timepoints (4 and 12 hours). This

finding provides further evidence of NCOR1 being preferentially recruited by VDR. The continuity of this response between isoforms of both NCOR1 and NCOR2/SMRT is not known. As the affinity exhibited toward them by VDR may alter. Truncations in the receptor interacting domains of these CoRs may produce differing levels of activity not yet investigated.

Epigenetic inheritance indicates that there maybe transmission of gene regulatory information through placement of histone modifications from one generation of cell to the next [238]. However, not all marks contribute to such a cellular memory and it has become apparent that some marks may be used for short-term regulation of a genes transcription. Thus, aberrant epigenetic marks or their absence can lead to a disease state through aberrant gene expression or repression [239] Such modifications to the histone tails can regulate the extent of access transcription factors have the DNA by increasing or decreasing the level of chromatin compaction. However, in addition, histone marks have also been shown to have the ability to 'flag' specific DNA sequences. For example H3K4 monomethylation has been demonstrated to mark enhancer regions and H3K4 tri-methylation associated with enhancers and TSS [240]. This indicates the potential existence of an 'epigenomic map' with levels of various histone marks being used to indicate the presence of specific regions coded within the genome. These marks can be used to recruit transcriptionaly repressive regulators such as HDACs.

As part of this investigation the well-studied *CDKN1A* gene was examined for responses mediated by the VDR ligand dependent transcription factor. These data show upon treatment with $1\alpha,25(OH)_2D_3$ there was depletion and enrichment of the NR at the response elements encoded within its promoter. In addition the pattern of response

observed differed at each response element. The *CDKN1A* transcription start site also showed high levels of VDR interaction and was consistent with of high levels of chromatin looping from VDREs to the TSS. These effects were measured over a prolonged time period in order to obtain an extended view of the transcriptional activation process. Chromatin immunoprecipitation gives a snapshot of interactions on a scale of minutes. This helps monitor the measurement of stochastic interactions that have also been previously shown to occur in transcription factors including the GR receptor and NF-kB [241, 242]. Analysis of *CDKN1A* mRNA over the same time periods yielded a fluctuating profile of transcription, of particular interest it the early peak of production after 0.5 hours $1\alpha,25(OH)_2D_3$ (100nm) stimulation. This was shown to be a productive to a protein level and examination of the xChIP data suggested that a loss of NCOR1 from the *CDKN1A* TSS may be an important factor in the rapidity of the mRNA transcription. This was further supported by the accumulation of NCOR1 at the *CDKN1A* TSS in PC-3 cells. Thus aberrant accumulation of CoRs at TSS may be a key change acquired by cancer cells to attain insensitivity to nuclear receptor transcription.

Future studies should be focused on establishing the nature of NCOR1 bound complex recruitment to the CDKN1A TSS. Particular attention should be paid to the ubiquitination mechanisms that mediate corepressor release from NR heterodimers such as the examination of the transducin β-like1 (TBL1) transducin β-like related 1 (TBLR1) proteins responsible for the recruitment of the 19s proteosome that induces release and degradation of NCOR1. Phosphorylation of the TBL1 and TBLR1 has been demonstrated to modulate their actions toward CoRs [243]. Therefore, inhibition of this post-translational modification may prevent the molecular activity of the TBL1 and TBLR1.

Consequently, it is hypothesized that foci of deregulated/impaired TBL1 and/or TBLR1 activity, whose placement is dictated by specific histone marks, may permit the accumulation of CoR at a normally transcriptionally active region. It is also suggested that such marks may include those indicating transcription start sites such as the H3K9ac and H3K4me3, increased presence of these marks may hold dual consequences for the cell. In non-transformed cells they indicate TSS positions and active chromatin. However, in malignancy their position may remain but additional deregulations such as impaired TBL1 and TBLR1 activity may exist. Such investigations may reveal how epigenetic modifications can contribute to the activity of NRs and importantly how their deregulation impacts upon NR target gene expression. In the future these investigations will be used to design new therapeutic compounds capable of specifically targeting aberrantly placed histone modifications or the enzymes responsible for their placement or 'reading'.

Collectively these data suggest there are progressive epigenetic distortions to NR signaling in CaP. NCOR1 levels are elevated, and preferentially change in response to VDR activation. In addition it is increasingly recruited to target gene promoters in response to VDR ligand presence. The net result of increased NCOR1 and NCOR2/SMRT association at VDR target genes is the loss of H3K9ac and accumulation of H3K9me2. In turn this epigenetic mark is recognised by the CpG methylation machinery and allows for the potential for DNA methylation at adjacent CpG regions for example through the recruitment of DNMT associated complexes include heterochromatin binding protein 1 (HP1)[244] (reviewed in [245]). Further links exist between NCOR1 and DNA methylation through its interaction with KAISO, to regulate

DNA methylation [246]. Jointly this elevation of CoR action thereby converts a transient epigenetic silencing process that is part of the normal NR-transcriptional cycle into a stable and heritable event. In this manner the ability of the VDR to regulate key anti-proliferative target genes is altered into a process that leads to their the stable silencing. As a consequence this may release the burden for elevated NCOR1 and NCOR2/SMRT requirement.

Journal Publications Related To This Thesis

- Ligand induced co-repressor recruitment by the vitamin D receptor target gene promoters in 1a,25(OH)2D3-recalcitrant prostate cancer cells. Doig CL, Pitzonka L, Godoy A, Thorne JL, Battaglia S, Singh P, Sobolewski M, Maguire O, Mohler JL, Turner BM, McCabe CJ, Campbell MJ. In preparation.

- The steroidogeneis enzyme AKR1C3 in androgen independent prostate cancer cells. **Doig CL**, McCabe CJ, Khanim F, Campbell MJ, Bunce CM. In preparation.

- Epigenetic control of a VDR-governed feed forward loop that regulates $p21^{(waf1/cip1)}$ expression and function in non-malignant prostate cells. Thorne JL, Maguire O, **Doig CL**, Battaglia S, O'Neill LP Turner BM, McCabe CJ, Campbell MJ. Nucleic Acids Res. 2010 Nov 17.

- Elevated NCOR1 disrupts PPARalpha/gamma signaling in prostate cancer and forms a targetable epigenetic lesion. Battaglia S, Maguire O, Thorne JL, Hornung LB, **Doig CL**, Liu S, Sucheston LE, Bianchi A, Khanim F, Gommersall LM, Coulter HS, Rakha S, Giddings I, O'Neill LP, Cooper CS, McCabe CJ, Bunce CM, Campbell MJ. Carcinogenesis. 2010 May 13.

- Pituitary tumor transforming gene binding factor: a new gene in breast cancer. Watkins RJ, Read ML, Smith VE, Sharma N, Reynolds GM, Buckley L, **Doig C**, Campbell MJ, Lewy G, Eggo MC, Loubiere LS, Franklyn JA, Boelaert K, McCabe CJ. Cancer Res. 2010 May 1;70(9):3739-49.

References

1. **Abate-Shen, C. and M.M. Shen, *Molecular genetics of prostate cancer.* Genes Dev, 2000. 14(19): p. 2410-34.**
2. **Goldstein, A.S., et al., *Identification of a cell of origin for human prostate cancer.* Science, 2010. 329(5991): p. 568-71.**
3. **Jemal, A., et al., *Cancer statistics, 2009.* CA Cancer J Clin, 2009. 59(4): p. 225-49.**
4. **Rowan, S., et al., *Survival from prostate cancer in England and Wales up to 2001.* Br J Cancer, 2008. 99 Suppl 1: p. S75-7.**
5. **Whittemore, A.S., et al., *Prostate cancer in relation to diet, physical activity, and body size in blacks, whites, and Asians in the United States and Canada.* J Natl Cancer Inst, 1995. 87(9): p. 652-61.**
6. **Gronberg, H., *Prostate cancer epidemiology.* Lancet, 2003. 361(9360): p. 859-64.**
7. **Mills, P.K., et al., *Cohort study of diet, lifestyle, and prostate cancer in Adventist men.* Cancer, 1989. 64(3): p. 598-604.**
8. **Yamashita, K., et al., *In vitro reaction of hydroxyamino derivatives of MeIQx, Glu-P-1 and Trp-P-1 with DNA: 32P-postlabelling analysis of DNA adducts formed in vivo by the parent amines and in vitro by their hydroxyamino derivatives.* Mutagenesis, 1988. 3(6): p. 515-20.**
9. **Parkin, D.M., et al., *Global cancer statistics, 2002.* CA Cancer J Clin, 2005. 55(2): p. 74-108.**
10. **Townsend, K., et al., *Biological actions of extra-renal 25-hydroxyvitamin D-1alpha-hydroxylase and implications for chemoprevention and treatment.* J.Steroid Biochem.Mol.Biol., 2005. 97(1-2): p. 103-109.**
11. **MacLean, C.H., et al., *Effects of omega-3 fatty acids on cancer risk: a systematic review.* JAMA, 2006. 295(4): p. 403-15.**
12. **Ruijter, E., et al., *Molecular genetics and epidemiology of prostate carcinoma.* Endocr Rev, 1999. 20(1): p. 22-45.**
13. **Crawford, E.D., *Challenges in the management of prostate cancer.* Br J Urol, 1992. 70 Suppl 1: p. 33-8.**
14. **Rachet, B., et al., *Population-based cancer survival trends in England and Wales up to 2007: an assessment of the NHS cancer plan for England.* Lancet Oncol, 2009. 10(4): p. 351-69.**
15. **Gonzalez, C.A. and E. Riboli, *Diet and cancer prevention: Contributions from the European Prospective Investigation into Cancer and Nutrition (EPIC) study.* Eur J Cancer, 2010. 46(14): p. 2555-62.**
16. **Gudmundsson, J., et al., *Genome-wide association and replication studies identify four variants associated with prostate cancer susceptibility.* Nat Genet, 2009. 41(10): p. 1122-6.**
17. **Luscombe, C.J., et al., *Exposure to ultraviolet radiation: association with susceptibility and age at presentation with prostate cancer.* Lancet, 2001. 358(9282): p. 641-642.**

18. **Grant, W.B., *Geographic variation of prostate cancer mortality rates in the United States: Implications for prostate cancer risk related to vitamin D.* Int J Cancer, 2004. 111(3): p. 470-1; author reply 472.**
19. **Freedman, D.M., M. Dosemeci, and K. McGlynn, *Sunlight and mortality from breast, ovarian, colon, prostate, and non-melanoma skin cancer: a composite death certificate based case-control study.* Occup Environ Med, 2002. 59(4): p. 257-62.**
20. **Luscombe, C.J., et al., *Outcome in prostate cancer associations with skin type and polymorphism in pigmentation-related genes.* Carcinogenesis, 2001. 22(9): p. 1343-1347.**
21. **Garland, C.F. and F.C. Garland, *Do sunlight and vitamin D reduce the likelihood of colon cancer?* Int J Epidemiol, 1980. 9(3): p. 227-31.**
22. **Giovannucci, E., et al., *Prospective study of predictors of vitamin D status and cancer incidence and mortality in men.* J Natl Cancer Inst, 2006. 98(7): p. 451-9.**
23. **Deeb, K.K., D.L. Trump, and C.S. Johnson, *Vitamin D signalling pathways in cancer: potential for anticancer therapeutics.* Nat Rev Cancer, 2007. 7(9): p. 684-700.**
24. **Haussler, M.R., et al., *The vitamin D hormone and its nuclear receptor: molecular actions and disease states.* J Endocrinol, 1997. 154 Suppl: p. S57-73.**
25. **Chen, K.S., J.M. Prahl, and H.F. DeLuca, *Isolation and expression of human 1,25-dihydroxyvitamin D3 24-hydroxylase cDNA.* Proc Natl Acad Sci U S A, 1993. 90(10): p. 4543-7.**
26. **Colston, K., M.J. Colston, and D. Feldman, *1,25-dihydroxyvitamin D3 and malignant melanoma: the presence of receptors and inhibition of cell growth in culture.* Endocrinology, 1981. 108(3): p. 1083-1086.**
27. **Holick, M.F., *Vitamin D: importance in the prevention of cancers, type 1 diabetes, heart disease, and osteoporosis.* Am J Clin Nutr, 2004. 79(3): p. 362-71.**
28. **Woodworth, C.D., et al., *Human cervical and foreskin epithelial cells immortalized by human papillomavirus DNAs exhibit dysplastic differentiation in vivo.* Cancer Res, 1990. 50(12): p. 3709-15.**
29. **Yankaskas, J.R., et al., *Papilloma virus immortalized tracheal epithelial cells retain a well-differentiated phenotype.* Am J Physiol, 1993. 264(5 Pt 1): p. C1219-30.**
30. **Bello, D., et al., *Androgen responsive adult human prostatic epithelial cell lines immortalized by human papillomavirus 18.* Carcinogenesis, 1997. 18(6): p. 1215-23.**
31. **Anwar, K., et al., *Presence of ras oncogene mutations and human papillomavirus DNA in human prostate carcinomas.* Cancer Res, 1992. 52(21): p. 5991-6.**
32. **Sobel, R.E. and M.D. Sadar, *Cell lines used in prostate cancer research: a compendium of old and new lines--part 2.* J Urol, 2005. 173(2): p. 360-72.**
33. **Kaighn, M.E., et al., *Establishment and characterization of a human prostatic carcinoma cell line (PC-3).* Invest Urol, 1979. 17(1): p. 16-23.**

34. **Ching, K.Z., et al., *Expression of mRNA for epidermal growth factor, transforming growth factor-alpha and their receptor in human prostate tissue and cell lines.* Mol Cell Biochem, 1993. 126(2): p. 151-8.**
35. **Mickey, D.D., et al., *Characterization of a human prostate adenocarcinoma cell line (DU 145) as a monolayer culture and as a solid tumor in athymic mice.* Prog Clin Biol Res, 1980. 37: p. 67-84.**
36. **Horoszewicz, J.S., et al., *The LNCaP cell line--a new model for studies on human prostatic carcinoma.* Prog Clin Biol Res, 1980. 37: p. 115-32.**
37. **Thalmann, G.N., et al., *Androgen-independent cancer progression and bone metastasis in the LNCaP model of human prostate cancer.* Cancer Res, 1994. 54(10): p. 2577-81.**
38. **Gingrich, J.R., et al., *Androgen-independent prostate cancer progression in the TRAMP model.* Cancer Res, 1997. 57(21): p. 4687-91.**
39. **Robinson-Rechavi, M., et al., *How many nuclear hormone receptors are there in the human genome?* Trends Genet, 2001. 17(10): p. 554-6.**
40. **Kliewer, S.A., et al., *Retinoid X receptor interacts with nuclear receptors in retinoic acid, thyroid hormone and vitamin D3 signalling.* Nature, 1992. 355(6359): p. 446-9.**
41. **Privalsky, M.L., *The role of corepressors in transcriptional regulation by nuclear hormone receptors.* Annu Rev Physiol, 2004. 66: p. 315-60.**
42. **Rochette-Egly, C., et al., *Phosphorylation of the retinoic acid receptor-alpha by protein kinase A.* Mol Endocrinol, 1995. 9(7): p. 860-71.**
43. **Perissi, V. and M.G. Rosenfeld, *Controlling nuclear receptors: the circular logic of cofactor cycles.* Nat Rev Mol Cell Biol, 2005. 6(7): p. 542-54.**
44. **Horlein, A.J., et al., *Ligand-independent repression by the thyroid hormone receptor mediated by a nuclear receptor co-repressor.* Nature, 1995. 377(6548): p. 397-404.**
45. **Jepsen, K., et al., *Combinatorial roles of the nuclear receptor corepressor in transcription and development.* Cell, 2000. 102(6): p. 753-63.**
46. **Jepsen, K., et al., *Cooperative regulation in development by SMRT and FOXP1.* Genes Dev, 2008. 22(6): p. 740-5.**
47. **Cohen, R.N., et al., *The specificity of interactions between nuclear hormone receptors and corepressors is mediated by distinct amino acid sequences within the interacting domains.* Mol.Endocrinol., 2001. 15(7): p. 1049-1061.**
48. **Makowski, A., et al., *Determination of nuclear receptor corepressor interactions with the thyroid hormone receptor.* Mol Endocrinol, 2003. 17(2): p. 273-86.**
49. **Li, J., et al., *Both corepressor proteins SMRT and N-CoR exist in large protein complexes containing HDAC3.* Embo J, 2000. 19(16): p. 4342-50.**
50. **Guenther, M.G., O. Barak, and M.A. Lazar, *The SMRT and N-CoR corepressors are activating cofactors for histone deacetylase 3.* Mol Cell Biol, 2001. 21(18): p. 6091-101.**
51. **Balk, S.P. and K.E. Knudsen, *AR, the cell cycle, and prostate cancer.* Nucl Recept Signal, 2008. 6: p. e001.**

52. **Locke, J.A., et al., *Androgen levels increase by intratumoral de novo steroidogenesis during progression of castration-resistant prostate cancer.* Cancer Res, 2008. 68(15): p. 6407-15.**

53. **Creighton, C.J., *Multiple oncogenic pathway signatures show coordinate expression patterns in human prostate tumors.* PLoS ONE, 2008. 3(3): p. e1816.**

54. **Edwards, J. and J.M. Bartlett, *The androgen receptor and signal-transduction pathways in hormone-refractory prostate cancer. Part 2: Androgen-receptor cofactors and bypass pathways.* BJU Int, 2005. 95(9): p. 1327-35.**

55. **Lu, D. and D.A. Carson, *Repression of beta-catenin signaling by PPAR gamma ligands.* Eur J Pharmacol, 2010. 636(1-3): p. 198-202.**

56. **Choudhary, R., et al., *Peroxisome proliferator-activated receptor-gamma inhibits transformed growth of non-small cell lung cancer cells through selective suppression of Snail.* Neoplasia, 2010. 12(3): p. 224-34.**

57. **Dionne, S., et al., *PPARgamma ligand 15-deoxy-delta 12,14-prostaglandin J2 sensitizes human colon carcinoma cells to TWEAK-induced apoptosis.* Anticancer Res, 2010. 30(1): p. 157-66.**

58. **Yu, J., et al., *Inhibitory role of peroxisome proliferator-activated receptor gamma in hepatocarcinogenesis in mice and in vitro.* Hepatology, 2010. 51(6): p. 2008-19.**

59. **Nunez, N.P., H. Liu, and G.G. Meadows, *PPAR-gamma ligands and amino acid deprivation promote apoptosis of melanoma, prostate, and breast cancer cells.* Cancer Lett, 2006. 236(1): p. 133-41.**

60. **Jaeckel, E.C., et al., *Correlation of expression of cyclooxygenase-2, vascular endothelial growth factor, and peroxisome proliferator-activated receptor delta with head and neck squamous cell carcinoma.* Arch Otolaryngol Head Neck Surg, 2001. 127(10): p. 1253-9.**

61. **Suchanek, K.M., et al., *Peroxisome proliferator-activated receptor alpha in the human breast cancer cell lines MCF-7 and MDA-MB-231.* Mol Carcinog, 2002. 34(4): p. 165-71.**

62. **Sarraf, P., et al., *Differentiation and reversal of malignant changes in colon cancer through PPARgamma.* Nat Med, 1998. 4(9): p. 1046-52.**

63. **Osawa, E., et al., *Peroxisome proliferator-activated receptor gamma ligands suppress colon carcinogenesis induced by azoxymethane in mice.* Gastroenterology, 2003. 124(2): p. 361-7.**

64. **Altiok, S., M. Xu, and B.M. Spiegelman, *PPARgamma induces cell cycle withdrawal: inhibition of E2F/DP DNA-binding activity via down-regulation of PP2A.* Genes Dev, 1997. 11(15): p. 1987-98.**

65. **Morrison, R.F. and S.R. Farmer, *Role of PPARgamma in regulating a cascade expression of cyclin-dependent kinase inhibitors, p18(INK4c) and p21(Waf1/Cip1), during adipogenesis.* J Biol Chem, 1999. 274(24): p. 17088-97.**

66. **Chambon, P., *A decade of molecular biology of retinoic acid receptors.* FASEB J, 1996. 10(9): p. 940-54.**

67. **Elstner, E., et al., *Novel 20-epi-vitamin D3 analog combined with 9-cis-retinoic acid markedly inhibits colony growth of prostate cancer cells.* Prostate, 1999. 40(3): p. 141-149.**
68. **Campbell, M.J., et al., *Expression of retinoic acid receptor-beta sensitizes prostate cancer cells to growth inhibition mediated by combinations of retinoids and a 19-nor hexafluoride vitamin D3 analog.* Endocrinology, 1998. 139(4): p. 1972-1980.**
69. **Blutt, S.E., et al., *1,25-dihydroxyvitamin D3 and 9-cis-retinoic acid act synergistically to inhibit the growth of LNCaP prostate cells and cause accumulation of cells in G1.* Endocrinology, 1997. 138(4): p. 1491-1497.**
70. **Ikeda, N., et al., *Combination treatment with 1alpha,25-dihydroxyvitamin D3 and 9-cis-retinoic acid directly inhibits human telomerase reverse transcriptase transcription in prostate cancer cells.* Mol Cancer Ther, 2003. 2(8): p. 739-46.**
71. **Baker, A.R., et al., *Cloning and expression of full-length cDNA encoding human vitamin D receptor.* Proc Natl Acad Sci U S A, 1988. 85(10): p. 3294-8.**
72. **Haussler, M.R., et al., *The nuclear vitamin D receptor: biological and molecular regulatory properties revealed.* J Bone Miner Res, 1998. 13(3): p. 325-49.**
73. **Liu, M., et al., *Transcriptional activation of the Cdk inhibitor p21 by vitamin D3 leads to the induced differentiation of the myelomonocytic cell line U937.* Genes Dev., 1996. 10(2): p. 142-153.**
74. **Campbell, M.J., et al., *Inhibition of proliferation of prostate cancer cells by a 19-nor-hexafluoride vitamin D3 analogue involves the induction of p21waf1, p27kip1 and E-cadherin.* J Mol Endocrinol, 1997. 19(1): p. 15-27.**
75. **Saramaki, A., et al., *Regulation of the human p21(waf1/cip1) gene promoter via multiple binding sites for p53 and the vitamin D3 receptor.* Nucleic Acids Res, 2006. 34(2): p. 543-54.**
76. **Thorne, J.L., et al., *Epigenetic control of a VDR-governed feed-forward loop that regulates p21(waf1/cip1) expression and function in non-malignant prostate cells.* Nucleic Acids Res, 2010.**
77. **Abbas, T. and A. Dutta, *p21 in cancer: intricate networks and multiple activities.* Nat Rev Cancer, 2009. 9(6): p. 400-14.**
78. **Sohn, D., et al., *p21 blocks irradiation-induced apoptosis downstream of mitochondria by inhibition of cyclin-dependent kinase-mediated caspase-9 activation.* Cancer Res, 2006. 66(23): p. 11254-62.**
79. **Suzuki, A., et al., *Resistance to Fas-mediated apoptosis: activation of caspase 3 is regulated by cell cycle regulator p21WAF1 and IAP gene family ILP.* Oncogene, 1998. 17(8): p. 931-9.**
80. **Xu, S.Q. and W.S. El-Deiry, *p21(WAF1/CIP1) inhibits initiator caspase cleavage by TRAIL death receptor DR4.* Biochem Biophys Res Commun, 2000. 269(1): p. 179-90.**
81. **Anderson, S.P., et al., *Overlapping transcriptional programs regulated by the nuclear receptors peroxisome proliferator-activated receptor alpha, retinoid X receptor, and liver X receptor in mouse liver.* Mol Pharmacol, 2004. 66(6): p. 1440-52.**

82. **Bookout, A.L., et al., *Anatomical profiling of nuclear receptor expression reveals a hierarchical transcriptional network.* Cell, 2006. 126(4): p. 789-799.**
83. **Hendriksen, P.J., et al., *Evolution of the androgen receptor pathway during progression of prostate cancer.* Cancer Res, 2006. 66(10): p. 5012-20.**
84. **Tomlins, S.A., et al., *Recurrent fusion of TMPRSS2 and ETS transcription factor genes in prostate cancer.* Science, 2005. 310(5748): p. 644-648.**
85. **Battaglia, S., O. Maguire, and M.J. Campbell, *Transcription factor co-repressors in cancer biology: roles and targeting.* Int J Cancer, 2010. 126(11): p. 2511-9.**
86. **Minucci, S. and P.G. Pelicci, *Histone deacetylase inhibitors and the promise of epigenetic (and more) treatments for cancer.* Nature Reviews, 2006. 6: p. 38-51.**
87. **Rowley, J.D., et al., *Further evidence for a non-random chromosomal abnormality in acute promyelocytic leukemia.* Int J Cancer, 1977. 20(6): p. 869-72.**
88. **Ito, K., et al., *PML targeting eradicates quiescent leukaemia-initiating cells.* Nature, 2008. 453(7198): p. 1072-8.**
89. **Lin, R.J., et al., *Role of the histone deacetylase complex in acute promyelocytic leukaemia.* Nature, 1998. 391(6669): p. 811-814.**
90. **Goll, M.G. and T.H. Bestor, *Eukaryotic cytosine methyltransferases.* Annu Rev Biochem, 2005. 74: p. 481-514.**
91. **Suzuki, M.M. and A. Bird, *DNA methylation landscapes: provocative insights from epigenomics.* Nat Rev Genet, 2008. 9(6): p. 465-76.**
92. **Weber, M. and D. Schubeler, *Genomic patterns of DNA methylation: targets and function of an epigenetic mark.* Curr Opin Cell Biol, 2007. 19(3): p. 273-80.**
93. **Eden, S., et al., *DNA methylation models histone acetylation.* Nature, 1998. 394(6696): p. 842.**
94. **Hashimshony, T., et al., *The role of DNA methylation in setting up chromatin structure during development.* Nat Genet, 2003. 34(2): p. 187-92.**
95. **Muller, C.I., et al., *DNA hypermethylation of myeloid cells, a novel therapeutic target in MDS and AML.* Curr Pharm Biotechnol, 2006. 7(5): p. 315-21.**
96. **Taverna, S.D., et al., *How chromatin-binding modules interpret histone modifications: lessons from professional pocket pickers.* Nat Struct Mol Biol, 2007. 14(11): p. 1025-40.**
97. **Barski, A., et al., *High-resolution profiling of histone methylations in the human genome.* Cell, 2007. 129(4): p. 823-37.**
98. **Choi, S.H., et al., *Identification of preferential target sites for human DNA methyltransferases.* Nucleic Acids Res, 2011. 39(1): p. 104-18.**
99. **Mikkelsen, T.S., et al., *Genome-wide maps of chromatin state in pluripotent and lineage-committed cells.* Nature, 2007. 448(7153): p. 553-60.**
100. **Sidransky, D., *Emerging molecular markers of cancer.* Nat Rev Cancer, 2002. 2(3): p. 210-9.**
101. **Issa, J.P., *Methylation and prognosis: of molecular clocks and hypermethylator phenotypes.* Clin Cancer Res, 2003. 9(8): p. 2879-81.**

102. van Straten, E.M., et al., *The liver X-receptor gene promoter is hypermethylated in a mouse model of prenatal protein restriction.* Am J Physiol Regul Integr Comp Physiol, 2010. 298(2): p. R275-82.

103. Li, L.C., et al., *Frequent methylation of estrogen receptor in prostate cancer: correlation with tumor progression.* Cancer Res, 2000. 60(3): p. 702-6.

104. Hansen, K.H., et al., *A model for transmission of the H3K27me3 epigenetic mark.* Nat Cell Biol, 2008. 10(11): p. 1291-300.

105. Bernstein, B.E., et al., *A bivalent chromatin structure marks key developmental genes in embryonic stem cells.* Cell, 2006. 125(2): p. 315-26.

106. Guenther, M.G., et al., *A chromatin landmark and transcription initiation at most promoters in human cells.* Cell, 2007. 130(1): p. 77-88.

107. Schuettengruber, B., et al., *Genome regulation by polycomb and trithorax proteins.* Cell, 2007. 128(4): p. 735-45.

108. Kondo, Y., et al., *Gene silencing in cancer by histone H3 lysine 27 trimethylation independent of promoter DNA methylation.* Nat Genet, 2008. 40(6): p. 741-50.

109. Ruthenburg, A.J., C.D. Allis, and J. Wysocka, *Methylation of lysine 4 on histone H3: intricacy of writing and reading a single epigenetic mark.* Mol Cell, 2007. 25(1): p. 15-30.

110. Baker, L.A., C.D. Allis, and G.G. Wang, *PHD fingers in human diseases: disorders arising from misinterpreting epigenetic marks.* Mutat Res, 2008. 647(1-2): p. 3-12.

111. Bower, M., et al., *Prevalence and clinical correlations of MLL gene rearrangements in AML-M4/5.* Blood, 1994. 84(11): p. 3776-80.

112. Dorrance, A.M., et al., *Mll partial tandem duplication induces aberrant Hox expression in vivo via specific epigenetic alterations.* J Clin Invest, 2006. 116(10): p. 2707-16.

113. Varambally, S., et al., *The polycomb group protein EZH2 is involved in progression of prostate cancer.* Nature, 2002. 419(6907): p. 624-629.

114. Yu, J., et al., *Integrative genomics analysis reveals silencing of beta-adrenergic signaling by polycomb in prostate cancer.* Cancer Cell, 2007. 12(5): p. 419-31.

115. Morin, R.D., et al., *Somatic mutations altering EZH2 (Tyr641) in follicular and diffuse large B-cell lymphomas of germinal-center origin.* Nat Genet, 2010. 42(2): p. 181-5.

116. Shi, Y., et al., *Histone demethylation mediated by the nuclear amine oxidase homolog LSD1.* Cell, 2004. 119(7): p. 941-53.

117. Wang, Y., et al., *LSD1 is a subunit of the NuRD complex and targets the metastasis programs in breast cancer.* Cell, 2009. 138(4): p. 660-72.

118. Metzger, E., et al., *LSD1 demethylates repressive histone marks to promote androgen-receptor-dependent transcription.* Nature, 2005. 437(7057): p. 436-9.

119. Metivier, R., et al., *Estrogen receptor-alpha directs ordered, cyclical, and combinatorial recruitment of cofactors on a natural target promoter.* Cell, 2003. 115(6): p. 751-763.

120. Krum, S.A., et al., *Unique ERalpha cistromes control cell type-specific gene regulation.* Mol Endocrinol, 2008. 22(11): p. 2393-406.

121. Jenuwein, T. and C.D. Allis, *Translating the histone code.* Science, 2001. 293(5532): p. 1074-1080.

122. Turner, B.M., *Cellular memory and the histone code.* Cell, 2002. 111(3): p. 285-91.

123. Turner, B.M., *Histone acetylation and an epigenetic code.* Bioessays, 2000. 22(9): p. 836-845.

124. Reid, G., et al., *Cyclic, proteasome-mediated turnover of unliganded and liganded ERalpha on responsive promoters is an integral feature of estrogen signaling.* Mol Cell, 2003. 11(3): p. 695-707.

125. Wang, Q., J.S. Carroll, and M. Brown, *Spatial and temporal recruitment of androgen receptor and its coactivators involves chromosomal looping and polymerase tracking.* Mol Cell, 2005. 19(5): p. 631-42.

126. Saramaki, A., et al., *Cyclical chromatin looping and transcription factor association on the regulatory regions of the p21 (CDKN1A) gene in response to 1alpha,25-dihydroxyvitamin D3.* J Biol Chem, 2009. 284(12): p. 8073-82.

127. Teboul, M., et al., *The nuclear hormone receptor family round the clock.* Mol Endocrinol, 2008. 22(12): p. 2573-82.

128. Shang, Y., et al., *Cofactor dynamics and sufficiency in estrogen receptor-regulated transcription.* Cell, 2000. 103(6): p. 843-852.

129. Abedin, S.A., et al., *Elevated NCOR1 disrupts a network of dietary-sensing nuclear receptors in bladder cancer cells.* Carcinogenesis, 2009. 30(3): p. 449-56.

130. Malinen, M., et al., *Distinct HDACs regulate the transcriptional response of human cyclin-dependent kinase inhibitor genes to Trichostatin A and 1alpha,25-dihydroxyvitamin D3.* Nucleic Acids Res, 2008. 36(1): p. 121-32.

131. Banwell, C.M., et al., *Altered nuclear receptor corepressor expression attenuates vitamin D receptor signaling in breast cancer cells.* Clin Cancer Res, 2006. 12(7 Pt 1): p. 2004-13.

132. Rashid, S.F., et al., *Synergistic growth inhibition of prostate cancer cells by 1a,25 Dihydroxyvitamin D3 and its 19-nor-hexafuoride analogs in combination with either sodium butyrate or trichostatin A.* Oncogene, 2001. 20: p. 1860-1872.

133. Khanim, F.L., et al., *Altered SMRT levels disrupt vitamin D3 receptor signalling in prostate cancer cells.* Oncogene, 2004. 23(40): p. 6712-25.

134. Ting, H.J., et al., *Increased expression of corepressors in aggressive androgen-independent prostate cancer cells results in loss of 1alpha,25-dihydroxyvitamin D3 responsiveness.* Mol Cancer Res, 2007. 5(9): p. 967-80.

135. Rabbitt, E.H., et al., *Prereceptor regulation of glucocorticoid action by 11beta-hydroxysteroid dehydrogenase: a novel determinant of cell proliferation.* FASEB J, 2002. 16(1): p. 36-44.

136. Penning, T.M., et al., *Pre-receptor regulation of the androgen receptor.* Mol Cell Endocrinol, 2008. 281(1-2): p. 1-8.

137. Wako, K., et al., *Expression of androgen receptor through androgen-converting enzymes is associated with biological aggressiveness in prostate cancer.* J Clin Pathol, 2008. 61(4): p. 448-54.

138. Bauman, D.R., et al., *Transcript profiling of the androgen signal in normal prostate, benign prostatic hyperplasia, and prostate cancer.* Endocrinology, 2006. 147(12): p. 5806-16.

139. Penning, T.M., et al., *Human 3alpha-hydroxysteroid dehydrogenase isoforms (AKR1C1-AKR1C4) of the aldo-keto reductase superfamily: functional plasticity and tissue distribution reveals roles in the inactivation and formation of male and female sex hormones.* Biochem J, 2000. 351(Pt 1): p. 67-77.

140. Penning, T.M. and M.C. Byrns, *Steroid hormone transforming aldo-keto reductases and cancer.* Ann N Y Acad Sci, 2009. 1155: p. 33-42.

141. Smuc, T. and T.L. Rizner, *Expression of 17beta-hydroxysteroid dehydrogenases and other estrogen-metabolizing enzymes in different cancer cell lines.* Chem Biol Interact, 2009. 178(1-3): p. 228-33.

142. Campbell, M.J., C. Carlberg, and H.P. Koeffler, *A Role for the PPARgamma in Cancer Therapy.* PPAR Res, 2008. 2008: p. 314974.

143. Das, C. and T.K. Kundu, *Transcriptional regulation by the acetylation of nonhistone proteins in humans -- a new target for therapeutics.* IUBMB Life, 2005. 57(3): p. 137-49.

144. Glozak, M.A., et al., *Acetylation and deacetylation of non-histone proteins.* Gene, 2005. 363: p. 15-23.

145. Kawahara, T.L., et al., *SIRT6 links histone H3 lysine 9 deacetylation to NF-kappaB-dependent gene expression and organismal life span.* Cell, 2009. 136(1): p. 62-74.

146. Jung-Hynes, B., et al., *Role of sirtuin histone deacetylase SIRT1 in prostate cancer. A target for prostate cancer management via its inhibition?* J Biol Chem, 2009. 284(6): p. 3823-32.

147. Rous, P., *A Sarcoma of the Fowl Transmissible by an Agent Separable from the Tumor Cells.* J Exp Med, 1911. 13(4): p. 397-411.

148. Rous, P., *The Influence of Diet on Transplanted and Spontaneous Mouse Tumors.* J Exp Med, 1914. 20(5): p. 433-451.

149. Guarente, L. and F. Picard, *Calorie restriction--the SIR2 connection.* Cell, 2005. 120(4): p. 473-82.

150. Boily, G., et al., *SirT1 regulates energy metabolism and response to caloric restriction in mice.* PLoS ONE, 2008. 3(3): p. e1759.

151. Seligson, D.B., et al., *Global histone modification patterns predict risk of prostate cancer recurrence.* Nature, 2005. 435(7046): p. 1262-6.

152. Huffman, D.M., et al., *SIRT1 is significantly elevated in mouse and human prostate cancer.* Cancer Res, 2007. 67(14): p. 6612-8.

153. Kojima, K., et al., *A role for SIRT1 in cell growth and chemoresistance in prostate cancer PC3 and DU145 cells.* Biochem Biophys Res Commun, 2008. 373(3): p. 423-8.

154. Dai, Y., et al., *Sirtuin 1 is required for antagonist-induced transcriptional repression of androgen-responsive genes by the androgen receptor.* Mol Endocrinol, 2007. 21(8): p. 1807-21.

155. Fu, M., et al., *Hormonal control of androgen receptor function through SIRT1.* Mol Cell Biol, 2006. 26(21): p. 8122-35.

156. Saunders, L.R. and E. Verdin, *Sirtuins: critical regulators at the crossroads between cancer and aging.* Oncogene, 2007. 26(37): p. 5489-504.

157. Rodgers, J.T., et al., *Nutrient control of glucose homeostasis through a complex of PGC-1alpha and SIRT1.* Nature, 2005. 434(7029): p. 113-118.

158. Liu, M., et al., *Transcriptional activation of the Cdk inhibitor p21 by vitamin D3 leads to the induced differentiation of the myelomonocytic cell line U937.* Genes Dev, 1996. 10(2): p. 142-53.

159. Rank, G., M. Prestel, and R. Paro, *Transcription through intergenic chromosomal memory elements of the Drosophila bithorax complex correlates with an epigenetic switch.* Mol Cell Biol, 2002. 22(22): p. 8026-34.

160. Zink, B. and R. Paro, *In vivo binding pattern of a trans-regulator of homoeotic genes in Drosophila melanogaster.* Nature, 1989. 337(6206): p. 468-71.

161. Yoon, H.G., et al., *N-CoR mediates DNA methylation-dependent repression through a methyl CpG binding protein Kaiso.* Mol.Cell, 2003. 12(3): p. 723-734.

162. Pillaire, M.J., et al., *A 'DNA replication' signature of progression and negative outcome in colorectal cancer.* Oncogene, 2010. 29(6): p. 876-87.

163. Shi, Y.K., et al., *Inhibition of prostate cancer growth and metastasis using small interference RNA specific for minichromosome complex maintenance component 7.* Cancer Gene Ther, 2010.

164. Feng, C.J., et al., *Expression of Mcm7 and Cdc6 in oral squamous cell carcinoma and precancerous lesions.* Anticancer Res, 2008. 28(6A): p. 3763-9.

165. Shi, Y.K., et al., *MCM7 interacts with androgen receptor.* Am J Pathol, 2008. 173(6): p. 1758-67.

166. Ambs, S., et al., *Genomic profiling of microRNA and messenger RNA reveals deregulated microRNA expression in prostate cancer.* Cancer Res, 2008. 68(15): p. 6162-70.

167. Chomczynski, P. and N. Sacchi, *Single-step method of RNA isolation by acid guanidinium thiocyanate-phenol-chloroform extraction.* Anal Biochem, 1987. 162(1): p. 156-9.

168. Watkins, R.J., et al., *Pituitary tumor transforming gene binding factor: a new gene in breast cancer.* Cancer Res, 2010. 70(9): p. 3739-49.

169. Bentwich, I., et al., *Identification of hundreds of conserved and nonconserved human microRNAs.* Nat Genet, 2005. 37(7): p. 766-70.

170. Esquela-Kerscher, A. and F.J. Slack, *Oncomirs - microRNAs with a role in cancer.* Nat Rev Cancer, 2006. 6(4): p. 259-69.

171. Huang, Z., et al., *Plasma microRNAs are promising novel biomarkers for early detection of colorectal cancer.* Int J Cancer, 2010. 127(1): p. 118-26.

172. Rosenfeld, M.G., V.V. Lunyak, and C.K. Glass, *Sensors and signals: a coactivator/corepressor/epigenetic code for integrating signal-dependent programs of transcriptional response.* Genes Dev., 2006. 20(11): p. 1405-1428.

173. Perissi, V., et al., *Deconstructing repression: evolving models of co-repressor action.* Nat Rev Genet. 11(2): p. 109-23.

174. Newling, D., et al., *Assessment of hormone refractory prostate cancer.* Urology, 1997. 49(4A Suppl): p. 46-53.

175. **Mueller, E., et al., *Effects of ligand activation of peroxisome proliferator-activated receptor gamma in human prostate cancer.* Proc Natl Acad Sci U S A, 2000. 97(20): p. 10990-5.**
176. **Battaglia, S., et al., *Elevated NCOR1 disrupts PPAR{alpha}/{gamma} signaling in prostate cancer and forms a targetable epigenetic lesion.* Carcinogenesis, 2010.**
177. **Liao, G., et al., *Regulation of androgen receptor activity by the nuclear receptor corepressor SMRT.* J Biol Chem, 2003. 278(7): p. 5052-61.**
178. **Hodgson, M.C., et al., *The androgen receptor recruits nuclear receptor CoRepressor (N-CoR) in the presence of mifepristone via its N and C termini revealing a novel molecular mechanism for androgen receptor antagonists.* J Biol Chem, 2005. 280(8): p. 6511-9.**
179. **Segawa, Y., et al., *Expression of peroxisome proliferator-activated receptor (PPAR) in human prostate cancer.* Prostate, 2002. 51(2): p. 108-116.**
180. **Penning, T.M., R.B. Sharp, and N.R. Krieger, *Purification and properties of 3 alpha-hydroxysteroid dehydrogenase from rat brain cytosol. Inhibition by nonsteroidal anti-inflammatory drugs and progestins.* J Biol Chem, 1985. 260(28): p. 15266-72.**
181. **Khanim, F.L., et al., *Combined bezafibrate and medroxyprogesterone acetate: potential novel therapy for acute myeloid leukaemia.* PLoS ONE, 2009. 4(12): p. e8147.**
182. **Desmond, J.C., et al., *The aldo-keto reductase AKR1C3 is a novel suppressor of cell differentiation that provides a plausible target for the non-cyclooxygenase-dependent antineoplastic actions of nonsteroidal anti-inflammatory drugs.* Cancer Res, 2003. 63(2): p. 505-12.**
183. **Cang, S., et al., *Deficient histone acetylation and excessive deacetylase activity as epigenomic marks of prostate cancer cells.* Int J Oncol, 2009. 35(6): p. 1417-22.**
184. **Battaglia, S., et al., *Elevated NCOR1 disrupts PPARalpha/gamma signaling in prostate cancer and forms a targetable epigenetic lesion.* Carcinogenesis, 2010. 31(9): p. 1650-60.**
185. **Byrns, M.C., et al., *Aldo-keto reductase 1C3 expression in MCF-7 cells reveals roles in steroid hormone and prostaglandin metabolism that may explain its over-expression in breast cancer.* J Steroid Biochem Mol Biol, 2010. 118(3): p. 177-87.**
186. **Wu, J.S., et al., *Ligand-activated peroxisome proliferator-activated receptor-gamma protects against ischemic cerebral infarction and neuronal apoptosis by 14-3-3 epsilon upregulation.* Circulation, 2009. 119(8): p. 1124-34.**
187. **Girnun, G., *PPARG: a new independent marker for colorectal cancer survival.* Gastroenterology, 2009. 136(4): p. 1157-60.**
188. **Bonofiglio, D., et al., *Peroxisome proliferator-activated receptor gamma activates fas ligand gene promoter inducing apoptosis in human breast cancer cells.* Breast Cancer Res Treat, 2009. 113(3): p. 423-34.**
189. **Nagata, D., et al., *Peroxisome proliferator-activated receptor-gamma and growth inhibition by its ligands in prostate cancer.* Cancer Detect Prev, 2008. 32(3): p. 259-66.**

190. Picard, F., et al., *Sirt1 promotes fat mobilization in white adipocytes by repressing PPAR-gamma.* Nature, 2004. 429(6993): p. 771-776.

191. Kim, M.Y., et al., *Acetylation of estrogen receptor alpha by p300 at lysines 266 and 268 enhances the deoxyribonucleic acid binding and transactivation activities of the receptor.* Mol Endocrinol, 2006. 20(7): p. 1479-93.

192. Lara, E., et al., *Salermide, a Sirtuin inhibitor with a strong cancer-specific proapoptotic effect.* Oncogene, 2009. 28(6): p. 781-91.

193. Ashraf, N., et al., *Altered sirtuin expression is associated with node-positive breast cancer.* Br J Cancer, 2006. 95(8): p. 1056-61.

194. Wilson, B.J., et al., *An acetylation switch modulates the transcriptional activity of estrogen-related receptor alpha.* Mol Endocrinol, 2010. 24(7): p. 1349-58.

195. Nosho, K., et al., *SIRT1 histone deacetylase expression is associated with microsatellite instability and CpG island methylator phenotype in colorectal cancer.* Mod Pathol, 2009. 22(7): p. 922-32.

196. Butler, R., et al., *Nonapoptotic cell death associated with S-phase arrest of prostate cancer cells via the peroxisome proliferator-activated receptor gamma ligand, 15-deoxy-delta12,14-prostaglandin J2.* Cell Growth Differ, 2000. 11(1): p. 49-61.

197. Gommersall, L.M., et al., *Epigenetic repression of transcription by the Vitamin D3 receptor in prostate cancer cells.* J Steroid Biochem Mol Biol, 2004. 89-90(1-5): p. 251-6.

198. Rashid, S.F., et al., *1alpha,25-dihydroxyvitamin D(3) displays divergent growth effects in both normal and malignant cells.* Steroids, 2001. 66(3-5): p. 433-440.

199. Ribas, J. and S.E. Lupold, *The transcriptional regulation of miR-21, its multiple transcripts, and their implication in prostate cancer.* Cell Cycle, 2010. 9(5): p. 923-9.

200. Ozen, M., et al., *Widespread deregulation of microRNA expression in human prostate cancer.* Oncogene, 2008. 27(12): p. 1788-93.

201. Sun, R., et al., *Global gene expression analysis reveals reduced abundance of putative microRNA targets in human prostate tumours.* BMC Genomics, 2009. 10: p. 93.

202. DeVere White, R.W., et al., *MicroRNAs and their potential for translation in prostate cancer.* Urol Oncol, 2009. 27(3): p. 307-11.

203. Shi, X.B., C.G. Tepper, and R.W. White, *MicroRNAs and prostate cancer.* J Cell Mol Med, 2008. 12(5A): p. 1456-65.

204. Weber, M.J., *New human and mouse microRNA genes found by homology search.* FEBS J, 2005. 272(1): p. 59-73.

205. Ivanovska, I., et al., *MicroRNAs in the miR-106b family regulate p21/CDKN1A and promote cell cycle progression.* Mol Cell Biol, 2008. 28(7): p. 2167-74.

206. Rohan, J.N. and N.L. Weigel, *1Alpha,25-dihydroxyvitamin D3 reduces c-Myc expression, inhibiting proliferation and causing G1 accumulation in C4-2 prostate cancer cells.* Endocrinology, 2009. 150(5): p. 2046-54.

207. Verlinden, L., et al., *1alpha,25-Dihydroxyvitamin D3-induced down-regulation of the checkpoint proteins, Chk1 and Claspin, is mediated by the pocket proteins p107 and p130.* J Steroid Biochem Mol Biol, 2007. 103(3-5): p. 411-5.

208. **Brungs, M., et al., *Sequential induction of 5-lipoxygenase gene expression and activity in Mono Mac 6 cells by transforming growth factor beta and 1,25-dihydroxyvitamin D3.* Proc Natl Acad Sci U S A, 1995. 92(1): p. 107-11.**

209. **Sorg, B.L., et al., *Analysis of the 5-lipoxygenase promoter and characterization of a vitamin D receptor binding site.* Biochim Biophys Acta, 2006. 1761(7): p. 686-97.**

210. **Seuter, S., et al., *Functional characterization of vitamin D responding regions in the human 5-Lipoxygenase gene.* Biochim Biophys Acta, 2007. 1771(7): p. 864-72.**

211. **Zandbergen, F., et al., *The G0/G1 switch gene 2 is a novel PPAR target gene.* Biochem J, 2005. 392(Pt 2): p. 313-24.**

212. **Kitareewan, S., et al., *G0S2 is an all-trans-retinoic acid target gene.* Int J Oncol, 2008. 33(2): p. 397-404.**

213. **Abedin, S.A., et al., *Epigenetic corruption of VDR signalling in malignancy.* Anticancer Res, 2006. 26(4A): p. 2557-66.**

214. **Graham, J.D., et al., *Nuclear receptor conformation, coregulators, and tamoxifen-resistant breast cancer.* Steroids, 2000. 65(10-11): p. 579-84.**

215. **Humeniuk-Polaczek, R. and E. Marcinkowska, *Impaired nuclear localization of vitamin D receptor in leukemia cells resistant to calcitriol-induced differentiation.* J Steroid Biochem Mol Biol, 2004. 88(4-5): p. 361-6.**

216. **Kaeding, J., et al., *Activators of the farnesoid X receptor negatively regulate androgen glucuronidation in human prostate cancer LNCAP cells.* Biochem J, 2008. 410(2): p. 245-53.**

217. **Ren, B., et al., *MCM7 amplification and overexpression are associated with prostate cancer progression.* Oncogene, 2006. 25(7): p. 1090-8.**

218. **Calin, G.A. and C.M. Croce, *MicroRNA signatures in human cancers.* Nat Rev Cancer, 2006. 6(11): p. 857-66.**

219. **Zhang, H.L., et al., *Serum miRNA-21: Elevated levels in patients with metastatic hormone-refractory prostate cancer and potential predictive factor for the efficacy of docetaxel-based chemotherapy.* Prostate, 2010.**

220. **Basu, S., et al., *Spatiotemporal control of gene expression with pulse-generating networks.* Proc Natl Acad Sci U S A, 2004. 101(17): p. 6355-60.**

221. **Palomero, T., et al., *NOTCH1 directly regulates c-MYC and activates a feed-forward-loop transcriptional network promoting leukemic cell growth.* Proc Natl Acad Sci U S A, 2006. 103(48): p. 18261-6.**

222. **Muller, M., et al., *Network topology determines dynamics of the mammalian MAPK1,2 signaling network: bifan motif regulation of C-Raf and B-Raf isoforms by FGFR and MC1R.* FASEB J, 2008. 22(5): p. 1393-403.**

223. **Majid, S., et al., *Regulation of minichromosome maintenance gene family by microRNA-1296 and genistein in prostate cancer.* Cancer Res, 2010. 70(7): p. 2809-18.**

224. **Nariculam, J., et al., *Utility of tissue microarrays for profiling prognostic biomarkers in clinically localized prostate cancer: the expression of BCL-2, E-cadherin, Ki-67 and p53 as predictors of biochemical failure after radical prostatectomy with nested control for clinical and pathological risk factors.* Asian J Androl, 2009. 11(1): p. 109-18.**

225. **Sanchez-Martinez, R., et al., *Vitamin D-dependent recruitment of corepressors to vitamin D/retinoid X receptor heterodimers.* Mol Cell Biol, 2008. 28(11): p. 3817-29.**
226. **Tagami, T., et al., *The interaction of the vitamin D receptor with nuclear receptor corepressors and coactivators.* Biochem Biophys Res Commun, 1998. 253(2): p. 358-63.**
227. **Townsend, K., et al., *Autocrine metabolism of vitamin D in normal and malignant breast tissue.* Clin Cancer Res, 2005. 11(9): p. 3579-86.**
228. **Gasser, S.M., *Positions of potential: nuclear organization and gene expression.* Cell, 2001. 104(5): p. 639-42.**
229. **Cimbora, D.M. and M. Groudine, *The control of mammalian DNA replication: a brief history of space and timing.* Cell, 2001. 104(5): p. 643-6.**
230. **Perissi, V., et al., *A corepressor/coactivator exchange complex required for transcriptional activation by nuclear receptors and other regulated transcription factors.* Cell, 2004. 116(4): p. 511-526.**
231. **Yan, F., et al., *Specific ubiquitin-conjugating enzymes promote degradation of specific nuclear receptor coactivators.* Mol Endocrinol, 2003. 17(7): p. 1315-31.**
232. **Risbridger, G.P., et al., *Breast and prostate cancer: more similar than different.* Nat Rev Cancer, 2010. 10(3): p. 205-12.**
233. **Dozmorov, M.G., et al., *Elevated AKR1C3 expression promotes prostate cancer cell survival and prostate cell-mediated endothelial cell tube formation: implications for prostate cancer progressioan.* BMC Cancer, 2010. 10: p. 672.**
234. **Desmond, J.C., et al., *The aldo-keto reductase AKR1C3 is a novel suppressor of cell differentiation that provides a plausible target for the non-cyclooxygenase-dependent antineoplastic actions of nonsteroidal anti-inflammatory drugs.* Cancer Res., 2003. 63(2): p. 505-512.**
235. **Skowronski, R.J., D.M. Peehl, and D. Feldman, *Vitamin D and prostate cancer: 1,25 dihydroxyvitamin D3 receptors and actions in human prostate cancer cell lines.* Endocrinology, 1993. 132(5): p. 1952-1960.**
236. **Coppola, V., R. De Maria, and D. Bonci, *MicroRNAs and prostate cancer.* Endocr Relat Cancer, 2010. 17(1): p. F1-17.**
237. **Gilad, S., et al., *Serum microRNAs are promising novel biomarkers.* PLoS ONE, 2008. 3(9): p. e3148.**
238. **Schulz, W.A. and J. Hatina, *Epigenetics of prostate cancer: beyond DNA methylation.* J Cell Mol Med, 2006. 10(1): p. 100-25.**
239. **Luo, W., et al., *Epigenetic regulation of vitamin D 24-hydroxylase/CYP24A1 in human prostate cancer.* Cancer Res, 2010. 70(14): p. 5953-62.**
240. **He, H.H., et al., *Nucleosome dynamics define transcriptional enhancers.* Nat Genet, 2010. 42(4): p. 343-7.**
241. **Voss, T.C., S. John, and G.L. Hager, *Single-cell analysis of glucocorticoid receptor action reveals that stochastic post-chromatin association mechanisms regulate ligand-specific transcription.* Mol Endocrinol, 2006. 20(11): p. 2641-55.**
242. **Bosisio, D., et al., *A hyper-dynamic equilibrium between promoter-bound and nucleoplasmic dimers controls NF-kappaB-dependent gene activity.* Embo J, 2006. 25(4): p. 798-810.**

243. Perissi, V., et al., *TBL1 and TBLR1 phosphorylation on regulated gene promoters overcomes dual CtBP and NCoR/SMRT transcriptional repression checkpoints.* Mol Cell, 2008. 29(6): p. 755-66.

244. Mohn, F. and D. Schubeler, *Genetics and epigenetics: stability and plasticity during cellular differentiation.* Trends Genet, 2009. 25(3): p. 129-36.

245. Cheng, X. and R.M. Blumenthal, *Coordinated chromatin control: structural and functional linkage of DNA and histone methylation.* Biochemistry. 49(14): p. 2999-3008.

246. Yoon, H.G., et al., *N-CoR mediates DNA methylation-dependent repression through a methyl CpG binding protein Kaiso.* Mol Cell, 2003. 12(3): p. 723-34.

Section A: Full list of genes contain on the microfluidic gene card.

Gene Symbol	Common name	Function
ABCA1	ABCA1	ATP-binding cassette (ABC) transporter
ABCB8	ABCB8	ATP-binding cassette (ABC) transporter
ABCC3	ABCC3	ATP-binding cassette (ABC) transporter
ABCG2	ABCG2	ATP-binding cassette (ABC) transporter
ACADM	ACADM	Oxidoreductase
AKR1C1/2	AKR1C1/2	Oxidoreductase
AKR1C3	AKR1C3	Oxidoreductase
ALOX5	ALOX5	Oxidoreductase
AOF2	LSD1/KIAA	Oxidoreductase
APOA1	APOA1	Transfer/carrier protein
AR	AR	Nuclear hormone receptor
BAX	BAX	Apoptotic regulator
CARM1	CARM	Methyltransferase
CASP4	CASP4	Cysteine protease
CCNB1	Cyclin B1	Kinase modulator
CCND1	Cyclin D1	Kinase modulator
CCNE1	Cyclin E1	Kinase modulator
CDC2	CDC2	Serine/threonine protein kinase
CDH1	Arc-1/CDH1	Cell adhesion molecule
CDK5	CDK5	Serine/threonine protein kinase
CDKN1A	p21/cip/waf	Kinase modulator
CDKN1B	p27	Kinase modulator
CDKN2A	p16	Kinase modulator
CEBPA	C/EBPa	Transcription factor
COPS2	ALIEN/TRIP15	Transcription factor corepressor
CREBBP	CREBBP	Transcription cofactor
CRSP2	DRIP150/TRAP170	Transcription factor
CRSP6	TRAP80/DRIP80	Transcription factor
CYP24A1	Cyp24	Oxidoreductase
CYP27B1	Cyp27	Oxidoreductase
CYP3A4	Cyp3A4	Oxidoreductase
EGFR	EGFR	Tyrosine protein kinase receptor
ESR1	ESR1	Nuclear hormone receptor
ESR2	ESR2	Nuclear hormone receptor
G0S2	G0S2	Cell cycle regulator
GADD45A	GADD45a	Cell cycle regulator
GATA3	GATA3	Zinc finger transcription factor
HDAC1	HDAC1	Histone Deacetylase
HDAC10	HDAC10	Histone Deacetylase
HDAC2	HDAC2	Histone Deacetylase
HDAC3	HDAC3	Histone Deacetylase
HDAC4	HDAC4	Histone Deacetylase
HDAC5	HDAC5	Histone Deacetylase
HDAC6	HDAC6	Histone Deacetylase

HDAC7A	HDAC7	Hydrolase,Deacetylase
ID1	ID1	Transcription factor
IGFBP1	IGFBP1	Growth factor binding protein
IGFBP3	IGFBP3	Growth factor binding protein
IGFBP5	IGFBP5	Growth factor binding protein
IKBKB	IKKB	Protein kinase
IKBKG	IKKG	Protein kinase
MAPK4	MAPK4	Non-receptor serine/threonine protein kinase
MAPKAPK2	MAPKAP2	Protein kinase
MAPKAPK5	MAPKAPK5	Protein kinase
MYB	MYB	Other transcription factor
NCOA1	NCoA1/RIP160	Transcription cofactor
NCOA2	NCo-A2	Transcription factor,Transcription cofactor
NCOA3	NCOA3	Transcription factor,Transcription cofactor
NCOA4	NCoA4	Transcription factor,Transcription cofactor
NCOR1	NCOR1	Transcription factor corepressor
NCOR2	SMRT/NCOR2	Transcription factor corepressor
NR0B1	DAX1	Nuclear hormone receptor
NR1H2	LXRb	Nuclear hormone receptor
NR1H3	LXRa	Nuclear hormone receptor
NR1H4	FXR	Nuclear hormone receptor
NR1I2	PXR	Nuclear hormone receptor
NR1I3	CAR	Nuclear hormone receptor
NR3C1	GR	Nuclear hormone receptor
PADI4	PADI4	Hydrolase
PPARA	PPARa	Nuclear hormone receptor
PPARBP	DRIP/TRAP220	Transcription cofactor
PPARD	PPARd	Nuclear hormone receptor
PPARG	PPARg	Nuclear hormone receptor
PPARGC1A	PPARGC1	Transcription cofactor
PTGS1	COX-1	Oxidoreductase
PTGS2	COX-2	Oxidoreductase
RARA	RARa	Nuclear hormone receptor
RARB,	RARb	Nuclear hormone receptor
RARG	RARg	Nuclear hormone receptor
RBBP4	RBBP4	Chromatin-binding protein
RXRA	RXRa	Nuclear hormone receptor
RXRB	RXRb	Nuclear hormone receptor
SET7	SET7/KIAA	Chromatin-binding protein
SIN3A	SIN3A/KIAA	Chromatin-binding protein
SIRT2	SIRT2	Chromatin-binding protein
SIRT6	SIRT6	Chromatin-binding protein
SNAI1	SNAI1	Zinc finger transcription factor
SULT2A1	SULT2A	Transferase
SUV39H1	SUV39A	Chromatin-binding protein
TGFB2	TGFB2	Growth factor
TGIF	TGIF	Homeobox transcription factor
THRB	THRB	Nuclear hormone receptor
TP53	p53	Transcription factor
VDR	VDR	Nuclear hormone receptor
YY1	YY1	Zinc finger transcription factor